# Non-RSSI based energy efficient transmission power control protocol for low power indoor wireless sensor networks

A thesis presented in partial fulfilment of the
requirement for the degree of
PhD
in
Engineering

at
Massey University
Palmerston North
New Zealand

Debraj Basu
2016

# Acknowledgement

First and foremost I offer my deepest gratitude to my primary supervisor, A/Prof Gourab Sen Gupta and secondary supervisors Dr. Giovanni Moretti and Dr. Xiang Gui, for their relentless support and guidance throughout my thesis. It is because of their untiring effort and belief in me that have helped me to finish my PhD.

I would like to thank the members of the Massey University Smart Environment (MUSE) team for the intellectually stimulating sessions that have immensely shaped my research skills. In particular, I covey my heartfelt gratitude to Prof. Stephen Marsland for the time he offered to help me with tackling some mathematical nuances.

My appreciation also extend to Mr. Ken Mercer, senior tutor with the school of Engineering and Advanced Technology, Massey University, who has been absolutely supportive with my building of electronic circuitry and testing for experimental purposes.

For all kind of administrative support, I am grateful to Mrs. Michele Wagner and Mrs. Linda Lowe from the school of Engineering and Advanced Technology, Massey University.

I would also like to thank my friends in New Zealand and overseas for keeping me company (and sane) during my studies.

I am indebted to my parents for their selfless act to bring me up and take care of me all throughout.

My final words of gratitude and appreciation go to my wife, Tamalika, who has been the primary source of my inspiration to complete my thesis. Without any doubt, I acknowledge that this thesis would never have seen the light of the day without her sacrifice and understanding.

# Abstract

In this thesis, we present the state-based adaptive power control (S-APC) protocol that is aimed to reduce energy consumption in low power wireless sensors while maintaining an application specific packet success rate requirement. The state-based approach is unique of its kind that dynamically adapt to the varying path losses caused by the movement of mobile sensors, by obstructions appearing between the stationary sensor and the base-station and movements of objects or humans in between two communicating stations. Since the primary reason for a drop in transmitted packets is the poor signal-to-noise ratio, it is important for the sensor to select a set of RF transmission power levels that will deliver the packets within a specified error rate while using the least amount of energy. In a battery-powered wireless sensor node, the use of ARQ (Automatic Repeat reQuest) protocol will lead to retransmissions when an attempt to send a packet fails. The proposed adaptive protocol does not use received signal strength indication (RSSI) based beacon or probe packets nor does it listen to the channel before transmitting for channel estimation. The use of the proposed S-APC protocol is not limited to only sensor network. It is applicable to any kind of radio communication when the transmitting radio frequency (RF) modules have configurable output power and options for retransmission. This proposed protocol can comfortably work on top of existing MAC protocol that is contention based and listens to channel before transmitting.

The hardware used for evaluating the protocol parameters is the nRF24L01p transceiver module from Nordic Semiconductor Inc. This radio module is cheaper than other modules that provide the RSSI values to the chip and the application of the adaptive power control protocol can further reduce the overall deployment and running cost of a sensor network.

The proposed protocol is designed to respond to an unknown and variable radio channel in an energy-efficient manner. The adaptive protocol uses past transmission experience or memory to decide the power level at which the new packet transmission will start. It also uses a drop-off algorithm to ramp down power level as and when required. Simulation has been used to compare the performance with the existing RSSI and non-RSSI based adaptive power control protocol. Results have shown that when the channel condition is between average and poor (ratio of bit energy ($E_b$) and noise power spectral density ($N_0$) is less than 20 dB), the RSSI based adaptive protocol consumes 10-20% more energy. Following the simulations, exhaustive experimental trials were done to compare S-APC with the existing protocols. It was found that there can be an increase of energy efficiency up-to 33% over fixed power transmission. This protocol could be applied in mobile robots that collect data in real time from sensors and transmit to the base station as well as to body wearable sensors used for monitoring the health conditions of patients in a health facility centre. Overall, this adaptive protocol can be used in radio communication

where the channel has dynamic temporal and spatial characteristics to enhance the lifetime of battery powered wireless sensors.

# Table of Content

# List of Figures

# List of Tables

# Chapter 1 Introduction

Over the last decade, sensor networks and applications relying on wireless sensor networks have become widespread, as has research in academia and a burgeoning industry in sensor networking devices. Over the last decade sensor devices have evolved to support various applications, such as asset monitoring, surveillance, structural health monitoring, habitat monitoring, and even underwater sensing. Wireless sensors are finding increasing importance in developing smart network like smart power grids, smart buildings and smart industrial process control that significantly contribute to more efficient use of resources and a reduction of greenhouse gas emissions and other sources of pollution. In the next section we would briefly discuss some application areas, their application requirements and relevance of energy conservation in sensor nodes [1].

## 1.1 Sensor Network Applications

### 1.1.1 Habitat and environmental monitoring

Habitat and environmental monitoring represent a class of sensor network applications with enormous potential benefits for scientific communities and society as a whole. A mesh of numerous networked micro-sensors can enable long-term data collection at scales and resolutions that are difficult, if not impossible, to obtain otherwise. Researchers in the life sciences are becoming increasingly concerned about the potential impacts of human presence in monitoring plants and animals in field condition. One such project was undertaken by College of the Atlantic (COA) to primarily monitor the usage pattern of nesting burrows of different birds by field testing with in-situ sensor networks. Some of the important application requirements for such habitat and environment monitoring are listed below.

- **Hierarchal network**: hierarchal network connectivity is required between the sensor nodes and the database system at the base station as distance between them can be several kilometres.
- **Sensor network longevity:** the network is expected to run for 9-12 months without recharging or replacing the battery.
- **System behaviour:** sensor networks should provide reliable data on regular basis
- **Inconspicuous operation:** the presence of the sensor network should not disrupt the natural processes or behaviours under study [2].

### 1.1.2 Structural health monitoring

Structural health monitoring (SHM) refers to the continual or periodic monitoring of the state or 'health" of large structures such as bridges, buildings, ships etc. Aging and degradation of transportation infrastructure can pose significant safety concerns, especially in light of increasing use of these structures. Like habitat monitoring, structural monitoring also has specific application requirements:

- **Large-scale multi-hop network:** for structures spanning large distances, the choice is between single hop and multi-hop connectivity between nodes or motes, as they are known, and the monitoring base station.
- **Lifetime of nodes:** node batteries that are meant for structural monitoring must last for years as replacing them in the big structures is an arduous and expensive task.
- **Reliable command dissemination and data collection:** motes or sensor nodes must receive the proper commands to perform theirs task. Data from the motes must be transferred reliably as missing samples can make the analysis hard or even impossible. [3] [4]

### 1.1.3 Human health monitoring and assisted living

Applications in this category include tele-monitoring of human physiological data, tracking and monitoring of doctors and patients inside a hospital, drug administrator in hospitals. This may also include scenarios of assisted living.

Body sensor networks are a key technology that use sensor data from patients and help in long term health monitoring. This technology is also used to prevent the occurrence of myocardial infarction, monitoring episodic events or any abnormal condition [5]. Activity tracking sensor network can also be installed in residential houses that support assisted living. These networks promise to revolutionize health care by allowing inexpensive, non-invasive, continuous, ambulatory health monitoring with near real time updates of medical records via the Internet. It is important to note that for effective in-situ human health monitoring systems, the sensor network application must meet the following requirements:

- **Reliable communication:** Data from wearable devices in Wearable Wireless Body/Personal Area Network (WWBAN) must be reliably transferred as their importance in medical applications can potentially be enormous**.**
- **Long-term, low duty cycle monitoring:** The communication requirements of different medical sensors vary with required sampling rates; from less than 1 Hz

to 1000 Hz. Sampling rate is related to duty cycle of communicating nodes, which has impact on the energy consumption of the sensor node. [6]

These sensors are constantly in touch with the wireless gateway or the access point. Most of these sensors are non-invasive and therefore a patient is allowed to move in freely. Therefore, the distance between the transmitting nodes and the access point also changes constantly. Power control can reduce the energy consumption and increases the lifetime of these body wearable sensors.

These nodes, capable of sensing, processing, and communicating one or more vital signs, can be seamlessly integrated into wireless personal or body area networks (WPANs or WBANs) for health monitoring

### 1.1.4 Workplace applications

The current generation of interactive devices and networks foster a wide class of interactive ubiquitous computing applications. The recent trend to integrate wireless networking into interactive devices such as PDAs, cellular phones, and portable computers has led to the availability of information such as news and stock quotes, as well as services such as email, appointment tracking, and multimedia content from any location at any time. Hundreds of sensors may scattered throughout workplaces in both industrial and non-industrial office environments. These wireless sensors can play the important role of interconnecting the devices so as to provide ubiquitous access to remote information and actuation capabilities. Application requirements include:

- **Low power wireless sensor** for prolonged battery life
- **Reliable data communication**
- **Acceptable data throughput** to support the applications [7]

### 1.1.5 Ubiquitous sensor network application (USN)

The proliferation of low power wireless sensor networks and their discreet presence have introduced a new paradigm in data collection and analysis of target parameters in both indoor and outdoor environments. This has been differently named in the literature and the industry, like ‘invisible”, “pervasive” or “ubiquitous” [8] computing. Others prefer to refer to it as “ambient intelligence” [9]. The broad idea is that there will be sensors (with or without for example, RFID tags) that are able to exchange information with a certain base station or hub and perform an assigned task. The sensors, the computational and the communication units, along with the hub, form the ubiquitous sensor network (USN). The term ubiquitous is applied to the collection and utilization of information in real time, and at any-time and any-where. The technology has enormous potential and a wide range of applications such as environmental monitoring, health monitoring for assisted

living (smart home environments) and industrial and plant monitoring (Industrial automation).

The general characteristics of a USN are:

- Limited power requirements (usually battery powered)
- Able to withstand harsh environmental conditions
- Fault tolerant and designed to cope with high possibility of node failures
- Support for mobility
- Dynamic network topology
- Able to withstand partial communication failures
- Heterogeneity of nodes
- Large scale of deployment [10]

### 1.1.6 Industrial automation using mobile robot

In industrial automation, the process monitoring and control applications range from data sensing, measurement, record and diagnosis, to machine/equipment operation and emergency action. These operations are classified by the ISA100 committee into six different classes with increased priority as following [11]

- Class 5: Monitoring without immediate operational consequences.
- Class 4: Monitoring with short-term operational consequences
- Class 3: Open-loop control
- Class 2: Closed-loop, supervisory control
- Class 1: Closed-loop, regulatory control
- Class 0: Emergency action[1]

Data communication in these process control applications includes periodic data dissemination and asymmetric or event-driven data traffic. The major concern is the quality of service (QoS), which requires the correct data at the right time, i.e., the reliability of the data and a real-time guarantee.

Mobile robots can play a pivotal role in making information available anytime and anywhere when they are used for applications that are delicate, heavy, and repetitive or labour intensive [12]. They can be used in assembly lines, in moving stacks of containers in warehouses, asset tracking, cleaning industrial floors etc. In process monitoring and

[1] Slide taken from ISA100 Overview & Status (ISA100 Roadshow Presentation) is used with permission of ISA – The International Society of Automation ©2008. All rights reserved.

control, process data such as pressure, humidity, temperature, flow, level, viscosity, density and vibration intensity measurements can be collected through sensing units and transferred wirelessly to a control system for operation and management [13]. Wireless sensor equipped mobile robots can also help in reducing the "blind spots" by their ability to collect measurement values on rotating or moving equipment and in remote location [14].

In [15], Tomioka Katsumi et al. have shown the applicability of ubiquitous wireless sensor networks especially in certain monitoring systems. This paper has listed application areas where mobile robots can be used advantageously. Some of the application areas are

- Facility status monitoring
- Temperature and humidity monitoring systems for warehouses
- Quality control for manufacturing and inspection processes

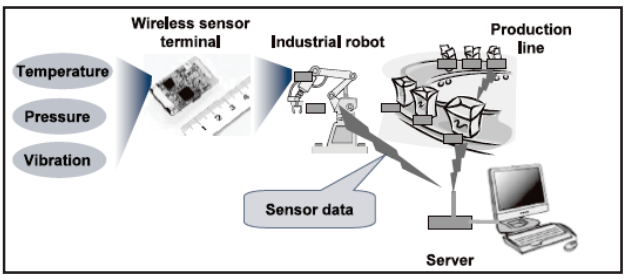


**Figure 1.** *Facility status monitoring [15].*

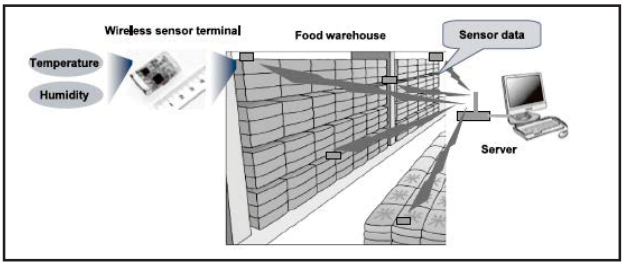


**Figure 2.** *Temperature and Humidity Monitoring System at a Warehouse [15].*

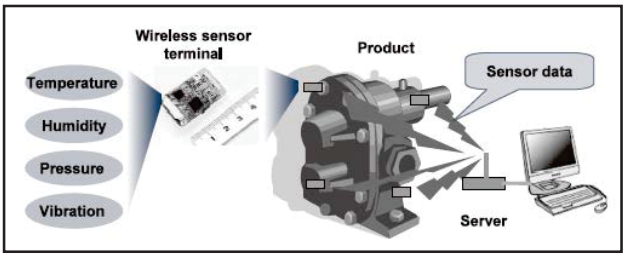


**Figure 3.** *Quality control for manufacturing and inspection processes [15].*

Figures 1-3 shows the placement of sensors and their communication with a server for further data processing. The key challenges in these scenarios are access and maintenance of sensors. To avoid human intervention and errors, a mobile robot can be used to perform different tasks like the replacement of equipment or batteries for sensors. The mobile robot can also be used to collect data from these sensors and transmit to the server in real time.

### 1.1.7 Healthcare application

In healthcare, traditionally human intervention is required to transport medical equipment, samples, and meals for patients, getting rid of medical waste. Mobile robots can eliminate the need for manual transport of laboratory specimens, medications, supplies and other materials, allowing healthcare technicians to focus on patient-related tasks [16] [17].

The different applications that are discussed in section 1.1 show that wireless sensors need to meet the mix of the following criteria:

- Reliability
- Mobility
- Real time data delivery
- Data security
- Lifetime prolongation

The target application areas of the wireless transmission power protocol are:

- Healthcare
- Industrial automation

There are primarily two kinds of sensor systems used in healthcare. They are vital status monitoring and remote healthcare surveillance [18]. In vital status monitoring, the patients wear sensors that monitors their vital health parameters in order to identify emergency situations and allow caregivers to respond effectively. Applications include wearable ECG-recording system for continuous arrhythmia monitoring in a wireless tele-homecare environment [19], monitoring and detection of epileptic seizures [20] and rehabilitation application where human motion tracking system is used [21]. In remote healthcare surveillance, body wearable sensors are used to collect medically related data from elderly or physically impaired person.

Industrial automation also requires continuous data collection from different control processes, remote health monitoring of components in a plant, mobile robot applications, etc.

In all these applications, the data transmission protocol should aim to meet the objectives of data reliability, support of mobility, minimum delay and prolonged sensor operational life. In order to ensure data reliability, transmission protocols apply error control mechanisms to send data with minimum error. These error control mechanisms are principally divided into error correction and error detection methods [22]. The most common and simple error correction mechanism is the stop-and-wait protocol [23]. In this protocol, the sender transmits a packet and waits for an acknowledgement from the receiver before it transmits a new packet. If no acknowledgement is received within a given time set by the transmitter, it assumes that the packet has been lost. It will continue to retransmit the lost packet until an acknowledgement is received or the maximum allowed retransmission attempts has been reached. Retransmission of packets leads to delay and additional energy expenditure. Mobility of sensors also becomes a major issue when the distance between the transmitter and the receiver is not fixed. Variable distance causes change in link quality with time and affects the data reliability and energy usages. Overall, there is a trade-off between reliable data communication and energy conservation in low power wireless sensor networks.

Another imposing reason for energy conservation is the operational expenditure to replace the batteries of these wireless sensors. Section 1.2 discusses the practical problems with battery powered sensors, the replacement of batteries and its economic implications on the industry.

## 1.2 Limitations of battery powered wireless sensors

The power sources of the wireless sensors are mainly disposable batteries. The primary challenge is that sensors are often in hard-to-find service locations. Hard-to-service locations can add significant cost to the already high replacement cost of batteries for wireless sensors and can even limit the deployment of more sensors, potentially reducing the effectiveness of the overall deployment. On the other hand, for continuing performance, the batteries are required to be replaced in bulk on regular basis. This results in wasted battery life. Otherwise, the users have to accept the risk of changing sensor batteries when the operating voltage goes below threshold [24]. Sensor operation will continue as long as the battery terminal voltage is above the usable limit, referred to as the Functional End Point (FEP) [25]. When the battery terminal voltage falls below the FEP value, the transmission link becomes very unstable as sensors cannot maintain the same transmission power level. Replacement of batteries in bulk number is a continuous and cost prohibitive undertaking. The cost of the batteries themselves is a small fraction of the overall costs; the storage, handling and labour costs being much more. Additionally, there are costs associated with the disruption caused to the sensor network which can be significant in a critical application. Over the life of the sensor it can be a

substantial expense, dramatically eroding the ROI (return of investment) of wireless sensor deployments [26]. “ON World” estimates the labour cost for changing batteries in wireless sensors will be greater than $1 billion over the next several years, assuming no energy-harvesting methods are used [27]. The network disruption and cost of battery replacement are significant factor constraining the growth of wireless sensor networks. It is therefore, important to design intelligent power saving algorithms to extend the lifetime of sensor nodes and reduce the overall operational cost of wireless sensor networks.

One of the other important aspects of batteries that are used to power wireless sensors is the size. This is because the focus of the current sensor design is to make them unobtrusive and inexpensive [28]. In that respect, the role of the coin cell batteries has become crucial. CR2032 [29] is one of the most popular coin cell lithium batteries that are used to power wireless sensor modules, primarily because of its small size and cheap price. A number of wireless sensor manufacturers like Monnit [30], WirelessTag [31] and Microstrain [32] use CR2032 lithium coin cell batteries in their sensor modules. They have far less capacity as compared to the batteries used by mobile cellular devices (~1500 -3500 mAh) [33] [34] [35].

High data refreshment rate and harsh wireless environment can adversely affect the battery lifetime. Figures in [25] have shown the battery discharge patterns of CR2032 coin cell batteries when continuous and pulse currents with different intervals are drawn. Most batteries used in wireless sensors are subjected to pulse discharge [36]. Pulsed discharge is different from continuous discharge because in pulse discharge a charge recovery takes place at the electrode when the sensor module is not transmitting. However, in harsh radio environment, a sensor transceiver may have to retransmit the same packets frequently because of high packet error rate. Battery voltage drain plots vs. the different duty cycles in [25] indicate that the more frequently the current is drawn from batteries the lesser will be its lifetime.

To summarise, for successful monitoring of target subjects and building a reliable communication network that can be used for an appreciably long time without significant human interventions (replacement of batteries, recharging etc.), the primary requirements are that sensor nodes must be

- Energy efficient
- Send data reliably with minimum number of errors

This research thesis has considered single hop network with battery powered wireless sensors that are placed for home, industrial, office-space and health monitoring and automation purposes and have certain common impediments in communicating the information over a dynamic radio channel. These sensors may be static or mounted on

mobile robots or worn by patients to monitor vital health parameters like heart rate, blood pressure, blood sugar level.

## 1.3 Error control mechanisms in wireless communication

The error control mechanism in wireless or wireline systems is handled by the data link layer [37]. The primary responsibility of this layer is to maintain a reliable communication between two sensor nodes. The most common correction mechanisms that are used are:

- Redundancy of information bits
- Retransmission of packets lost due to error
- Transmit power of radio transmitter

Other methods include the choice of parameters like the packet size and data rate.

In the context of the thesis, the error control method using retransmission and power control is used. Error control by retransmission of lost packets falls broadly under the purview of ARQ protocol [23]. ARQ stands for automatic repeat request. The basic idea of the ARQ protocol is that the transmitting node creates a link layer packet by adding a header and checksum to the data packet before transmitting. The receiving node checks the integrity of the packet with help of the checksum and sends the acknowledgement regarding the success of the packet transmission. If a negative or no acknowledgement is received within a specific time, the packet transmission is considered unsuccessful and the transmitter performs a retransmission. There is broadly three categories ARQ protocol. They are

- Stop-and-Wait ARQ
- Go-Back-N ARQ
- Selective-repeat ARQ

The go-back-N and selective-repeat protocols are categorized as sliding window protocol as both use variable buffer size to accept packets instead of one packet at a time as part of their flow control.

Figure 4 shows the pictorial representation of the stop-and-wait protocol. In this protocol, the sender sends a message to the receiver and waits for an acknowledgement. When an acknowledgement is received, then the next packet is sent. If the message is lost, the transmitter waits till the retransmission timer expires and resends the last lost packet. In section 2 of chapter 3, a detail explanation including results of channel utilization of the different error control protocols are presented. Based on the results, it is found that that the stop-and-wait protocol can deliver same channel utilization performance as the other two, while it is simple and easy to implement.

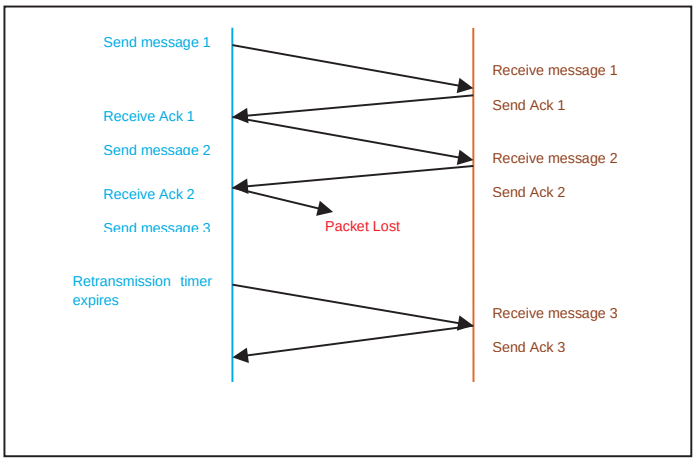


**Figure 4.** *Error correction using simple Stop-and-Wait protocol.*

## 1.4 Wireless transceiver module and its operation

A wireless node has three broad modes of operation. They are

- Sensing mode
- Computational mode (possibly a microcontroller)
- Trans-receiving mode

The computational and communication module structure of a sensor is shown in Figure 5. The communication module is the dominant energy consumer compared to computation and sensing [37].

During each transmission cycle, the transmitter radiates electromagnetic energy through the antenna using the power amplifier (PA). The current consumption during the transmission cycle depends on the amount of power that is radiated and the data packet size for a given channel data rate.

During reception, the receiver section of the radio transceiver is active. The amount of energy consumed during reception is dependent on the received packet size (for a given channel data rate) as the current consumption during reception is usually fixed.

Hence when an error control protocol like the Stop-and-Wait is used for error control, the transmitter has to resend the lost packets and waits for acknowledgement from the receiver by constantly listening to the channel. All these increase the total energy consumption of the wireless transceiver module and can curtail the battery lifetime.

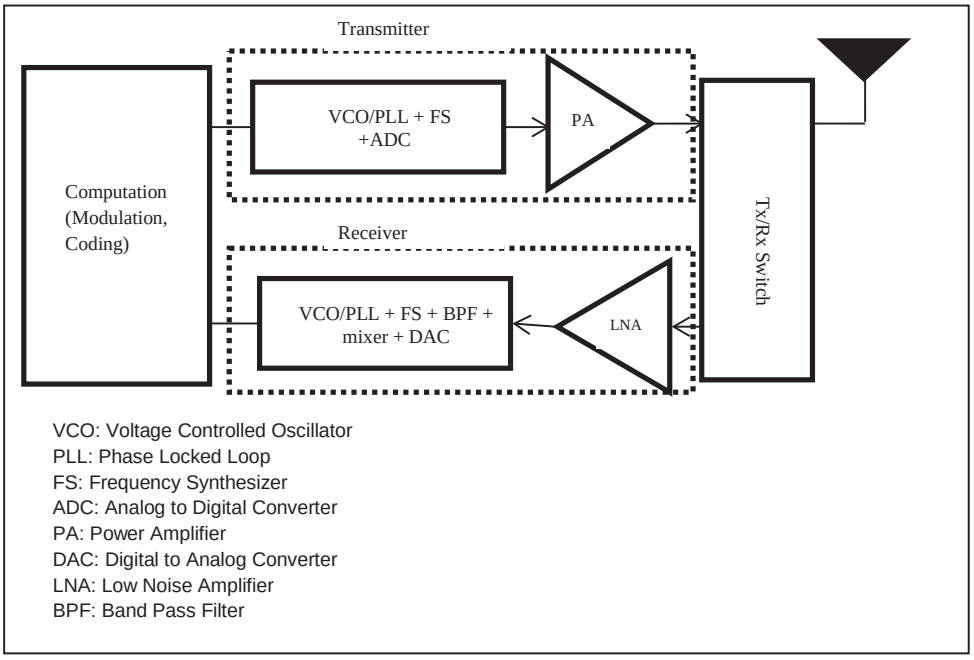


**Figure 5.** *Computation and Communication module of a wireless sensor transceiver.*

## 1.5 Adaptive power control with configurable output power

The primary objective of the research work is to design, implement and test a transmission power control protocol that will make use of the configurable output power levels of radio transmitter to transmit at the optimal power level to save energy. This can be achieved by setting the power level to the minimum level as and when necessary while still achieves correct reception of a packet despite intervening path loss and fading.

Most of the real world radio devices have configurable, finite and discrete power levels. Especially for wireless sensors, the transmission power level approximately ranges between -25 dBm to 0 dBm. The current consumption is the maximum at the maximum output power level and decreases with lower power levels. Table 1 shows the range of configurable power levels of some of the low power sensor radios along with the current consumption range during transmission and reception.

In Table 1, note that, surprisingly, the current consumption during reception is same or greater than during transmission. Therefore, the more the sensor has to retransmit, the more is the energy wasted in listening and receiving the acknowledgement packets.

**Table 1. Sensor radio power levels**

| Radio device | Description | Output Power range | Current consumption range during transmission | Current consumption during reception |
|---|---|---|---|---|
| CC2420 (Texas Instruments) | 2.4 GHz IEEE 802.15.4 / ZigBee-ready RF Transceiver | The output power is programmable in 8 steps from approximately –25 to 0 dBm. [38] | 8.5 mA to 17.4 mA | 18.8 mA |
| nRF24L01p (Nordic Semiconductors Inc.) | 2.4 GHz Transceiver | The output power is programmable in 4 steps from -18 to 0 dBm. [39] | 7 mA to 11.3 mA | 12.3 mA |
| CC2500 (Texas Instruments) | 2.4 GHz Transceiver | The output power is programmable in 4 steps from -12 to 0 dBm. [40] | 11.1 mA to 21.2 mA | 18.8 mA |

## 1.6 Thesis organization

The rest of the thesis is organized as follows:

Chapter 2 discusses the relevant research work in the field of energy efficiency of wireless sensor nodes and outlines the research statement about how S-APC may be more energy efficient in indoor low power wireless communication and even can fare better than existing power control protocols in certain scenarios.

In Chapter 3, the general performance parameter of transmission protocol has been presented. It also discusses the validation process using experiments and simulations to compare the variation of the packet success rate (PSR) with the benchmark theoretical success rate against the average $E_b/N_0$ values.

Chapter 4 specifically looks into adjusting the delay values between retries in ARQ scheme for indoor low power wireless communication. It was found through experiments that the proper choice of the delay between retries can reduce the packet error rate and the consumption of energy by retrying less often.

In Chapter 5, the proposed adaptive power control protocol is introduced, that does not use RSSI side information for channel estimation. This chapter also presents the comparative analysis of the energy expenditure values of the proposed adaptive protocol and the fixed power transmission that are obtained from experiments.

Chapter 6 has explored the use of the proposed adaptive power control protocol in mobile sensors. Several simulation results using MATLAB simulations have shown that the use of the adaptive protocol can outperform the fixed power transmission in terms of energy consumption while maintaining the PSR above a given threshold. Experiments have been conducted to validate the simulation results.

In Chapter 7, the proposed adaptive power control protocol is compared with RSSI based power control protocol that exchanges beacon packets, either with its neighbouring node or with the hub, to estimate the link quality before actual data packet transmission. The periodic link sampling can add to the cost of transmission. Simulation using Matlab has been conducted to compare the performance parameters of the beacon based power control protocol with the proposed adaptive power control protocol not using any beacon based channel estimation method.

Chapter 8 has compared the performance of the proposed adaptive power control protocol with ATPC (Adaptive transmission power control). ATPC is the first adaptive power control protocol for wireless sensor network. It uses RSSI values of the transmitted packet at a given power level that are sent as feedback or acknowledged packet from the receiver to estimate link quality and set the appropriate power. In this chapter, real world RSSI data from different indoor radio environments, such as shopping mall and University dining hall during the busy hours are collected from the beacon packets with the strongest signal strength that are periodically transmitted by the WIFI access points (AP). These beacon packets contain the RSSI values and they can emulate the working of the ATPC protocol if these RSSI values are considered to be received from the hub. In simulation, the ATPC protocol is designed accordingly and the different RSSI values are passed as input parameters to ATPC to calculate the PSR and other performance parameters. These parameter values are compared with the performance of the proposed adaptive protocol under the same scenario as the ATPC protocol.

The thesis is concluded in Chapter 9.

# Chapter 2 Literature survey and the research statement

This chapter discusses the relevant research work in the field of energy efficiency of wireless sensor nodes, finds out the research gaps and proposes the research hypothesis.

## 2.1 Existing power saving algorithms/protocols

Power saving approaches can be broadly classified into media access control (MAC) layer solutions and network level solutions [41].

The medium access control (MAC) layer controls when and how each sensor node can access the shared wireless channel to transmit packets. The primary responsibilities of MAC layer are

- collision avoidance
- energy efficiency
- scalability and adaptability
- fairness
- throughput
- bandwidth utilization

An energy efficient MAC protocol is meant to

- reduce collisions
- reduce idle listening
- avoid overhearing
- reduce control packet overhead

Most existing contention-based WSN MAC protocols attempt to limit transmissions and idle listening, but fail to prevent the nodes from actively monitoring channel contention periods before transitioning to sleep. Idle listening occurs when a radio monitors an inactive channel. The existing contention-based protocols reduce idle radio listening by concentrating the network's data transmissions into smaller active periods, and then transitioning to sleep for the remainder of the cycles. Concentrating the transmissions into a smaller active period increases the probability of collisions, thus wasting precious bandwidth and energy. Existing reservation-based protocols like the time division multiple access (TDMA) establish fixed time periods for nodes to communicate to eliminate the channel contention and idle listening energy costs. To use the bandwidth effectively, these protocols expend significant energy in exchanging control packets to reallocate unused time slots or require complex algorithms to allocate time slots based upon previous traffic requirements.

In a general contention based protocol, energy is wasted because of the following reasons:

- collisions
- control packet overhead
- overhearing unnecessary traffic
- long idle time

It has been estimated that idle listening consumes almost the same energy as when required for receiving a packet.

In paper [42], Injong Rhee et al. have done a brief comparison of CSMA and TDMA based protocols in general. The CSMA protocol is simple, robust and flexible. It does not require much infrastructural support in terms of clock synchronization, global topology information and handling of dynamic node joining and leaving. However, that comes at the cost of collisions when more than two nodes transmit at the same time causing corrupted received packets. For example, if two nodes, B and C which cannot hear each other, transmit packets at the same time to node A (which can hear both B and C), then there is very high probability of collision of packets transmitted by both B and C. This is called hidden node problem. The use of Request-to-Send (RTS) and Clear-to-Send (CTS) messages can alleviate this hidden terminal problem. In RTS/CST scheme, when node B wants to send a packet to node A, node B first sends a RTS message to A. On receiving the RTS message, node A responds by sending Clear-to-Send (CTS) message, provided node A is able to receive the packet. When another node, say C, overhears a CTS message, it keeps quiet for the duration of the transfer [43]. But usage of this scheme can incur high overhead (40% to 75% of the channel capacity) in sensor networks because data packets are typically very small in sensor networks. TDMA alleviates this problem by scheduling the transmission time of nodes. However, as the number of nodes increases, efficient time scheduling becomes harder. During low contention, TDMA gives much lower channel utilization and higher delays than CSMA because in TDMA, a node can transmit only during its scheduled time slots whereas in CSMA, nodes can transmit at any time as long as there is no contention. In [42], the authors have proposed ZMAC that combines the strengths of TDMA and CSMA while offsetting their weaknesses. The main feature of Z-MAC is its adaptability to the level of contention in the network so that under low contention, it behaves like CSMA, and under high contention, like TDMA. It is also robust to dynamic changes in topology and the time synchronization failures commonly occurring in sensor networks.

The energy efficiency is achieved by scheduling the sleep/wake-up times of the sensors. One major issue with energy-saving MAC protocols is the way they handle the data. If there is a fixed periodic sleep/wakeup time as in sensor-MAC protocol (S-MAC) [44], or dynamic SMAC which controls the periods of sleep/wake-up, then this can result in

latency issues, unlike in TDMA (time division multiple access), where the delay is constant. In wireless sensor networks, data transmission can be either periodic or event-driven. Under such circumstances, SMAC will fail completely because packets can get lost in between sleep/wake up time. In [45], Polastre et al. propose a Berkeley-MAC (B-MAC) protocol that provides a flexible interface to obtain ultra-low power operation, effective collision avoidance, and high channel utilization. However, the inherent weakness of low-duty-cycled MAC protocols are that, in order to synchronize with neighbouring nodes, preamble packets are required before receiving message data. Even in low power wireless transceivers, such as the CC2420, CC2500 and nRF24L01p, the energy cost for reception is comparable to that for transmission ( [38] [39] [40] and Table 1 in chapter 1). Therefore the cost of a preamble exchange cannot be ignored; even if the preamble packet reception time is small compared to that of actual data packets. The scheduling of nodes usually needs global time synchronization. It can be a major challenge if the clock drift issue is not properly addressed.

In contrast to MAC layer solution, the network layer solution utilizes adjusting the appropriate transmission parameters to achieve power saving. This thesis work investigates the different power control protocols that are employed for wireless communication to achieve energy efficiency. Network level solution modifies the different transmission parameters to achieve the set goal.

### 2.1.1 Network layer solution

There are several transmission parameters that can be varied to suite the requirement of the application:

- Power
- Modulation technique
- Data rate
- Error correction coding
- Retransmission number control if using ARQ protocol

However, as mentioned in [37], transceivers use the maximum energy during transreceiving; so this thesis focuses on adjusting transmission power to reduce the packet error rates, thereby minimizing the number of retries and extending the battery lifetime.

## 2.2 Basic approach of adaptive power control protocols

The framework for adaptive transmission has been explained by Andrea Goldsmith in chapters 4 and 9 of [46]. There are several adaptive transmission strategies in practice that try to maximize data throughput and minimize error rates. Link quality estimation is an integral part of adaptive transmission. It involves link monitoring, link measurement

and metric evaluation [47] [48]. In traditional link quality estimation, the transceiver sends probe packets to the destination nodes, either in uni-cast or broadcast modes, and senses the channel using the feedback packets before the actual transmission commences. Even during normal data transmission, the receiver usually piggybacks the link quality parameters like the received signal strength indication (RSSI) or the link quality indication (LQI). Based on these values, the transmitter can set the output power level and/or the retransmission limit of the next packet transmission. The objective of these power control algorithms is to find the power level that is sufficient to transmit the packet with the minimum number of retries and /or to minimise the number of packet losses and therefore to conserve energy. Certain adaptive protocols also us the packet reception rate (PRR) or the packet delivery ratio (PDR) within a given sample window to estimate link quality. They do not consider RSSI/LQI as reliable link quality indicators, especially in dynamic radio channels when the link quality changes with time. The next sections discuss the different adaptive approaches in details.

### 2.2.1 RSSI/LQI based adaptive power control with or without beacon packets for link quality estimation

RSSI is a measurement of signal power which is averaged over 8 symbols of each incoming packet [49]. On the other hand, LQI is usually vendor specific and is measured based on the first eight symbols of the received packet as a score between 50 and 100 [48]. The basic principle behind the RSSI/LQI based adaptive power control system is guided by closed loop control between the transmitting node and the receiving base station mechanism. The general steps are described below as

- The transmitter sends packet at an updated power level to the receiver
- Receiver measures the RSSI
- If the RSSI is below the threshold that is required for faithful packet delivery, then the receiver sends the control packet with the new transmission power level.
- At the transmitter, the control packet is received and the current power level is updated for packet delivery

During initialization phase, the transmitter needs to know the power level at which it should transmit to successfully deliver the packet. In this phase, the transmitter sends several packets at all its available power levels. In return, it receives RSSI values for each power levels. Based on the mapping of the RSSI and the output power level, the transmitter selects the required power level.

In paper [49], Shan Lin et al. have introduced adaptive transmission power control (ATPC) that maintains a neighbour table at each node and a feedback loop for transmission power control between each pair of nodes. ATPC is the first dynamic

transmission power protocol for WSN that uses all the available power output levels of CC2420 [38]. The CC2420 radio transceiver module operates in the ISM 2.4 GHz band and has 32 output power levels, ranging from 0 dBm to -25 dBm. Through exhaustive experiments, the authors of this paper have found strong linear correlation between the transmission power and the RSSI. In this adaptive transmission power protocol, the neighbour table contains the proper transmission power level that this node should use for its neighbour and the parameters for a linear predicative model. The aim is to find out the minimum power level to maintain a satisfactory link quality between two neighbouring nodes. The predictive model is used to describe the relationship between the transmission powers and link qualities. If a node receives a packet with the RSSI value that is different from the desired RSSI value, then a notification packet is sent to the sender. The notification packet is sent under two circumstances. They are

- the link quality falls below the desired level and required to ramp up
- the link quality is good but the signal energy is high enough to be wasted and therefore require to ramp down

The notification packet contains the difference between the measured and desired link quality. This difference is used as input to the predictive model that calculates the new transmission power level for its neighbour.

Sheu et.al have proposed an adaptive power control algorithm that also has an initialization phase and a maintenance phase while adjusting transmission power [41]. In the initialization phase, each of the sensor nodes uses the 8 power levels of CC2420 to send 100 probe packets in each of the power levels. It sets the packet delivery ratio (PDR) threshold to 80% instead of the RSSI threshold to determine the minimum power level with which the nodes must communicate with each other. In the maintenance phase, the aim is to adjust the transmission power level with the changing environment. It combines the RSSI and LQI values to determine the new transmission power. There are two RSSI thresholds that are maintained in each node. If the average of the RSSI is greater than the upper threshold, then it steps down one power level. If the RSSI is below the lower RSSI threshold, it will increase the power level by one step. If the RSSI is in between the RSSI thresholds, then it checks if the average LQI is less than the lower threshold LQI. If that condition is fulfilled, then it increases the transmission power by one level.

REAL (reliable energy adept link-layer) [50] protocol uses error correction mechanism to maintain reliable communication. It chooses its data recovery strategy based on the overall information distortion and the available energy at a sensor node. The data recovery actions have three options to choose from. They are

- Use of error correction code to recover the original data packet at the receiver

- Retransmit when the error correction mechanism has failed due to severe distortion
- Drop some packets to save energy for transmission of higher priority packets

REAL also uses RSSI/LQI as the channel side information to evaluate channel conditions.

In [51], the approach is similar to ATPC where the power-distance table is maintained at each node. The minimum transmission power of one node with the neighbouring node is considered as the 'distance' and packets will be routed through these nodes in a multihop sensor network topology. Therefore, the optimization of the transmission power is the shortest path problem based on the power-distance relationship. This protocol relies on broadcast-and-feedback mechanism to determine the minimum transmission power required for each neighbouring node. This protocol can optimize power consumption by choosing to transmit via one or multi-hop.

In paper [52], the authors have provided an empirical analysis of the impact of power control for mobile sensor network. The focus of this research paper is on residential health monitoring, in-hospital patient monitoring and sports monitoring that require mobile sensing. Cellular networks deal with mobility by using different types of hand-shake mechanism. However, the emphasis is on the energy-constrained sensor nodes. This paper suggested that RSSI data may not be sufficient to evaluate link quality when sensor nodes are mobile. The authors propose an active probing scheme for sensor applications that send data periodically and those which are triggered by an event (i.e. event-driven). In active probing scheme, the mobile node counts the number of consecutive packets that are successfully transmitted at the current power level. If that is more than a predefined threshold, then the power level is decremented by one level. However for any un-acknowledged packet, the transmission power level is incremented by one level, until the maximum power level is reached. This protocol has also modified this approach by using the LQI values that are provided by CC2420 transceiver modules. In order to make good use of the LQI values of the acknowledgement packets, it allowed the radio to transmit several packets at each of the power levels. It finds the optimal power level region where consistent LQI values higher than 100 is observed. This optimal value is used as the benchmark to set the new transmission power level.

The authors in [53] have proposed a power control algorithm in which each sensor node also uses beacon messages to determine its neighbours and the corresponding minimum transmission power. After the neighbours are discovered, the adaptive algorithm finds the optimal power so that it is able to meet its target of communicating with a given number of neighbouring nodes. Authors have combined dynamic transmission power control of the link layer protocol with the reduction of duty cycle of MAC layer to save energy. It

also investigates the effectiveness of duty cycling the nodes rather than put them in idle listening mode when not transmitting.

The application of an adaptive power control algorithm for IEEE 802.11 in the technical report of [54] aims to modulate the transmit power based on the distance between the communicating nodes to the minimum level such that the destination node still achieves correct reception of a packet despite intervening path loss and fading. In the experiments, Cisco Aironet 350 series radio was used that has discrete and configurable output power levels ranging between 0 and 20 dBm. Once the transmitter sends a packet to the receiver, it calculates the optimal transmit power for the new transmission based on the path loss and average RSSI values. The receiver only sends the control packet containing the optimal transmission power level when there are significant changes in the RSSI values.

***Discussion on the use of RSSI based adaptive power control protocols***

RSSI/LQI based adaptive power control protocols are an attractive alternative to save energy. It is to be noted that these protocols are mainly designed for multi-hop network where each sensor node broadcast beacon packets and discover its neighbour to which it can able to transmit at the minimum power. However, there are two factors that are worth considering. They are

- There is an initial overhead cost for building up the RSSI vs. Power level table.
- In case the sensor is mobile, the refreshing frequency of the table becomes crucial and that also adds to the cost.
- Even when the sensors are stationary, there is no clear indication in any of the papers ( [41], [49] - [54]) as to what would be the ideal channel sampling frequency that would optimise energy efficiency.

In this thesis, the standard RSSI based adaptive power control protocol is compared with the proposed novel non-RSSI based adaptive power control protocol in terms of energy efficiency when they maintain comparative packet success rate. The results point out the shortcomings of using the RSSI as the link quality estimator in dynamic radio channel condition and the additional energy cost that is incurred when probe/beacon packets are used to build up the neighbour table.

### 2.2.2 Non-RSSI based adaptive power control protocols

Practical-TPC [55] is a receiver oriented protocol that is considered robust in dynamic wireless environments and uses packet reception rate (PRR) values to compute the transmission power that should be used by the sender in the next attempt. The receiver monitors all incoming packet and counts the successes and failures of the packet transmission within the current sampling window. After the sampling window period is

over, the P-TPC protocol computes the next transmission power level and sends to the transmitter. This new power level will be used during the next sampling window. P-ATPC has two main components. One component (fast online model identification FID) estimates the model between the PRR and the transmission power. It initialises or reconfigures the second component proportional-integral with anti-Windup (PI-AW). The PI-AW computes the transmission power level based on the difference between the current PRR and the application specific PRR requirement. P-ATPC runs two feedback loops. The inner loop involves the PI-AW that adapts the transmission power based on the PRR measurement. The outer loop involves FID to adjust the parameters based on the updated power model that defines the relationship between the PRR and transmission power. P-ATPC also initializes the power model parameters before the feedback loops kick in. In this initial phase, each link is set to transmit a sequence of probe packets using highest to lowest power level to build the transmission power model.

ART (Adaptive and Robust Topology control) protocol [56] has been designed for complex and dynamic radio environments. It adapts the transmission power in response to variation in link quality or degree of contention. Empirical studies presented in this paper have shown that the PRR and the signal strength can vary over time. This is primarily due to effect of movements of objects and people in between the transmitter and the receiver during the busy hour of the day and corresponding fading of signal. Analysis of the paper has suggested that RSSI and LQI may not be good or the most reliable indicators of link quality, especially in dynamic indoor radio environment. ART changes the transmission power of a link based on the observed PRR. It has an initialization phase when the ART protocol monitors all the outgoing packets for its successful or failed transmission within a sliding window of predefined size. It compares the number of failures within that window with a minimum and a maximum threshold failure. Based on the comparison, it does anyone of the following:

1) Remains in the same power level or

2) Increases the transmission power level or

3) Reduces the transmission power level and enters a trial to compare the new failure rate count with the predefined threshold.

D.Lal et.al have introduced the term “link inefficiency” while characterizing the link quality metrics of energy constrained wireless sensor nodes [57]. Link inefficiency is defined as the inverse of the packet success probability as it represents the mean number of transmissions for a successful transmission at a given time. The expected energy consumption is therefore proportional to the link inefficiency. This paper proposes the time average energy consumption as the cost metrics.

The ART protocol in [56] uses two packet reception rate threshold values to adapt the output power level. These thresholds would depend on the channel conditions and requires to be made adaptive. Such protocols may not be suited for time varying radio channels as the two thresholds are required to be updated. The authors, however, have not indicated clearly about changing the thresholds as link quality changes.

***Discussion on the use of non-RSSI based adaptive power control algorithm***

The primary shortcoming of a non-RSSI based adaptive power control protocol is the choice of the sampling windows when the short term and long term relationship between the packet reception rate (PRR) and the output powers are built to determine the transmission power to meet the PRR requirement. Especially in temporally and spatially dynamic radio environment, it becomes a considerable challenge to balance between energy saving and energy consumption due to periodic sampling of radio channel to updated the output power vs. PRR model. This overhead cost can increase the average energy cost of transmitting a packet. A faulty model can either over-estimate or underestimate the channel quality. Things can get worse when sensors are mobile and randomly change their distance with respect to the base station.

In order to compare the performance parameters of a general non-RSSI adaptive power control protocol with the proposed one in this thesis, simulations have been used. It has been shown that when the radio link quality changes with time, the proposed adaptive protocol can perform better than the PRR based power control protocol.

### 2.2.3 Power, modulation order and code rate control in broadband access network and cellular network

The adaptive modulation and coding technique in WIMAX is meant to improve effective data throughput for the customers [58]. The adaptive modulation and coding (AMC) is modelled as a Moore's state machine. Each state represents a modulation order and a coding rate. The aim is to cater to the different application requirements, users' requests and system characteristics. There are two adaptive transmission approaches that are proposed in the paper. In the first approach the aim is to keep the target block error rate under a target limit. The other method maximises the total link throughput. The adaptive modulation and coding technique for WIMAX is primarily aimed at maximising the throughput within a threshold error rate. The objective of the thesis is to meet the application specific error rate requirement while save the maximum amount of energy without concerning about improving the throughput. Besides the application of different modulation orders and coding rates can increase the computational overhead of the sensor node, thereby consumes extra energy. Also the introduction of error correction coding increases the overhead cost because use of code (addition of redundant bits), especially with low code rate (ratio of the information message length and the generated code

length) can significantly reduce the throughput. In such situations, a block of information data can require more than one transmission which adds to the total cost of transmission.

In GSM, power control algorithm is employed to achieve desired signal strength for faithful communication between the mobile station (MS) and the base transceiver station (BTS). Power control also reduces interference and improves cell capacity. During a connection between the BTS and the MS in a cell, the MS measures the channel RF link quality every 480 ms [59]. In this way an acceptable link quality is maintained which can also improve the battery lifetime of the mobile device. As mentioned in the Introduction chapter, the drive for small and discreet sensor has prompted the use of coin cell batteries with capacity in the order of 250-300 mAh [29]. Their capacity is far less as compared to those that are used in mobile phones (~1500-3500 mAh) [33-35]. This link quality measurement and maintenance method will rapidly deplete the sensor battery even at a lower rate, primarily because of the limitation of the capacity of these batteries that are used in wireless sensors.

### 2.2.4 Dynamic or adaptive power control in the physical layer

Authors in [60] have proposed a power control algorithm that reduces energy consumption by utilizing retransmissions. It has suggested half power scheme for transmission where the transmission power is reduced to half and allowed to retransmit once. In essence, the transmitter is consuming the same amount of energy. But when it is allowed to retransmit twice at the half power, essentially the packet error rate (PER) is reduced. Reduction in the PER minimises the retransmission probability and therefore the energy consumption. The issue of delay due to retransmission is also considered. The dynamic power control algorithm that is proposed in this paper has set the retransmission limit to 1. If a packet transmission is not successful even after the retry limit, it doubles the power and transmits the same frame again. If there is an acknowledgement, the signal powered is lowered gradually to save energy.

***Limitation of using half-power approach***

The half power approach in paper [60] assumes that the output power has a proportional relationship with the drain current drawn by the power amplifier (PA) of the sensor transmitting module. Therefore the half-power with one retransmission scheme should be able to reduce the energy consumption of the transmitting sensor node. In this thesis, the half-power scheme has been simulated using Matlab. The simulation results show that the packet error rate using the scheme that is mentioned in [60] reduces the PER at higher ratio of energy per bit ($E_b$) to the noise spectral density ($N_0$), $E_b/N_0$ (> 15 dB). But they have similar values when the channel condition is poor. If the PER of full power transmission at power level S is denoted by $PER_s$, then the PER of the half power approach with one retransmission is given by $[PER_{s/2}]^2$. Plots of the PER at different

powers and their corresponding $E_b/N_0$s in figures 6 and 7 suggest that half power scheme with one retransmission performs better at higher $E_b/N_0$.

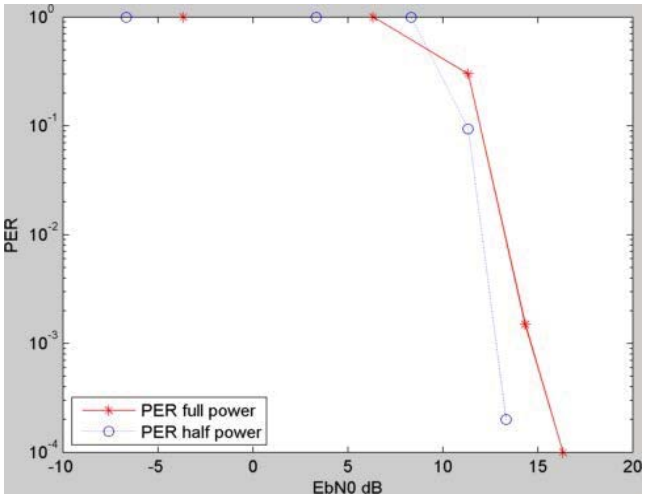


**Figure 6.** *Simulated PER vs. the $E_b/N_0$ for full power and half power schemes in AWGN channel shows that at higher $E_b/N_0$, the half power scheme can perform better.*

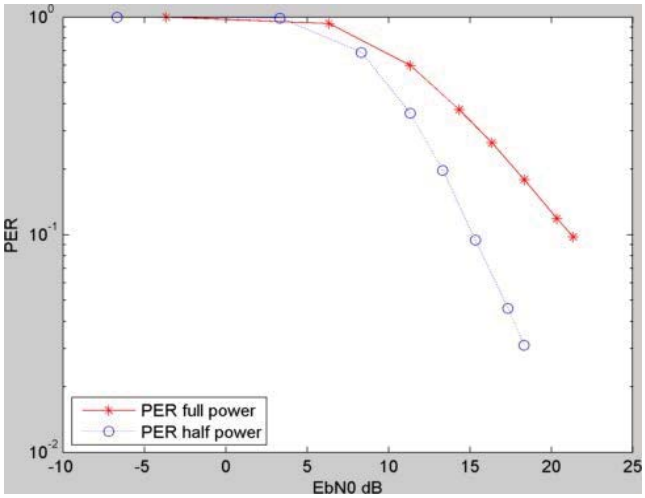


**Figure 7.** *Simulated PER vs. the $E_b/N_0$ for full power and half power schemes in fading channel shows that at higher $E_b/N_0$, the half power scheme can perform better.*

The paper has calculated the power consumption in each these cases using equations 1 and 2 . If the full power energy consumption is $E_s$, then

Full power average energy consumption

$$P_{FULL=} E_s \tag{1}$$

And half-power average energy consumption while allowing only one retransmission

$$P_{HALF} = \left(\frac{E_s}{2}\right) * \left(1 + PER_{\frac{s}{2}}\right) \quad (2)$$

However, in real world hardware, the power consumption values do not vary in a linear manner with the output power level. Example plots of CC2420 and nRF24L01p in Figure 8 demonstrate the relationship between the output power levels and the corresponding current consumptions and therefore the limitations of this type of half-power adaptive power control algorithm.

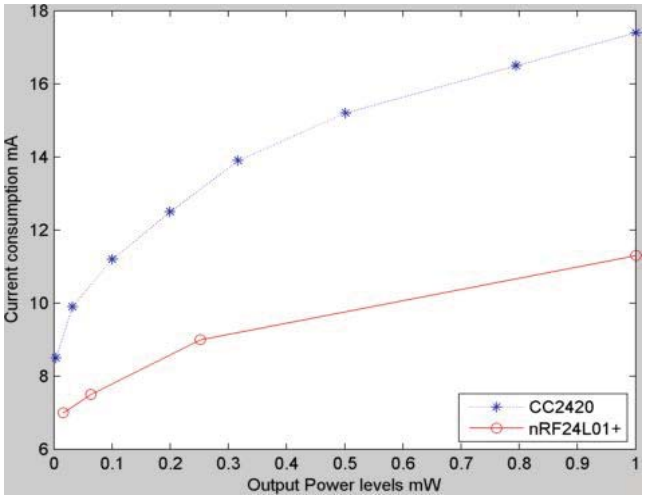


**Figure 8.** *Output power levels vs the current consumption values of CC2420 and nRF24L01p shows that their relationship is not linear and half output power does not mean half the current consumption of the full power.*

### 2.2.5 Power control with error detection and correction mechanism

Forward error correction (FEC) mechanism is used in wireless network to recover lost packets and thereby saves energy by reducing the number of retransmission of traditional ARQ error control protocols. Several papers have analysed the energy consumption issues when FEC is applied. In the light of WSN, some of these algorithms are discussed critically in the current section.

In contrast to 1-bit or 2-bit errors in outdoor environments, indoor radio channel suffers from multiple-bit errors in the same packet due to its slow fading nature [61]. The authors have shown through experiments with single (13, 8 and 30, 24) and double bit correction codes (16, 8), represented by SECDED (13, 8), SECDED (30, 24) and DECTED (16, 8) respectively, that the overall packet drop is less than when no FEC is used. The two values within parenthesis of SECDED and DECTED represent the lengths of the data bits and codeword respectively.

However, as the results suggest, the difference in the packet drop rates is low (2.32 % with no FEC as compared to 0.02 % with SECDED (13, 8) and 1.19% with SECDED (30, 24). On the other hand, the overheads for encoding are very high. The overhead is

the ratio of the difference of the length of the data bytes transmitted with and without error correction coding (ECC) and the length of data byte transmitted without ECC. The values are derived from the TinyOS [62] distribution for CC1000 radio [63] that has been used in [61]. Table 2 summarises the finding of the paper. The over-head values are quite high and can significantly add to the cost of transmission.

**Table 2. Comparison of the average packet drop rate and overhead of coded and un-coded system**

| | **No FEC** | **1-bit error correction (13,8)** | **1-bit error correction (30,24)** | **2-bit error correction (16,8)** |
|---|---|---|---|---|
| **Packet Drop Rate** | 2.32 % | 0.02 % | 1.19 % | 1.32 % |
| **Overhead** | 0 % | 64.3 % | 21.4 % | 64.3 % |

Authors in [64] have performed experiments with coded messages in lab setup where the main source of packet error was from the other wireless LANs (WLANs) in the 2.5 GHz band. Experimental results in that paper suggest that in a start topology, appropriate choice of error correction codes can help in achieving energy efficiency as compared to un-coded system with ARQ protocol. However, these results fail to capture the complex and dynamic multipath radio environment where the significant sources of error are due to signal losses due to fading and variation of the path losses over time.

In [65] authors have introduced the concept of cross-over distance which defines the boundary condition of employing error correction coding in an energy efficient manner as compared to un-coded communication. Due to significant overhead of FEC systems, the coding gain achieved due to FEC can only compensate for the energy overhead beyond a certain distance. The cross-over distance depends on several factors. They are

- The total circuit power which includes the power consumption of the ADC, DAC, frequency synthesize (FS), band pass filter (BPF), LNA etc.
- Computational energy
- The efficiency of the power amplifier (PA)
- The total ON-time of the transmitter
- Number of bits per modulation symbols
- Bandwidth
- Noise figure
- Error correction capability of the code (N, K, t), N = code-word length, K = message world length, t = error correction capability in terms of the number of bits
- The coding gain

- Gain of the transmitting and receiving antenna
- Operating frequency
- Noise spectral density

Analytical and simulation results with AWGN channel and different FEC systems suggest that the cross-over distance decreases as the computational energy decreases and vice versa. It means that if computational energy is low, then FEC can be employed at a smaller distance. On the other hand, if the efficiency of the PA increases, the cross-over distance increases. This is because the energy consumption of the PA i.e. transmission energy dominates over other sources of energy expenditures. Therefore, it is the balance of the computational energy and transmission energy that determines the cross-over distance. These cross-over values range from 80 to 150 m that depend on the PA efficiency and the computational expenditure (in terms of the error correction capability of the code). The experiments were conducted using CC2420 radio modules from Texas Instruments. The range of the cross-over distances may vary marginally if tested with other RF hardware modules because other low power radio transceivers also have similar current consumption values, like in CC2500 where the current consumption ranges between 11.1 mA to 21.5 mA corresponding to output power level between -12 dBm to 1 dBm [40]. CC1000 also have similar output power vs. current consumption profile (8.6 mA to 16.5 mA corresponding to -20 dBm to 0 dBm) [63]. These cross-over distance values are not realistic for indoor communication. They also mean that in order for the coding system to be energy saving compared to un-coded system, the distance between the transmitting sensor and the hub should be more than 80 m. Based on these observations, it can be concluded that existing encoding scheme may not be energy efficient in indoor radio environments where the distance between the sensor and the hub is usually within 40 m.

In [66], the authors have proposed a hybrid ARQ scheme with power ramping to improve throughput in a fading channel. In simulation, the hybrid type I ARQ (HARQ I) with packet combining scheme is used that stores erroneous packets after each failed retransmission. The receiver then uses maximum ratio combining (MRC) to combine each received channel bit with any previous transmissions of the same bit and the combined signal is fed to the decoder [67]. MRC is a diversity combining method where the signal from each diversity branches (example: multiple receive antennae) is multiplied by a weighted factor that is proportional to signal amplitude [68]. In HARQ I, the diversity branches are provided by the erroneous packets. Simulation results show that power ramping scheme with HARQ I has shown improvement in terms of average number of retransmissions.

The use of HARQ (types I, II and II) to optimize energy consumption in fading channel has been investigated by Igor Stanojev et.al [69]. The paper has adopted information

theoretic approach to evaluate the total energy consumptions. The authors have covered the scenario when the energy consumption due to electronic circuitry is comparable to the transmission power. The findings of the paper suggested that energy efficiency of HARQ protocols depends on the transmission range. At sufficiently large distance, the energy expenditure due to the power amplifier dominates the contribution of the transmission and the reception circuitry.

***Limitations of using error correction coding in slow fading channel and simple assumption of AWGN channel***

One of the main drawbacks of using error correction codes in slow fading channel is that error detection probability decays with the inverse of the average $E_b/N_0$ value. Therefore coding cannot significantly improve the error probability. This is because coding can average out the Gaussian white noise, but cannot average out the channel fade, that will affect all the coded symbols. Thus, deep fade, which is the typical error event in the un-coded case, is also the typical error event in the coded case [70] [71].

Papers [55], [50], [57], [60], [69] have proposed adaptive transmission algorithms that are based on the assumption that bit error rates are independent and uniformly distributed. However, the complex nature of indoor multi-path channel means that the bit errors occur in bursts. These papers also used simple path loss model which fails to capture the different degree of signal attenuation when it passes through different partitions in between the sensor and the hub or base station.

The simple additive white Gaussian noise (AWGN) channel model does not hold well in a very complex indoor multi-path radio environment. The relationship between bit error rate (BER) and packet error rate (PSR) is presented in equation (3) for AWGN channel when that assumes that bit errors are independent and uniformly distributed.

$$PSR = (1 - BER)^L \tag{3}$$

where $L$ = packet length in bits

Indoor radio channels are modelled as slow fading channels because the coherence time ($T_c$) of the fading channel is much greater than the symbol or bit period [72]. The Doppler spread and the coherence time describes the time varying nature of the channel in a small scale region. $T_c$ is the time duration over which two received signals have strong amplitude correlation. Since this thesis is dealing with fading channels, it assumes that either all the following three scenarios can exist:

a) there are movements in between the transmitting sensor and the receiver or

b) the sensor is mobile or

c) both (a) and (b)

Doppler spread is the measure of the spectral broadening caused by the time-rate of change of the radio channel. The coherence time of a fading channel is approximated as the inverse of the maximum Doppler spread ($F_d$). Empirical measurements of $F_d$ from different indoor environment including body area networks suggest that in the 2.5 GHz ISM band, the maximum Doppler spread value lies between 0 and 20 Hz [73] [74] [75]. The slow fading nature of the channel errors occur in blocks as the deep fades last long and affects a large number of transmitted symbols [70]. In other words, the bit or symbols errors occur in bursts and are not independent. Therefore the relationship between PSR and BER as mentioned in equation (3) does not hold true. Figures 11 and 12 have plotted the simulated PSR and the PSR that is derived from the BER vs the $E_b/N_0$ in AWGN and Rayleigh's fading channels. Simulation parameters are presented in Table 3. Results in figures 9 and 10 support the observation made.

**Table 3. Simulation parameters in MATLAB**

| | |
|---|---|
| Modulation technique | BFSK |
| Channel data Rate | 250 kbps |
| Maximum Doppler spread | 20 Hz |
| Packet size | 41 bytes |
| Multi-path Fading channel model | UMTS Indoor Office Test Environment [76] (based on Cost231 path loss model |

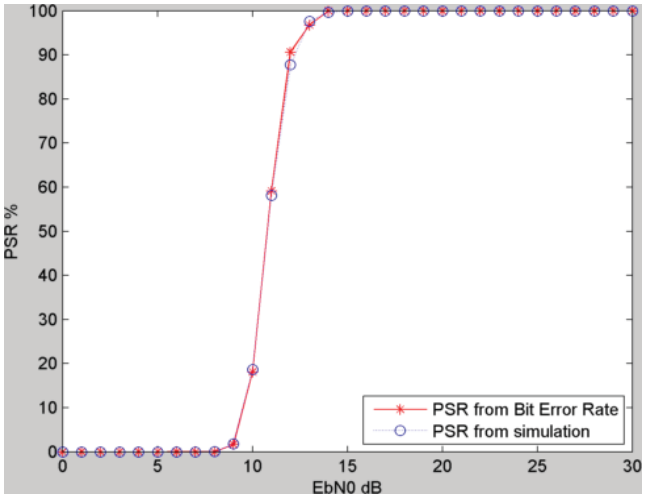


**Figure 9.** *Simulated PSR and PSR derived from BER vs. the $E_b/N_0$ in AWGN channel shows that bit errors are independent and uniformly distributed.*

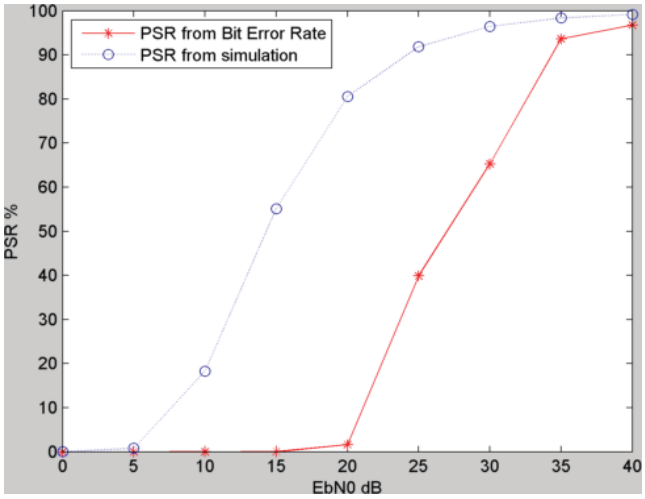


**Figure 10.** *Simulated PSR and PSR derived from BER vs. the $E_b/N_0$ in multi-path fading channel shows that bit errors are not independent and that errors occur in burst.*

***Use of Cost231 indoor path loss model and Indoor Office Test Environment***

In this simulation, the Cost231 path loss model for indoor above 900 MHz [76] has been used. This model takes into account the losses due to two different types of walls within a building and between floors. The two types of walls are

- Wall type I: Light internal walls
  - Plasterboards, walls with large number of holes
- Wall type II: Internal walls
  - Concrete, bricks, walls with minimum number of holes

It is therefore important to include the effect of these types of partitions when the adaptive algorithms are analysed. The proposed adaptive protocol is meant not only for sensors working in the ISM band but can be used in all RF modules that have configurable output power.

Lognormal shadowing model is simple and very basic as mentioned in [55] and suffers from inaccuracies in complex environment.

The ITU indoor path loss model [77] (between 900 MHz and 5.2 GHz) accounts for the penetration losses through floors. However, in indoor wireless communication signals also travel through different wall types. The ITU model does not account for the signal travelling through partitions or walls. From the different models in questions, Cost231 model is best able to explain the complexity of indoor radio environment.

### 2.2.6 Other methods of power control

Authors Xin Huang and Asuman Ozdaglar have also investigated the issues of power control and network design in mobile sensor networks in [78]. The objective of this

research paper is to maximise network lifetime in a multi-hop sensor network with the joint power control and area partitioning strategy.

Paper [79] has introduced an optimal power and retransmission control policies that uses Markov decision process (MDP) to formulate the underlying power and retransmission (modified ARQ) control.

Other energy efficient wireless transmission algorithm uses reinforcement learning method to optimise energy consumption [80] .

The use of reinforcement learning for energy efficient wireless transmission has been studied in [80]. It involves the use of Q-learning to control the transmission parameters to achieve maximum energy efficiency. The basic idea of Q-learning is that there will be the representation of the environmental states, 's', and possible actions in those states, 'a', and you learn the value of each of those actions in each of those states. At each state 's', Q-learning chooses the action 'a' that maximises a given function.

The parameters are the transmission power and the transmission rate. The state space includes the number of packets in the buffer, the transmitter mode and the channel condition. It assumes that the system has perfect knowledge of the channel condition that is obtained from the feedback of the receiver. The action space has the transmit power, the transmitter mode and the transmission rate. The final component of Q-learning is the cost function that is the weighted sum of energy consumption and penalty for buffer overflow.

In practice, the channel condition can only be known by sending beacon packets. The traffic patterns of practical wireless sensor network are not Poisson distributed. Moreover, the change in transmission rate can create significant alteration of the bandwidth and may not be recommended in ISM bands which are already over-crowded with WIFI channels and different ZigBee application channels. The approach, though unique, needs to align to the real world radio environments and answer the fundamental questions of when and how often to sample the radio link and how that affects the accuracy of link quality estimation.

### 2.2.6 Finite state Markov modelling of fading channel and its importance in adaptive transmission

Finite state channel modeling is an approach to divide the channel states based on noise level, fading gains or bit error probabilities. There are several works on finite state channel modeling. The first such major channel model was a two-state Markov channel introduced by Gilbert and Elliot and is known as the Gilbert-Elliott channel. In that proposed model, each state corresponds to a specific channel quality which is either noiseless or totally noisy. In general, a binary symmetric channel (BSC) with a given

crossover probability can be associated with each state so that the channel quality for each state can be identified. The Gilbert-Elliott channel is the special case where the crossover probabilities of the BSC's are 0 and 0.5, respectively.

But two-state Gilbert-Elliott channel is inadequate when the channel quality varies dramatically. A channel model with more than two states is needed so that "quantization error" can be minimized. This idea motivated researchers to extend the study from a two-state channel to a finite-state channel [81].

In [82], Paratoo Sadeghi et.al has discussed the benefit of treating the fading channel as a finite state Markov channel (FSMC). If an accurate modelling is present, the receiver may need to estimate few states for the fading level and send them to the transmitter as feedback. This will result in reduction of usage of bandwidth along the feedback path. Besides, a quantised version of channel fading amplitude means only a finite number of transmission strategies.

Markov channel models are used to characterise the wireless non-stationary channel. In [81], the FSMC was built by partitioning the received instantaneous ratio of bit energy and noise power spectral density ($E_b/N_0$) into intervals. However the choice of the number of states and $E_b/N_0$ partition was somewhat arbitrary as has been pointed out in paper [83]. The choice of interval cannot be arbitrary but will depend on the duration of time that the channel stays in a particular condition based on its $E_b/N_0$ value. The $E_b/N_0$ range in each state should be large enough to cover the $E_b/N_0$ variation during a packet time so that for most of the time, a received packet completely falls in the current state or one of the neighbouring states. On the other hand, the $E_b/N_0$ range of each state cannot be made too large. The reason is that if the $E_b/N_0$ range of a state increases, the time duration of the state also increases. Within a packet time period the received $E_b/N_0$ values are distributed in a smaller range than the state $E_b/N_0$ interval. Therefore the packets that are falling in the state may have bit error rates (BER) which is quite different from the BER for the state. The most important task in FSMC modelling is to determine the state boundaries. Therefore it is very important to track the dynamics of fading and quantise the channel based on this estimate.

In indoor radio environments, when the signal level can change dynamically, the use of FSMC for channel partitioning and setting the right power level is not a practical approach. The channel is required to be scanned for change in link quality frequently which in turn increases the overhead cost. The computational cost to do the channel partitioning also cannot be ignored.

## 2.3 Applicability of the existing adaptive protocols in indoor wireless sensor network

Over-all, the existing literature have been able to answer some of the challenges in indoor radio communication in terms of improving the packet success rate, the throughput and reducing energy consumption by adapting the output power, tracking the channel link quality with time and/or using forward error correction mechanism. The indoor radio channel is dynamic and link quality fluctuates over time. The RSSI/LQI based adaptive power control protocols use the instantaneous channel quality indicators (RSSI and/or LQI) to change the output power so that subsequent packets can be successfully transmitted and at the same time able to save energy. The PRR/PDR based protocols do not rely on RSSI/LQI values for link quality estimation in dynamic radio environment.

In general, during communication build-up phase, these adaptive power control protocols sets up the output power vs. the RSSI model or output power vs. the PRR model by transmitting short beacon packets to all its neighbours. The model gets refreshed every time a new packet is transmitted. Else the adaptive protocols can allow a specific number of transmission before the model can be re-profiled. Even during run time, the RSSI/LQI values are used to tweak the output power level. In order to maintain an up-to-date power model profile, it is important to send beacon packets at regular intervals. Especially in indoor radio environments, where link quality varies widely over time, the frequency of the refreshment can be extremely critical.

Some of the methods in literature have assumed that current consumption in a radio transceiver scales proportionally with the output power level and have proposed power control algorithms that can be energy efficient. In practice, the existing radio modules have non-linear current vs. power profiles. This is because of poor power converting efficiency of the power amplifier (PA) in the radio module that is responsible for pumping in electromagnetic energy through the antenna.

Error correction methods are an alternative approach in wireless link when there can be unpredictable losses. Error correction codes (ECC) can minimise the number of packet losses as well as the retries and therefore save energy. However, the limitation of using error correction codes in slow fading channel is that error detection probability decays with the inverse of the average $E_b/N_0$ value. Therefore coding cannot significantly improve the error probability. On the other hand, the overhead cost of processing the redundant bits can increase.

The adaptive power control approaches give an insight of the variety of techniques that can be employed to achieve maximum energy efficiency. Some of them can achieve 25-30% efficiency over fixed power solutions.

An ideal energy efficient adaptive power control protocol in dynamic radio environment should be able to track link quality per-packet transmission basis and adapts its output power and /or retransmission limits without the use of any overhead cost and not relying on the output power vs. PRR models or the output power vs. RSSI model which can be inaccurate.

A wide range of indoor radio environments must be chosen to ascertain the efficacy of the adaptive protocol. Most of the experiments in the literature have been either conducted in controlled environments like inside a laboratory or in open spaces in non-busy hours.

## 2.4 Research statement

The existing adaptive power control protocols have relied on the use of RSSI or LQI or the number of successful packet transmission to estimate channel quality and linked it with the output power. Some of the protocols have also used beacon packets at different power levels to discover and set the minimum required power level for acceptable communication. In dynamic indoor radio environments, the use of instantaneous RSSI or LQI to estimate channel state may give inaccurate or incomplete information. Moreover it can increase the overall cost of transmission. In this thesis, we explore the use of a non-RSSI approach to estimate link quality to adapt the output power and avoid using beacon packets for channel estimation. The adaptive algorithm is capable of tracking the changes in the link quality per transmission basis. Since this approach does not use beacon packets before the actual data transmission, the cost of transmission can be reduced. This approach will be tested in a dynamic indoor radio channel. In the process, extensive simulation with accurate indoor radio channel models from standards will be used to compare the performance of the proposed adaptive protocol with the RSSI/LQI or PRR based protocols that are most suited for indoor radio channel.

# Chapter 3 Performance parameters, experimental setup for validation, choice of ARQ and collision rate analysis

This chapter deals with the performance parameters that are used to evaluate transmission protocols. It also discusses the validation process using simulations and experiments to compare the variation of the packet success rate (PSR) with the benchmark theoretical success rate against the average $E_b/N_0$ values. This chapter also discusses the choice of the error control mechanism based on some analytical results. The wireless sensor network scenario is also introduced in this chapter along with results of collision error rate under different circumstances.

## 3.1 Performance parameters used to evaluate transmission protocols

S-APC uses output power and retransmissions to control error. There are two performance parameters based on one constraint. The constraint is the packet success rate (PSR) that is defined as the ratio of the successfully transmitted packets divided by the number of packets sent. Mathematically,

$$PSR = \frac{P_{succ}}{P_S} 100 \tag{4}$$

where

$P_S$ = total packets to send
$P_{succ}$ = successfully transmitted packets

$P_{succ}$ represents those packets that have been acknowledged by the receiver based on the CRC checksum match. In case of a CRC checksum mismatch, no acknowledgment is sent and the packet transmission is repeated. When all the retries elapse and no acknowledgment have arrived at the transmitter, the packet transmission is counted as permanently failed. The total packets to send in equation (4) only takes into account of the first transmission attempt when a new event occurs and does not include any retries.

The evaluation parameters are:

- **Average energy cost per successful transmission**
- **Expected success rate or protocol efficiency**

One of the parameters for the optimization is the energy consumed per useful bit transmitted over a wireless link [41] [64]. Similarly in this thesis, the cost per successful transmission has been considered.

$$C_{S\_avg} = \frac{C_T}{P_S - P_L} \tag{5}$$

where

$C_{S\_avg}$ = average energy cost per successful transmission
$C_T$ = total (energy) cost of transmission
$P_L$ = number of lost packets
Therefore, $P_{succ} = P_S - P_L$

All cost values are measured in millijoules (mJ). The total cost of transmission includes the expenditure for the first transmission attempt of a packet and the subsequent retries if the first attempt fails. The total packet-to-send count does not include the retry packets. Therefore the denominator in equation (5) is the count of successfully transmitted packets. Equation (6) represents the formula for calculating the cost per packet transmission ($C_P$).

$$C_P = V_t T_{ON} I_{PL} \tag{6}$$

where
$V_t$ = typical voltage (usually 3.3 or 5 volts)
$T_{ON}$ = the time duration when the transmitter is ON (in seconds)
$I_{PL}$ = drain current consumed in that power amplifier at a given power level( in mA)

Therefore the units of both $C_T$ and $C_{S\_avg}$ are mJ. $T_{ON}$ is the ratio of the packet size ($B_p$) and the channel data rate ($D_R$) [84] [85]. In case retransmissions are allowed, the cost will be simply added up. It will be shown in chapter 5 that by adjusting the delay between retries, the PSR value can be improved and total number of retries can decrease. However, there is a penalty for buffering the packet for the delay period. Under such circumstances, the total cost during one packet transmission cycle ($C_{p\_total}$) will be represented by equation (7).

$$C_{P\_total} = V_t N T_{ON} I_{PL} + V_t (N-1) T_B \, I_B \tag{7}$$

where,
$N (\leq R_L)$ = total number of transmissions used to transmit the packet
$R_L$ = Maximum limit of transmission
$T_B$ = Buffer time
$I_B$ = Current consumed during buffering

The expected success rate or protocol efficiency of the adaptive protocol is defined as the expected number of successes and takes into account the average number of retries [41]. It can also be defined as the expected number of successes per 100 transmissions. Mathematically,

$$Protocol_{eff} = \frac{P_S - P_L}{P_S + Ret_T} \tag{8}$$

where

$Protocol_{eff}$ = expected success rate
$Ret_T$ = total number of retries

Here $P_S - P_L$ = total number of successes ($Succ_T$)

If both the numerator and denominator are divided by $P_s$, then in percentage term,

$$Protocol_{eff}\ (\%) = \frac{PSR}{1 + Ret_{avg}} \tag{9}$$

where $Ret_{avg}$ = average number of retries per packet and is defined as

$$Ret_{avg} = \frac{Ret_T}{P_S} \tag{10}$$

$Protocol_{eff}$ indicates the total number of transmissions (on average) to achieve a given packet success rate (PSR). It also indicates the expected delays in transferring data as there are several applications that require delay-sensitive data.

Based on these parameters, simulation and experimental values are compared and analysed in the following chapters.

## 3.2 Choice of the error correction protocol based on the channel utilization values

The channel utilization is one important measure of protocol efficiency in flow control protocols that used for error detection and correction. It is defined as the percentage of the time that the channel is transferring data packets. Channel utilization of the ARQ protocol depends on two factors. They are

- The ratio of propagation time and packet transmission time ($A_{Link}$)
- The window size (N) [23] [86]

The window size is applicable to the last two variants of ARQ protocol.

For indoor wireless communication, the distance between communicating nodes or between a node and a base station generally lies between 0 and 40 m. For unguided transmission through air medium, the maximum propagation time ($T_{prop}$) will be approximately 133.33 ns. The transmission time ($T_p$) is also small as sensors generally sends small packets at reasonably high data rate (250 kbps and above).

Based on the literature references of [23] [86], it has been argued that channel utilization of Stop-and-Wait protocol is adversely affected by high value of $A_{Link}$. As mentioned

earlier, a wireless sensor usually sends small packets. If the packet size and data rate are taken as 50 bytes and 250 kbps, then

$A_{Link} = 0.0000833$

The channel utilization values of the three variants of ARQ are calculated based on the channel utilization equation of chapter 5 in [86] and presented in Table 4. The channel utilization values in Table 4 show that when the value of $A_{Link}$ is very small as is the case with wireless sensor communications, the channel utilization without any packet error is almost 100%. The plots in the figures 11 and 12 show the channel utilization when the packet error rates are set at 1% and 5% for a range of $A_{Link}$ values when the packet transmission time is normalized to 1.

**Table 4. Channel Utilization without any packet error**

| ARQ protocol | Channel Utilization |
|---|---|
| Stop-and-Wait | 99.98% |
| Go-Back-N ARQ - Window size 7 | 100% |
| Selective-repeat ARQ - Window size 7 | 100 % |

It can be concluded that when the propagation time is negligibly small, there is practically no difference in the channel utilization values of the three versions of the ARQ protocol. The Stop-and-Wait protocol is the simple and easy to implement. It also does not need buffer space to store packets. Therefore, in resource constrained wireless sensor modules, the stop-and-wait protocol is used to recover lost packets.

***Channel utilization with 1% packet error***

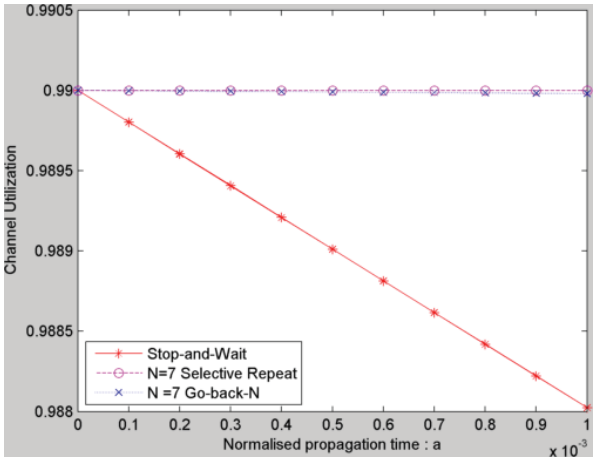


**Figure 11.** *Channel utilization plots of ARQ protocol at packet error rate of 1%. Stop-and-Wait protocol performs similarly with the sliding window protocols.*

***Channel utilization with 5% packet error rate***

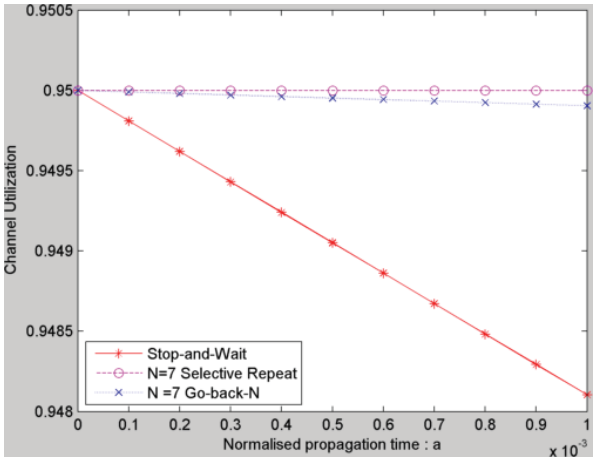


**Figure 12.** *Channel utilization plots of ARQ protocol at packet error rate of 5%. Stop-and-Wait protocol has comparable channel utilization values with the sliding window protocols.*

## 3.3 Hardware description and validation of setup

The packet success rate is calculated at the transmitter side which sends a packet to the receiver and waits for an acknowledgement from it. Retransmission happens when there is no response from the receiver within a specific time. A packet transmission is considered permanently failed when the number of retransmission has reached a pre-set maximum value. Therefore it is important to add two important features at the receiver end.

- The receiver must transmit the acknowledgement with enough power to ensure that the reverse link between the receiver and transmitter is practically error free as compared to the forward link between the transmitter and receiver. A front-end high gain power amplifier (PA) at the receiver side can pump out sufficient power so that the acknowledgement packet of successful packet transmission can be detected by the transmitting sensor
- The receiver should be able to extract the original signal from the transmitter even in presence of a high noise floor. A low noise amplifier (LNA) can capture extremely weak signal and amplify it to a useful level [87].

The hardware used in the research includes the nRF24L01p transceiver module that acts as a transmitting sensor. For the receiver, another nRF24L01p transceiver module is used that has an additional PA and LNA. The receiver has a maximum output power level of 20 dBm. The reason to choose a high power receiver is to make the path between the transmitter and the receiver practically error free. The primary features of the receiver and the transmitter receiver are presented in Table 5 and Table 6 respectively. The nRF24L01p transmitter and the receiver are shown in appendix A. The transmitter can

transmit at four power levels: -18 dBm, -12 dBm, -6 dBm and 0 dBm. In general a wireless transceiver has different modes of operation. They are mainly divided into active transmit mode, active receive mode, standby mode and sleep mode. In between retries, a transceiver module usually goes to a standby mode without shutting down its transmitter units. The transceiver module used in the experiment also has different modes of operations.

**Table 5. Features of nRF24L01p receiver [88]**

| Device: Receiver | nRF24L01p with PA and LNA |
|---|---|
| Maximum output power | + 20 dBm |
| Transmission mode peak current | 115 mA |
| Reception mode peak current | 45 mA |
| PA gain | 20 dB |
| LNA gain | 10 dB |

**Table 6. Features of nRF24L01p transmitter [39]**

| Device : Transmitter | nRF24L01p |
|---|---|
| Arduino Mega Development board with attached temperature sensor | Microcontroller board based on the ATmega2560 [89] |
| On air data rate | 250 kbps |
| Cyclic redundancy check | CRC-16 |
| Packet size | 41 bytes |
| Modulation method | Gausssian FSK |

The details of the modes and their current ratings are presented in Table 7.

**Table 7. Operational modes and current consumption of nRF24L01p**

| Operational mode | Current consumed mA |
|---|---|
| Transmission @ 0 dBm output power (MIN) | 11.3 |
| Transmission @ -6 dBm output power (LOW) | 9 |
| Transmission @ -12 dBm output power (HIGH) | 7.5 |
| Transmission @ -18 dBm output power (MAX) | 7 |
| Reception/Listening | 12.6 |
| Power down mode | 0.9 |
| Standby- I mode | 0.026 |
| Standby-II mode | 0.320 |

As expected, it can be seen from Table 7 that the transceiver consumes maximum current at the highest output transmission power of 0 dBm. Interestingly, the current consumptions at the different power levels do not scale proportionally with the output power levels. The current consumption almost halves when the output power level drops almost 100 times from 0 dBm to -18 dBm. This feature is common among existing low power wireless transceivers that have programmable output power levels. Noted among them are CC2420 [38] and CC2500 [40] from Texas instruments. The output power vs. current consumption behaviour in CC2420 is almost the same as nRF24L01p. In CC2500, the current consumption almost halves when the output power level drops approximately 20 times from +1 dBm to -12 dBm. This kind of disproportionate output power vs. current consumption characteristics poses stiff challenges in developing power control algorithms. This kind of characteristics is due to poor efficiency of the power amplifier (PA) of the RF module. The efficiency of a PA ($\eta_{PA}$) is defined by

$$\eta_{PA} = \frac{R_p}{I_{DC}} \tag{11}$$

Where,

$R_p$ = radiated power in W/mW

$I_{DC}$ = load current drawn by the PA in A/mA

Figure 13 shows that the when the radiated power changes more than 300 times from -25 dBm to 0 dBm, the current consumption is only reduced by half. Therefore it is important to consider the limitation of the RF hardware when designing the adaptive protocol.

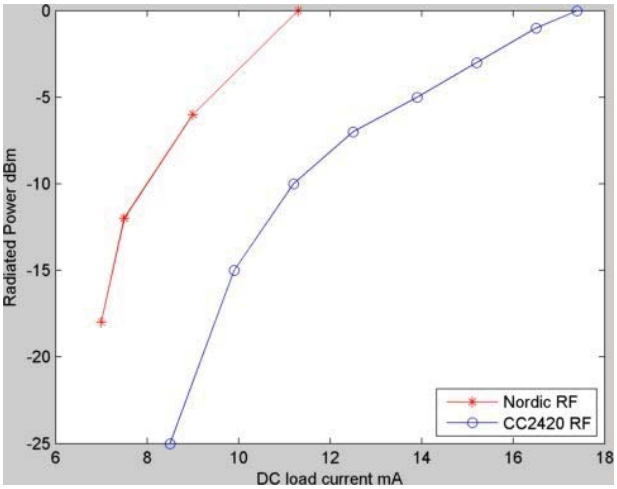


**Figure 13.** *DC load current drawn vs the radiated power curves of nRF24l01 and CC2420*

### 3.3.1 Theoretical background and validation of the hardware setup using simulation and experimental data

In this section, the theoretical plot of the PSR against the average $E_b/N_0$ will be compared and validated with the simulated and experimental results. In this thesis, simulations have been extensively used to test the proposed adaptive protocol. Based on the test results, the experiments have been conducted using the hardware. Therefore it is important to validate the both the simulation and experimental results with the theory.

The theoretical understanding of packet loss in a fading channel can be derived from the Gilbert-Elliot channel model that assumes that channel can be modelled as a Markov chain with a fade and a non-fade period. Since it is a memoryless model, the fade and non- fade intervals are independent and exponentially distributed.

The relationship between the PSR and the $E_b/N_0$ can be approximated by the sigmoid function [90] [91].The authors in these papers have done mathematical analysis and taken measurements in indoor radio environments. They have shown that the variation of the expected PSR with $E_b/N_0$ follows the sigmoid curve as mentioned in [92].

The PSR vs. the $E_b/N_0$ is also explained mathematically by Jean Paul Linnartz in [93]. Packet transmissions are assumed to be successful whenever the transmission starts in a non-fading interval and that the non-fade interval lasts for the whole duration of the packet transmission. We can define the probability of successful packet transmission as the product of two probabilities which are independent of each other.

Probability that the packet transmission starts in a non-fading interval $P_1$ is determined by the probability that the received signal amplitude is above the noise floor. For a Rayleigh fading channel, the probability distribution of received power is exponentially distributed. If the threshold power is $P_{th}$, then

$$P_1 = \exp\left(-\frac{P_{th}}{P_{avg}}\right) \tag{12}$$

where

$P_{th}$ = minimum received power required or threshold power
$P_{avg}$ = average received power and

The ratio of $P_{avg}$ and $P_{th}$ is referred as the fade margin ($M$). Therefore, equation (12) can be rewritten as

$$P_1 = \exp\left(-\frac{1}{M}\right) \tag{13}$$

The probability that the non-fade interval lasts for the full duration of the transmission is

$$P_2 = \exp\left(-\frac{T_p}{T_{nf}}\right) \tag{14}$$

where $T_p$ = packet duration or transmission time and

$T_{nf}$ = average non-fade duration

The theoretical probability of successful packet transmission PSR is, therefore,

$$PSR_T = P_1 * P_2 \tag{15}$$

The power terms of fade margin are conveniently replaced with average $E_b/N_0$ and threshold $E_b/N_0$. Hence from equations 14 and 15

$$PSR_T = \exp\left(-\frac{1}{M} - \frac{\sqrt{2\pi}}{\sqrt{M}} F_d T_p\right) \tag{16}$$

where

$$T_{nf} = \sqrt{\frac{M}{2\pi}}\, F_d \tag{17}$$

Therefore, PSR is a dependent on the maximum Doppler spread ($F_d$), the packet transmission time and the fade margin [93]. Figure 14 shows the theoretical plot of the PSR against the average received $E_b/N_0$ for different values of threshold $E_b/N_0$. The value of $T_p$ is calculated based on packet length of 41 bytes and channel data rate of 250 kbps. The value of $F_d$ is set as 20 Hz based on the discussion of section 2.2.4 in chapter 2.

***Theoretical PSR plot***

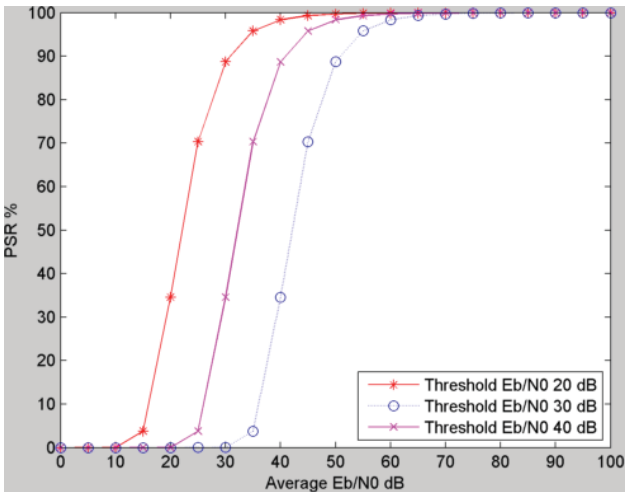


**Figure 14.** *Theoretical PSR plot against the average received $E_b/N_0$ at threshold $E_b/N_0$ values of 20 dB, 30 dB and 40 dB. A low threshold value indicates that very high PSR can be achieved at lower average received $E_b/N_0$. However, the nature of the curves remains the same.*

Figure 15 plots the simulated PSR when retries are allowed. The protocol efficiency is defined by equation (9) in chapter 3. It includes the total number of retries during transmission. Table 8 represents the simulation parameters.

**Table 8. Simulation parameters with MATLAB**

| | |
|---|---|
| Modulation technique | BFSK |
| Channel data Rate | 250 kbps |
| Maximum Doppler spread | 20 Hz |
| Packet size | 41 bytes |
| Cyclic redundancy check | CRC-16 |
| Multi-path Fading channel model | UMTS Indoor Office Test Environment [76] |
| Retry limit | 3 |

The shapes of PSR in Figure 14 (theoretical) and Figure 15 (simulated) are similar; indicating that the simulation set up is correct. The PSR and efficiency values that are obtained using experiments are plotted in figures 16 and 17.

### *Simulated PSR and efficiency plots with retries allowed*

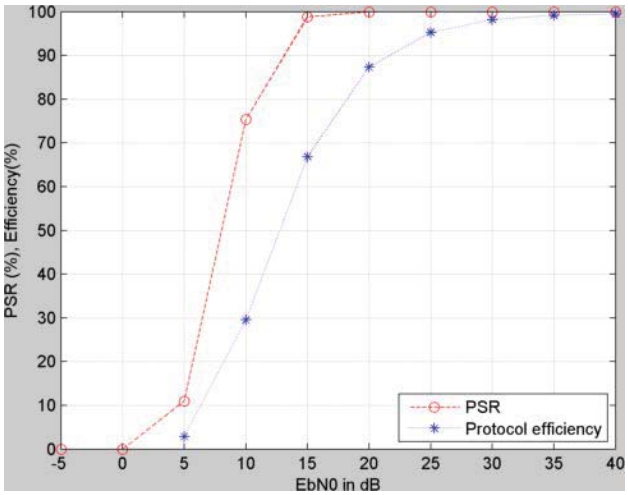


**Figure 15.** *Simulated PSR plotted with the efficiency that shows the actual work done in terms of retransmitting to achieve the PSR.*

### *Experimental PSR and efficiency plots with retries allowed*

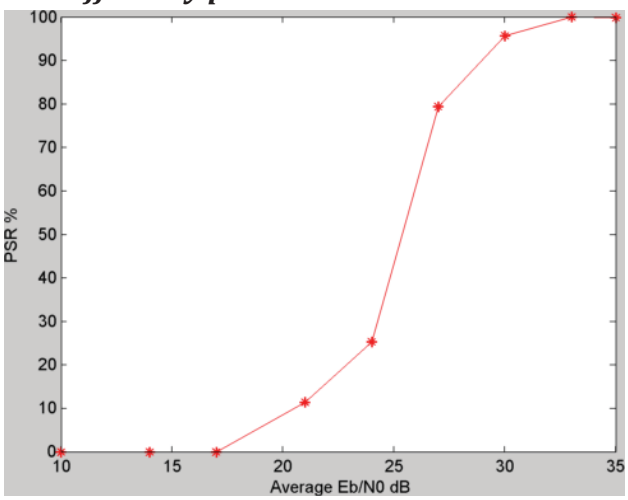


**Figure 16.** *Experimental values of PSR plotted when no retries are allowed.*

The nature of the curve in Figure 16 closely matches with the theoretical and simulated PSR. In Figure 17, the retry limit is changed to 3 in order to observe the behaviour of the efficiency and PSR and how closely they match the plots in Figure 15.

The average $E_b/N_0$ values are an approximation of the real values. They are derived using the Cost231 path-loss model. The objective of this chapter is to show that the experimental results match with the benchmark theoretical and simulated results. Figures 15 to 17 demonstrate that the hardware setup is correct and the nature of the curve of PSR against the $E_b/N_0$ values closely matches with the theoretical curves.

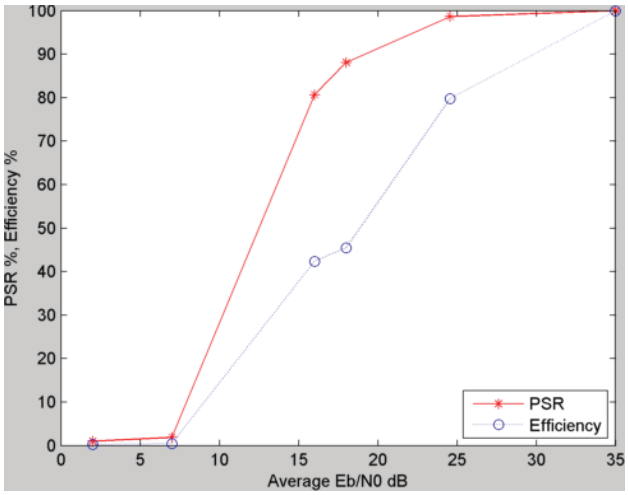


**Figure 17.** *Experimental values of PSR and efficiency plotted when retry limit is set at 3.*

In simulation, BFSK has been used as the modulation technique. However, the hardware RF module uses GFSK (Gaussian FSK). In terms of PSR and other measured parameters, this in not going to make any difference because the primary difference between FSK and

GFSK is that in GFSK, a Gaussian shape filter is used to reduce the spectral width for a given symbol rate. It is spectrally more efficient than BFSK [94].

## 3.4 Evaluating the impact of channel contention in WSN using Matlab simulation

It has been pointed out in [56] that in multihop WSN, transmission power control has an impact on the channel contention. The ramping up of the power level can be beneficial to improve the PSR up to a limit, but it can fall due to increase in contention if the output power is increased further. The MAC layer protocol controls when and how each node can transmit in the wireless channel. There are two different types of channel access mechanism. They are

- Without channel sensing before transmission (ALOHA, slotted ALOHA) [23]
- With channel sensing before transmission (carrier sense multiple access (CSMA),with collision avoidance (CA), optionally (clear-to-send CTS, request-to-send RTS) [43]

The first kind of random channel access method (ALOHA) is primarily meant for wired network. It works like following:

- When station has data to transmit, it transmit immediately
- When there is collision, it is treated as transmission error and packet is retransmitted
- Sender back-off for some random time after collision before it retransmits
- The collision or contention window is twice the packet transmission time indicating that any two packets that start transmitting within that contention will collide.

In a wireless sensor network, it is important to keep the channel access mechanism simple in order to avoid any computational overhead due to the implementation of the sophisticated access mechanisms. However that will depend on the network traffic load of

- the sensors in multi-hop network
- the sensors in single hop network transmitting to a single base station

The sensor network that is envisaged in this thesis has considered 50-75 sensors transmitting to a single base station at either at different rates or reporting an event when it occurs and within a communicating distance of 30-40 meters. These sensors can be static or mobile. They follow the principle of the ALOHA protocol, i.e. transmit a packet immediately without any channel sensing. Under these circumstances, it is important to understand the impact of the packet losses due to collision. Several simulation results

with realistic sensor network size and reporting rate to the base station are used in this thesis to outline their effect on the collision probability. In the ALOHA protocol, the collision window is twice the packet transmission time. Since only the impact of collision is studied, it is assumed that a sensor does not retransmit when a packet is dropped due to collision.

The simulation is designed in such a manner that the sensors start transmitting at any random point of time and are programmed to report at a fixed interval to the base station. A time window of 60 minutes was chosen to estimate the number of collisions. Within that specific time window, the transmission time stamp of the sensors are noted and the number of colliding sensors is counted when the difference in the timing falls within the collision or contention window. In order to make this simulation realistic, sets of sensors are allowed to transmit at fixed intervals. To account for the drift of the sensor crystal clock frequency, a drift with mean 1 and standard deviation of 0.0001 seconds are applied to all the sensors. Three different packet sizes were selected. They are 10 bytes, 20 bytes and 40 bytes with a fixed on-air data rate of 250 kbps. The contention windows are, therefore, 0.32 ms, 64 ms and 1.28 ms corresponding to the packet sizes of 10 bytes, 20 bytes and 40 bytes. A byte size of 10 will be sufficient as most of these sensors send humidity, temperature, on/off data etc. rather than multi-media data streams. Figure 18 shows the variation of the collision error with the number of sensors. The sets of sensors (25, 50, 75, and 100) are reporting to the base station at different rates. In this simulation, we have chosen arbitrary reporting rates of 1 sec, 9 secs, 19 secs, 59 secs, 111 secs in sets of 10 sensors.

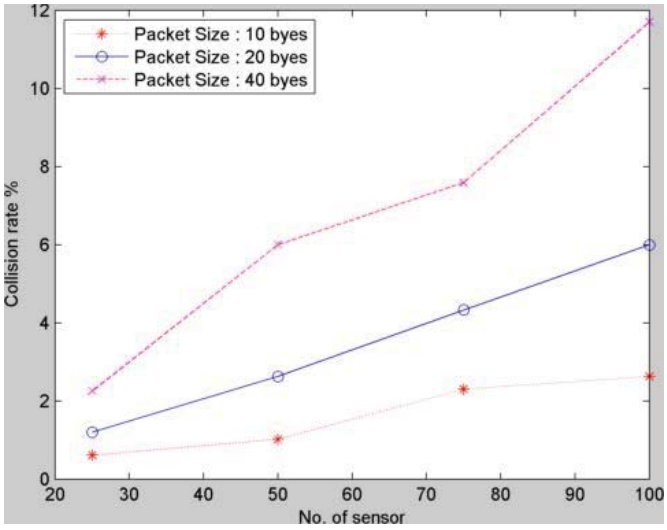


**Figure 18.** *Collision error increases with the number of sensor and also depends on the packet size*

As expected, the collision rate increases with the number of sensors. However, it also suggests that, packet losses due to collision also depend on the packet size. When the

sensors transmit humidity, temperature, on/off data, a small packet (10 -20 bytes) is enough to convey the information. Under this circumstance, the collision rate can be kept well under-checked (approximately 5%).

## 3.5 Discussion

This chapter has discussed about the performance parameters of the transmission protocols. In this thesis, extensive simulations followed by experiments have been conducted to evaluate and compare the performances of transmission protocols. Therefore it is important in the first place to validate the simulation and experimental results with the benchmark theoretical curves. In this thesis, the typical PSR vs. the $E_b/N_0$ curve has been used to validate the simulation and experimental setup. In simulation, the average $E_b/N_0$ values are calculated using the standard path loss model by varying the distance. The PSR values against each of these $E_b/N_0$ values are calculated using simulation. In practice, the position of the transmitter is changed to measure the PSR and the result is plotted against the average $E_b/N_0$ values. These $E_b/N_0$ values are derived using the Cost231 path-loss model and an approximation of the real values. The results show that the nature of the curves (from both simulation and experiments) is sigmoid in nature and matches closely with the theoretical one. In the next chapter, the same experimental setup is used with different retry delay values to find out if delay between retries has an impact on the energy efficiency.

# Chapter 4 Choice of retransmission delay in indoor wireless communication for enhanced energy efficiency

This chapter explores how the proper choice of delay values between retries in ARQ scheme for indoor low power wireless communication can cut down on the cost of total transmission. This in turn increases the lifetime of the battery powered wireless sensors. In an indoor wireless environment, the channel conditions change very slowly. The effect of block-fading has been discussed in chapter 2 that may lead to subsequent retries also failing, which adds to the total energy expenditure of transmission. The experiments have been performed inside a University building and nRF24L01p transceiver module has been used for measurement. The nRF24L01p module has a default range of retry delays. We have also used software delays to increase the range of delays. A retransmission penalty is added to the cost of transmission to account for the extended delay time. Results show that in a slowly changing channel, extended delay between retries can increase the battery lifetime by reducing the number of retries and therefore the average energy used per successful transmission. This delay analysis is only concerned about the behaviour of indoor radio channel and does not take into consideration of the random back-off delay to avoid packet collisions. This extended delay values were used for all subsequent experiments that compared the performance of the fixed power transmission, RSSI and non-RSSI approaches with S-APC.

The research focuses on losses due to multipath fading effect in indoor wireless and uncontrolled environment where packet losses due to other WLAN traffic has been avoided by selecting the RF channel away from the WLAN bands. It has included as much as realistic scenarios by collecting all the data during University busy hours.

## 4.1 Indoor radio channel with fading

The autocorrelation function of a fading radio channel provides some insight into the waiting or delay or buffering time that can be used to minimise the probability of high channel correlation. The term channel correlation defines the temporal similarity of the channel state. The autocorrelation function for an indoor fading radio channel is a sin(x)/x (sinc) function where x is the product of the maximum Doppler spread $F_d$ and delay ($T_d$) [95]. The autocorrelation expresses how significantly the channel has changed over a time delay ($T_d$) for a given $F_d$. A high correlation value indicates that channel state has not changed enough to make packet error rate independent in each time slot of transmission. Due to this bursty behaviour of the channel, errors tend to occur in blocks and the fading effect can persist through several packet transmissions.

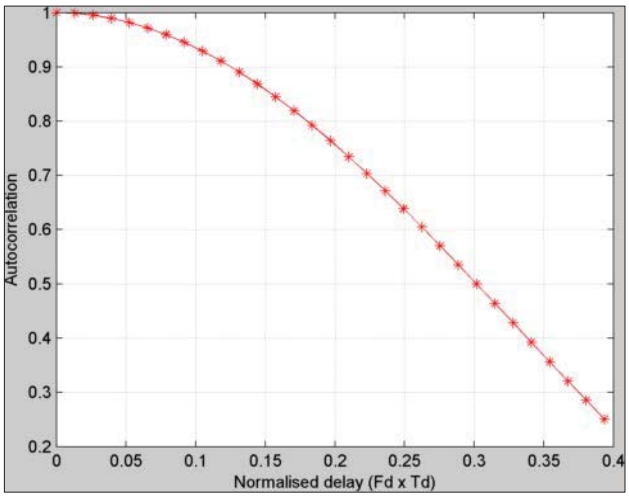


**Figure 19.** *Autocorrelation plot of indoor fading channel shows how significantly the channel has changed over a time delay (Td) for a given maximum Doppler spread (Fd). In order to avoid block fading effect, the autocorrelation value must be low. An autocorrelation value of 50% means that the normalised delay is around 0.3.*

Figure 19 shows the autocorrelation plot of indoor fading channel against the normalised delay. When the value along the x-axis increases, it indicates that for a given fading condition (assuming $F_d$ is constant), the delay between transmission of packets or bit interval increases. As indicated in chapter 2 page 47, the $F_d$ is inverse of the coherence time of the channel. Packets that are transmitted within the coherence time will be affected by fading and can be lost. However, if the delay between transmissions cab e increased, probability of correlation between channel states also decreases. Therefore, block fading effect can be reduced if packets are transmitted after a given delay so that consecutive packets are not affected.

## 4.2 Calculation of the delay between retries

In order to achieve an autocorrelation of less than or equal to 50%, the normalised delay will be around 0.3 (based on Figure 19). It is mentioned in section 2.2.4 of chapter 2 that the maximum Doppler spread ($F_d$) for indoor radio environment at 2.4 GHz can be around 20 Hz. Hence if the product of $F_d$ and delay ($T_d$) is 0.3, then

$$T_d = 15 \text{ ms}$$

## 4.3 Experimental design

In order to meet the requirement of low power wireless sensor and asymmetric link between the sensor and the hub, the nRF24L01p from Nordic semiconductor was chosen. It supports a single hop star topology. At the sensor side, an nRF24L01p module is used that consumes peak current of 11.3 mA at maximum output power of 0 dBm. At the hub, the nRF24L01p module has an additional power amplifier (PA) and a low noise amplifier

(LNA). The choice of the high power transmitter (with an additional LNA) at the hub end is made to make the link from the hub to the sensor practically error-free. This Nordic module at the hub has the added features that are presented in Table 5 of chapter 3.

In general, a wireless transceiver has different modes of operation. They are mainly divided into active transmit mode, active receive mode, standby modes, sleep mode etc. In between retries, a transceiver module usually go to a standby mode without shutting down its transmitter units. The transceiver module used in the experiment also has different modes of operations. The details of the modes and their current ratings are presented in Table 7 of chapter 3.

In normal operation where error correction requires retransmission of lost packets, the transmitter goes to standby-II mode until the automatic retry delay elapses and then retransmits. In case the packet transmission cycle is over (either due to successful transmission or the maximum number of allowed retries has elapsed) it goes to standby-I mode and wait for a new packet to be transmitted. Figure 10 of the nRF24L01p product specification manual has been redrawn in Figure 20 which shows the whole operation of transmission when the nRF24L01p module is in primary transmission mode. The time to waits for the retry is limited by the hardware and has a maximum value of 4 ms. As discussed in section 4.1, this delay value may not be enough, on average, for the channel to change in a slow fading channel. Using software control, the delay value can be extended.

All the software programming was done in C in the open-source Arduino (version 1.0.5-r2) software (IDE) [96]. The programs or sketches in Arduino are used to interface with the nRF24L01p modules and the sensors to do the necessary changes.

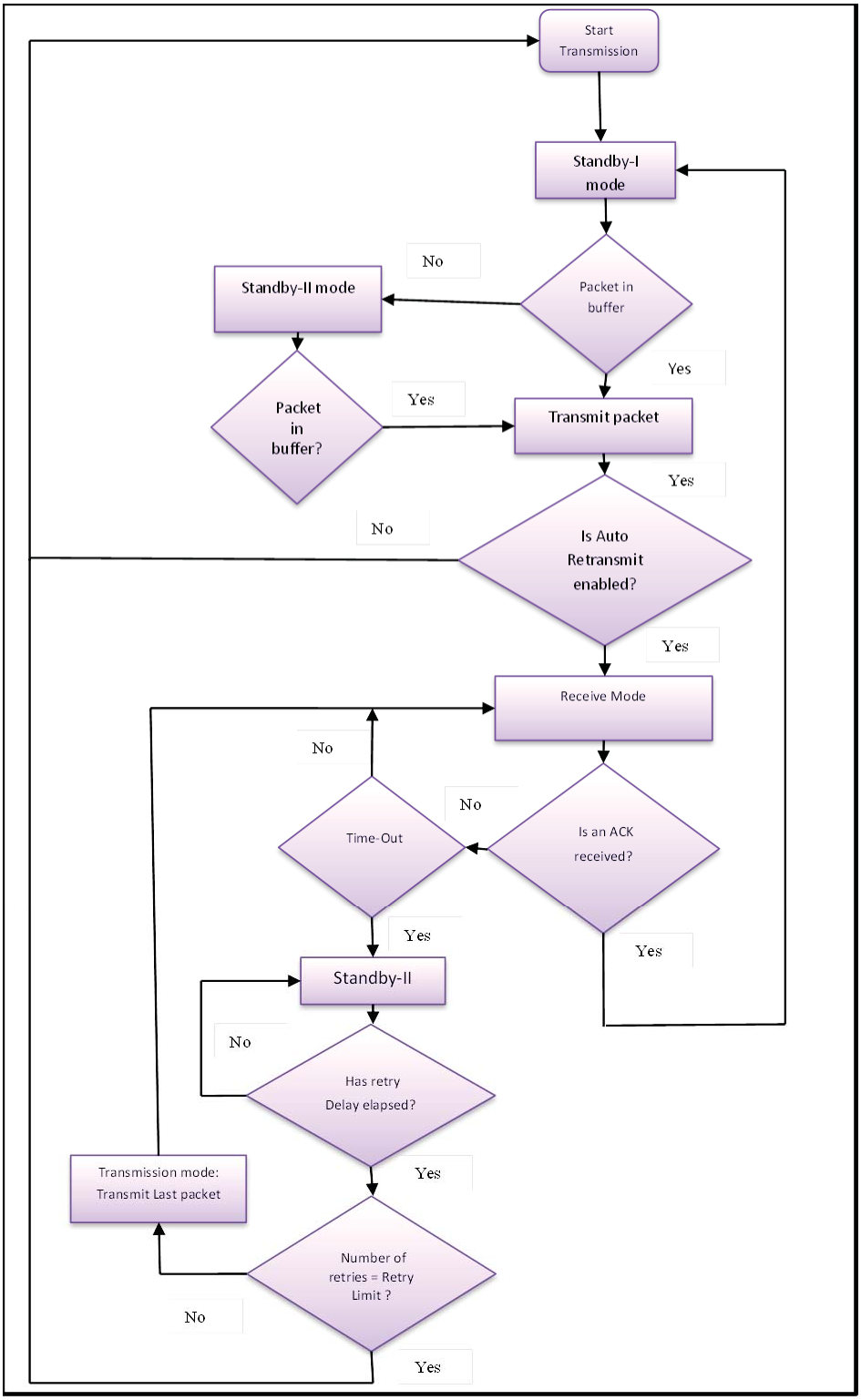


**Figure 20**. *Transmission operation cycle when the nRF24L01p module is in primary transmission mode* [39].

## 4.4 Visualization of the current consumption of the Nordic transceiver

As discussed in Section 4.3 of this chapter, the ARQ protocol can be enabled in the Nordic chip which takes care of the error correction process. After each transmission, it waits for the acknowledgement for a specific period of time. If no acknowledgement is received, it goes to standby mode II and waits for a fixed period of time before transmitting the same packet.

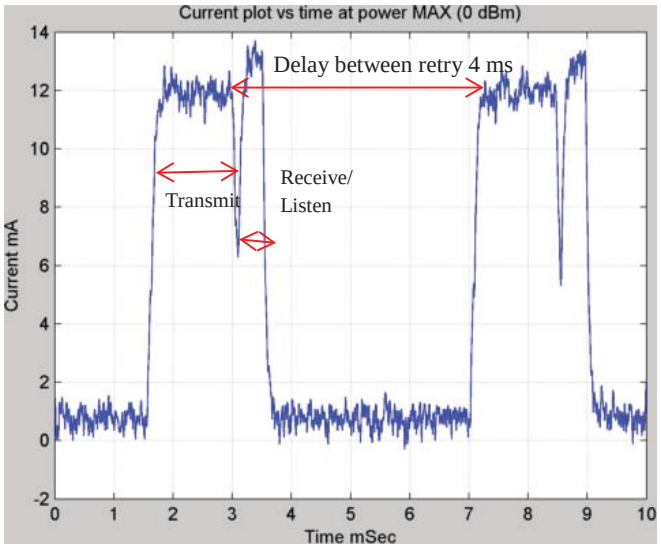


**Figure 21.** *The transmit mode curve showing the current consumption during transmission, reception of acknowledgement and retry delay when maximum hardware delay of 4 ms is applied. The average current consumption in between retries is 0.320 mA (standby-II mode current).*

Figure 21 shows the current (mA) plot vs. time (ms) of nRF24L01p when the transmitter is transmitting at output power of 0 dBm, the auto acknowledgement is enabled and the delay between retries are set at 4 ms. When auto acknowledgement is enabled, the transmitter switches to receive mode once the packet is transmitted to receive the acknowledgement packet. In Figure 22, a software delay of 15 ms over 4 ms is applied and the transmitter goes to standby mode I between retries. The plots of figures 21 and 22 are drawn from the measured values that are collected using an oscilloscope.

It can be noticed from figures 21 and 22 that there is a difference in the current consumption during the retry delay time although due to very small values of the current in original scale the difference may not be obvious. These current values correspond to the current values of standby II and standby I modes in Table 7. These current ratings are taken into account when the energy efficiency performances are compared in the next section.

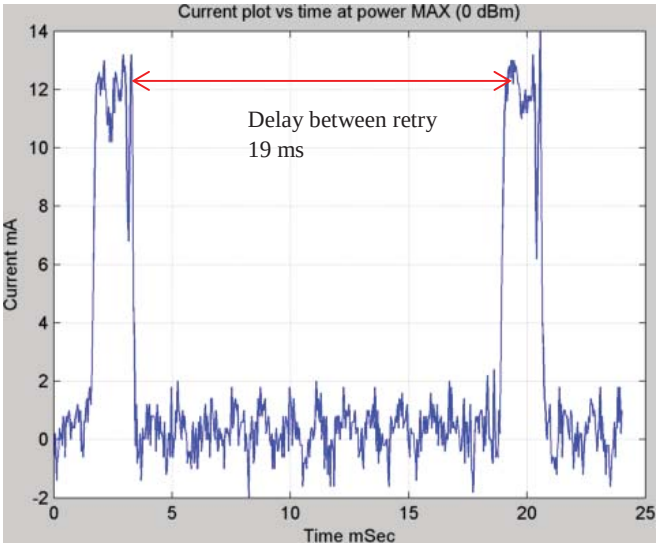


**Figure 22.** *The transmit mode curve showing the current consumption during transmission, reception of acknowledgement and retry delay when the hardware delay is overwritten by software delay of 15 ms+ 4 ms. The average current consumption in between retries is 0.026 mA (standby-I mode current).*

## 4.5 Experimental scenario

The experiments were performed inside the University campus building in an indoor setup with the transmitter and the receiver being placed at different distances from each other. The different scenarios are selected based on the distance and the number of partitions or walls. All the data were collected during the busy hours of the University where it can be expected to exhibit fading affect with Maximum Doppler spread of 20 Hz due to people moving in the environment. In this thesis, experimental results from 5 different scenarios are presented and analysed. These scenarios are selected based on the distance between the transmitter and receiver and the number of partitions in between them. They are presented in the results sections. The performance parameters are explained in the next section.

## 4.6 Experimental setup

In order to calculate the packet success rate, the average number of retries and the cost per successful transmission in the four different power levels and with four different delay values, in total 16 data packets are sent at each transmission instant. The number of retries in each of these cases is set at 3. The numbers of data samples that are collected per experiment are between 4000 and 5000.

## 4.7 Results

The theoretical calculations in section 4.2 show that a delay of 15 ms or more can achieve an autocorrelation of less than or equal to 50%. For exhaustive analysis, four sets of delay values are considered. They are classified as

- Hardware delays of 750 µs and 4 ms
- Software managed delays of 15 ms and 30 ms (over the maximum hardware delay of 4 ms)

As mentioned earlier, the cost calculation is based on equation (7) in chapter 3. Therefore, hardware and a software delay incur additional costs that are dependent on the delay value and the standby mode current values. The wall type I accounts for 3.4 dB signal loss per wall, while the wall type II accounts for 6.9 dB loss per wall. These wall types are mentioned in the Cost231 path loss model for indoor operations above 900 MHz [76] [97]. This model takes into account the losses due to two different types of walls within a building and between floors. Therefore, the inclusion of wall types may give rough approximation of the amount of attenuation that signals will suffer. The sample indoor radio propagation environments are presented in pictorial form in the appendix B.1 of the thesis.

### 4.7.1 Result Set I

| Distance between the sensor and the Hub | Number of Wall type I: Light internal walls | Number of Wall type II: internal walls |
|---|---|---|
| 30 m | 1 | 0 |

**Distance = 30 m. Transmit Power = -12 dBm**

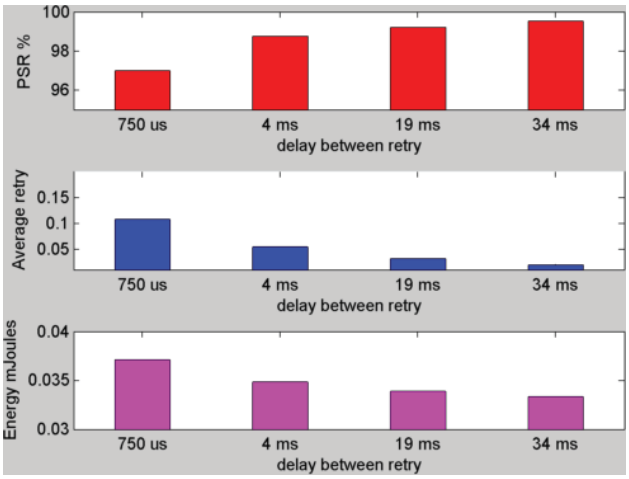

**Figure 23. Distance = 30 meters. Transmit Power = -12 dBm:** *Comparison of packet success rate (PSR), average number of retries and energy used per successful transmission with 1 partition in between the transmitter and the hub (receiver). The software delay has reduced the average number of retries significantly by 63%. The corresponding reduction in cost due to software delay is around just around 4.3 %. This small difference in costs is due to marginal difference of the PSR value of both types of delays. The average number of retries values and energy expenditures when software delays of 19 ms and 34 ms are used are almost same.*

## Distance = 30 m. Transmit Power = -6 dBm

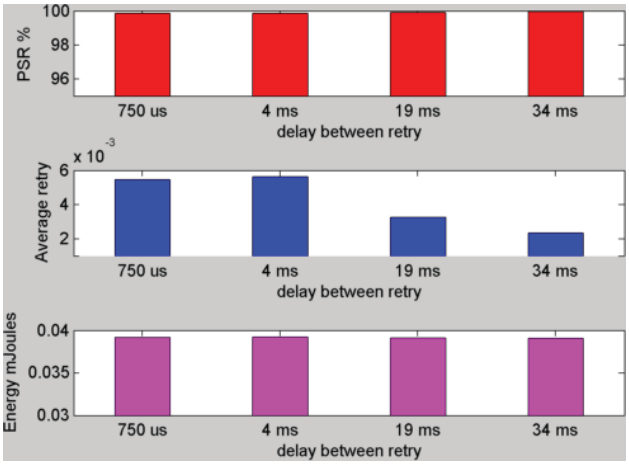


**Figure 24. Distance = 30 m. Transmit Power = -6 dBm.** *Comparison of packet success rate (PSR), average number of retries and energy used per successful transmission with 1 partition in between the transmitter and the hub (receiver). The software delay (19 ms) has reduced the average number of retries by 58% which is significant. The cost difference is however negligible. This is because the PSR of both types of delays are practically the same. The average number of retries values and energy expenditures when software delays of 19 ms and 34 ms are used are approximately equal.*

## Distance = 30 m. Transmit Power = 0 dBm

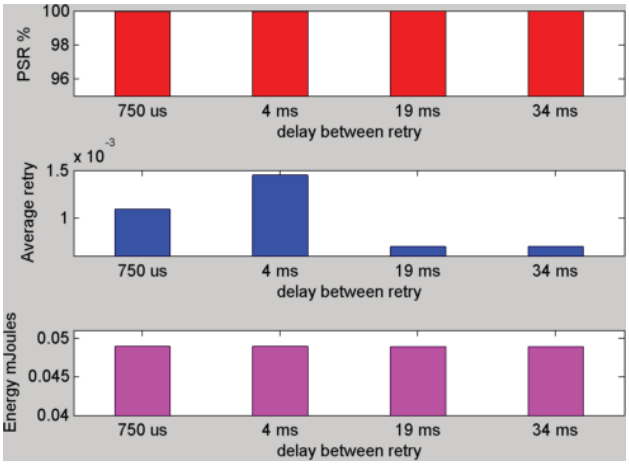


**Figure 25. Distance = 30 m. Transmit Power = 0 dBm.** *Comparison of packet success rate (PSR), average number of retries and energy used per successful transmission with 1 partition in between the transmitter and the hub (receiver). Practically there is no difference in the PSR, average retry and cost values.*

Figures 23 to 25 have compared the PSR, average number of retries and the energy used per successful transmission of three power levels (0 dBm, -6 dBm, -12 dBm) when four

sets of delay between retry values are used. No packets were received successfully at output power level -18 dBm and therefore no results are available. It can be observed from figures 23-25 that when the PSR values of software and hardware delays are comparable and around 100%, the difference in the energy consumption per successful transmission is negligible. The high difference in the average retries values (63% and 58 %) in figures 23 and 24 also could not make tangible reduction in cost as transmission cost is still significantly larger than the waiting time costs.

### 4.7.2 Result set II

| Distance between the sensor and the Hub | Number of Wall type I: Light internal walls | Number of Wall type II: internal walls |
|---|---|---|
| 16 m | 4 | 0 |

Figure 26 shows that the software delay has reduced the average number of retries significantly by 86%. The reduction in cost is around 10%. There is no large change in the cost from software delays of 19 ms to 34 ms.

**Distance = 16 m. Transmit Power = -12 dBm**

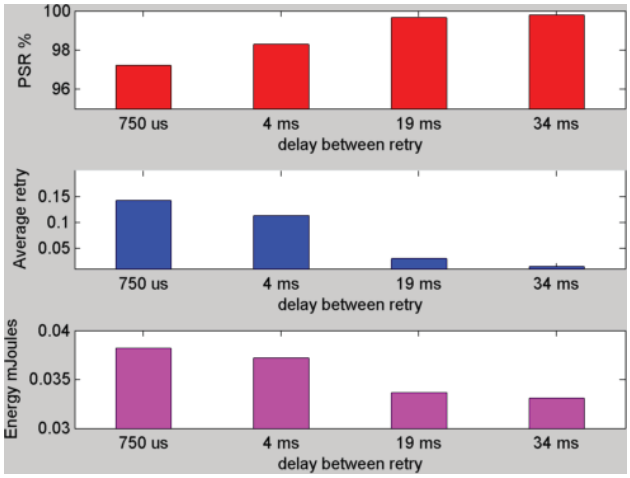


**Figure 26. Distance = 16 m. Transmit Power = -12 dBm** *Comparison of packet success rate (PSR), average number of retries and energy used per successful transmission with 4 partitions in between the transmitter and the hub (receiver). The software delay has reduced the average number of retries significantly by 86%. The reduction in cost is around 10%. There is no large change in the cost from software delays of 19 ms to 34 ms.*

No packets were received successfully at output power level -18 dBm and therefore no results are available. From figure 26-28 it can be observed that the use of software delay has significantly reduced the average number of retries. The % reduction has gone from 86 to 100 from transmission at -12 dBm to 0 dBm. Since the PSR values of hardware and software delays in each of these cases are almost comparable, the reduction in energy cost is not large.

### Distance = 16 m. Transmit Power = -6 dBm

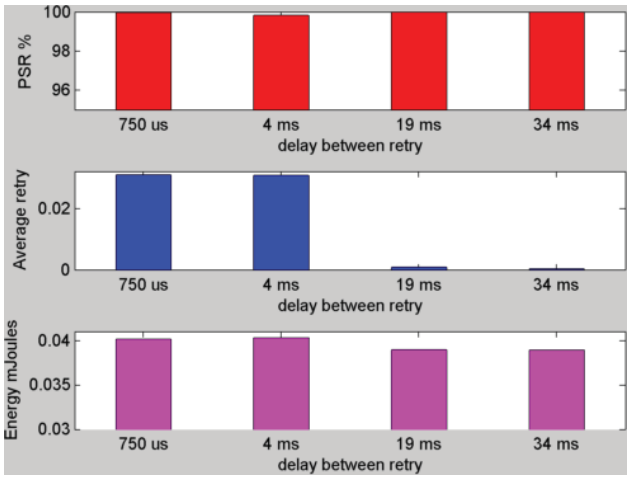


**Figure 27. Distance = 16 m. Transmit Power = -6 dBm** *Comparison of packet success rate (PSR), average number of retries and energy used per successful transmission with 4 partitions in between the transmitter and the hub (receiver). The software delay has reduced the average number of retries significantly by 98%. The reduction in cost is around 3% with no noticeable difference in the costs due to software delays.*

### Distance = 16 m. Transmit Power = 0 dBm

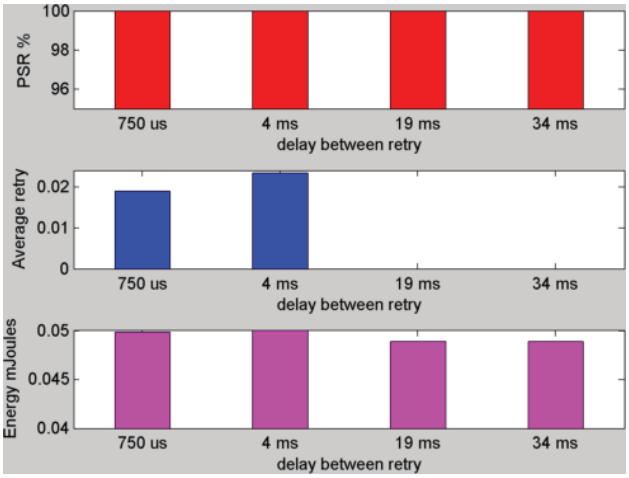


**Figure 28. Distance = 16 m. Transmit Power = 0 dBm** *Comparison of packet success rate (PSR), average number of retries and energy used per successful transmission at distance of 16 m between the transmitter and the receiver and 4 partitions in between them at output power of 0 dBm. The software delay has practically removed the need of retries. The reduction in cost is around just around 2.5 %. The average costs due to software delays are the same.*

### 4.7.3 Result set III

| Distance between the sensor and the Hub | Number of Wall type I: Light internal walls | Number of Wall type II: internal walls |
|---|---|---|
| 14 m | 5 | 0 |

**Distance = 14 m. Transmit Power = -12 dBm**

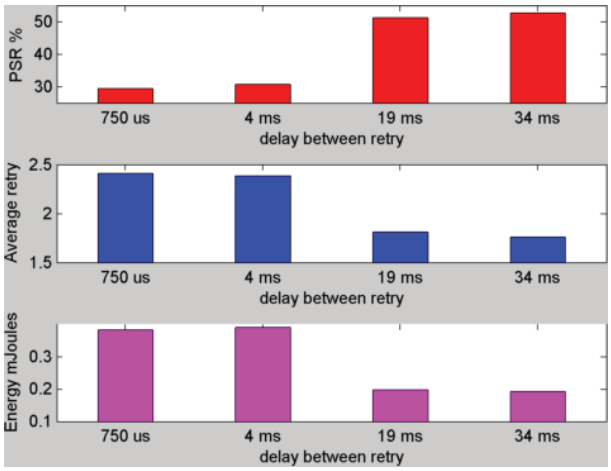


**Figure 29. Distance = 14 m. Transmit Power = -12dBm.** *Comparison of packet success rate (PSR), average number of retries and energy used per successful transmission with 4 partitions in between the transmitter and the hub (receiver). The software delay has reduced the average number of retries by 26%. The reduction in cost due to introducing a software delay is approximately 54 %. This huge difference in costs is due to a 50% rise in the PSR when software delay is used. Marginal differences are observed in the average number of retries values and energy expenditures when software delays of 19 ms and 34 ms are used.*

Results of Figure 29 demonstrate that a significant reduction of cost (54%) can be achieved when the difference in PSR due to software delay is high (~50%). In addition to that, the reduction in the number of retries by 26% has also contributed to the energy efficiency.

**Distance = 14 m. Transmit Power = -6 dBm**

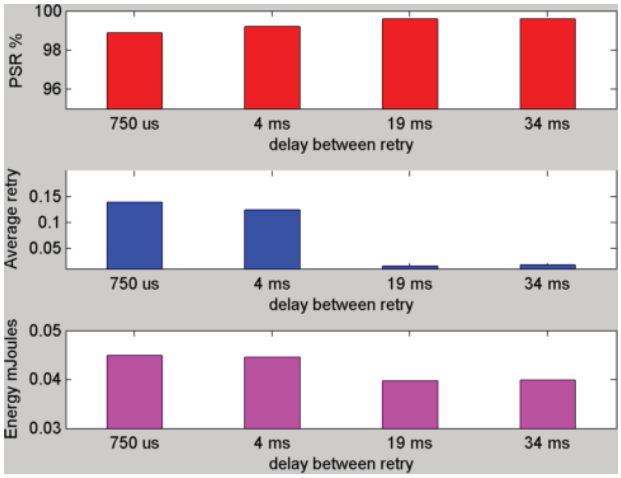


**Figure 30. Distance = 14 m. Transmit Power = -6 dBm.** *Comparison of packet success rate (PSR), average number of retries and energy used per successful transmission with 4 partitions in between the transmitter and the hub (receiver). The software delay has reduced the average number of retries significantly by 87%. The reduction in cost due to software delay is approximately 10 %. This small difference in costs is due to marginal change in PSR (~99-100%). In terms of average number of retries values and energy expenditures, there is no significant difference between delays of 19 ms and 34 ms.*

**Distance = 14 m. Transmit Power = 0 dBm**

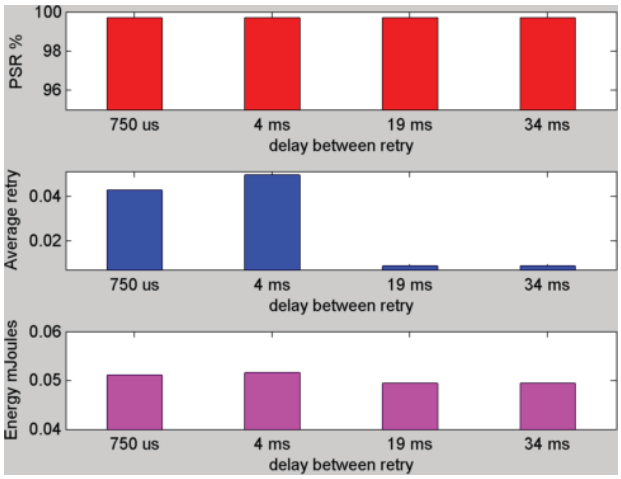


**Figure 31. Distance = 14 m. Transmit Power = 0 dBm.** *Comparison of packet success rate (PSR), average number of retries and energy used per successful transmission with 4 partitions in between the transmitter and the hub (receiver). The software delay has reduced the average number of retries significantly by 79%. The reduction in cost due to software delay is around 3 %. This small difference in costs is due to comparable PSR value of both types of delays. The average number of retries values and energy expenditures when software delays of 19 ms and 34 ms are used are same.*

Figures 29 to 31 have compared the PSR, average number of retries and the energy used per successful transmission of three power levels (0 dBm, -6 dBm, -12 dBm) for different delay values between retries and the transmission distance is 14 m across 4 partitions. No packets were received successfully at output power level -18 dBm and therefore no results are available. As discussed during the analysis of the results of set I, the high difference in the average retry values (87% and 79% in Figure 30 and Figure 31) also could not make marginal improvement in costs (10% and 3% respectively at -6 dBm and 0 dBm) because of comparable PSR values in each of the cases.

Comparing the result of **set I** with **II**, it can be observed that increasing the number of partitions have increased the packet loss rate (PSR) and therefore the average number of retries per transmission.

### 4.7.4 Result set IV

| Distance between the sensor and the Hub | Number of Wall type I: Light internal walls | Number of Wall type II: internal walls |
|---|---|---|
| 24 m | 5 | 0 |

**Distance = 24 m. Transmit Power = -6 dBm**

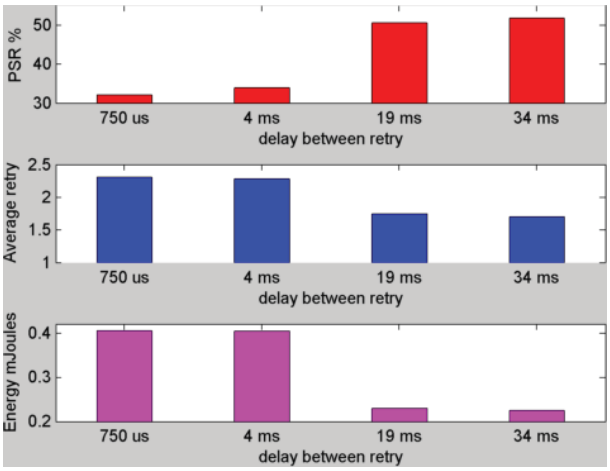


**Figure 32. Distance = 24 m. Transmit Power = -6 dBm** *Comparison of packet success rate (PSR), average number of retries and energy used per successful transmission with 5 partitions in between the transmitter and the hub (receiver).There is a huge jump in the PSR from ~30% (hardware) to ~50% (software). The software delay has reduced the average number of retries by ~25%. The reduction in cost is around 47 %. Very small differences are observed in the average number of retries values and energy expenditures when software delays of 19 ms and 34 ms are used.*

Figure 32 shows that there is a huge jump in the PSR from ~30% (hardware) to ~50% (software). The software delay has reduced the average number of retries by ~25%. The reduction in cost is around 47 %. Very small differences are observed in the average number of retries values and energy expenditures when software delays of 19 ms and 34 ms are used. Figure 33 shows that software delay has reduced the average number of retries by more than 50%. The reduction in cost is 28 %.

**Distance =24 m. Transmit Power = 0 dBm**

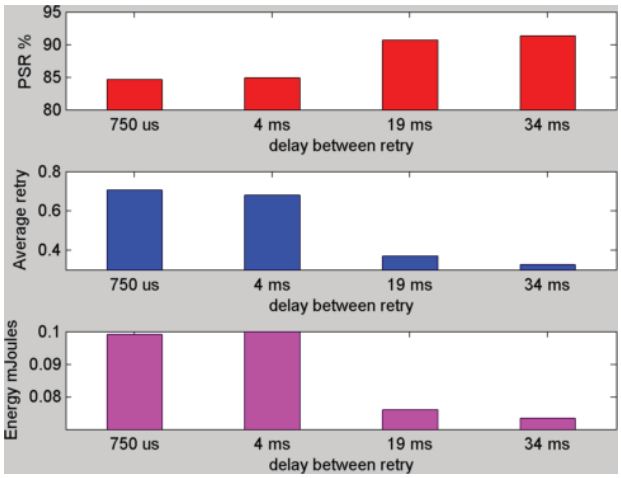


**Figure 33. Distance = 24 m. Transmit Power = 0 dBm** *Comparison of packet success rate (PSR), average number of retries and energy used per successful transmission with 5 partitions in between the transmitter and the hub (receiver). The software delay has reduced the average number of retries by more than 50%. The reduction in cost is around just around 28 %. Marginal differences are observed in the average number of retries values and energy expenditures when software delays of 19 ms and 34 ms are used.*

### 4.7.5 Result set V

| Distance between the sensor and the Hub | Number of Wall type I: Light internal walls | Number of Wall type II: internal walls |
|---|---|---|
| 20 m | 2 | 2 |

**Distance = 20 m. Transmit Power = -6 dBm**

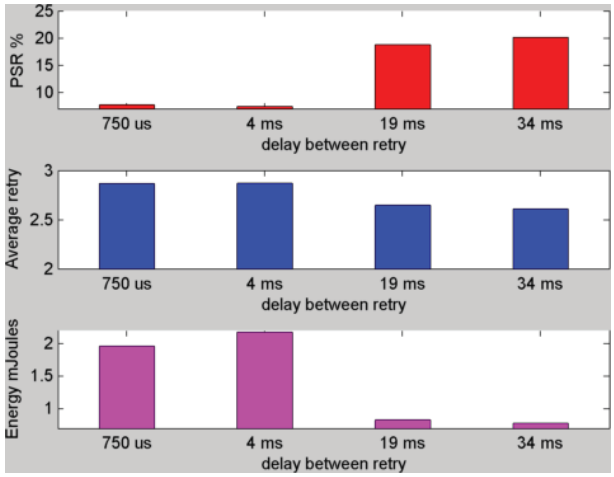


**Figure 34. Distance = 20 m. Transmit Power = -6 dBm** *Comparison of packet success rate (PSR), average number of retries and energy used per successful transmission with 4 partitions in between the transmitter and the hub (receiver). The software delay has reduced the average number of retries by 9%. The significant reduction in cost due to software delay is due to the PSR value getting doubled when software delays are used. The average number of retries values and energy expenditures when software delays of 19 ms and 34 ms are used are practically equal.*

**Distance = 20 m. Transmit Power = 0 dBm**

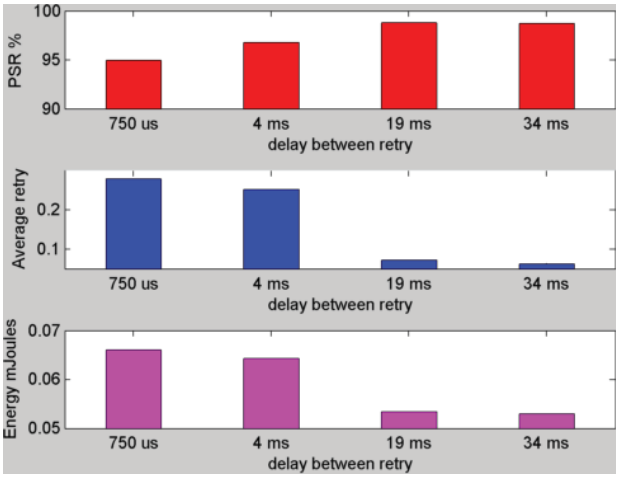


**Figure 35. Distance = 20 m. Transmit Power = 0 dBm** *Comparison of packet success rate (PSR), average number of retries and energy used per successful transmission with 4 partitions in between the transmitter and the hub (receiver). The software delay has reduced the average number of retries by 75%. The reduction in cost due to software delay is 18% due to the small change in the PSR value. The average number of retries values and energy expenditures when software delays of 19 ms and 34 ms are used are practically equal.*

No packets were received successfully at output power level -18 dBm and -12 dBm.

Therefore, no results are available. Figure 34 show that software delay has reduced the average number of retries by 9%. The significant reduction in cost of approximately 200% due to software delay is because of the PSR value getting more than doubled from 8% (at 4 ms hardware delay) to 18% (at 19 ms software delay). The average number of retries values and energy expenditures when software delays of 19 ms and 34 ms are used are practically equal. In figure 35, the software delay (19 ms) has reduced the average number of retries by 75%. The reduction in cost due to software delay is 18% due to the small change in the PSR value from the hardware delay and the software introduced delay.

Overall, it can be observed from figures 23 to 35 that the use of higher delay reduces the average number of retries and increases the over-all PSR. Even when the channel condition is good in terms of high $E_b/N_0$, the use of higher delay between retries reduces the average cost of successful transmission. It is also observed that increasing the delay between retries above 19 ms does not improve the PSR, the cost and the average number of retries as it is limited by the coherence time of the fading channel. Also, long delays are undesirable as this increases the current consumption while waiting. This is because after very high delays, the fading channel changes completely and behaves independently of the current channel state. Table 9 has tabulated the PSR, average number of retries and the average cost per successful transmission based on the data collected.

**Table 9 Tabulated PSR, cost and average retries at different distances and partitions in between**

| **Distance = 30 meters** | | | | |
|---|---|---|---|---|
| **Number of Walls (Type I) between transmitter and receiver = 1** | | | | |
| **Power levels** | **Delay between retries (ms)** | **PSR (%)** | **Avg. cost per successful transmission (mJ)** | **Average number of retries** |
| -12 dBm | 0.75 | 97 | 0.0371 | 0.108 |
| -12 dBm | 4 | 98.76 | 0.0349 | 0.0545 |
| -12 dBm | 19 | 99.21 | 0.0338 | 0.0320 |
| -12 dBm | 34 | 99.53 | 0.0333 | 0.0200 |
| -6 dBm | 0.75 | 99.95 | 0.0392 | 0.00545 |
| -6 dBm | 4 | 99.82 | 0.0392 | 0.00563 |
| -6 dBm | 19 | 100 | 0.0391 | 0.00327 |
| -6 dBm | 34 | 100 | 0.0390 | 0.00236 |
| 0 dBm | 0.75 | 100 | 0.0489 | 0.00109 |
| 0 dBm | 4 | 100 | 0.0489 | 0.00145 |
| 0 dBm | 19 | 100 | 0.0489 | 0.00070 |
| 0 dBm | 34 | 100 | 0.0489 | 0.00070 |

| **Distance = 14 meters** | | | | |
|---|---|---|---|---|
| **Number of Walls (Type I) between transmitter and receiver = 5** | | | | |
| **Power levels** | **Delay between retries (ms)** | **PSR (%)** | **Avg. cost per successful transmission (mJ)** | **Average number of retries** |
| -12 dBm | 0.75 | 29.47 | 0.38164 | 2.410 |
| -12 dBm | 4 | 30.76 | 0.38962 | 2.386 |
| -12 dBm | 19 | 51.20 | 0.18269 | 1.813 |
| -12 dBm | 34 | 52.62 | 0.17868 | 1.760 |
| -6 dBm | 0.75 | 98.88 | 0.04492 | 0.1388 |
| -6 dBm | 4 | 99.2 | 0.04461 | 0.1240 |
| -6 dBm | 19 | 99.58 | 0.03971 | 0.0159 |
| -6 dBm | 34 | 99.58 | 0.03982 | 0.0179 |
| 0 dBm | 0.75 | 99.70 | 0.05112 | 0.0426 |
| 0 dBm | 4 | 99.70 | 0.05163 | 0.0494 |
| 0 dBm | 19 | 99.70 | 0.04944 | 0.0088 |
| 0 dBm | 34 | 99.70 | 0.04945 | 0.0088 |
| **Distance = 16 meters** | | | | |
| **Number of Walls (Type I) between transmitter and receiver = 4** | | | | |
| -12 dBm | 0.75 | 97.21 | 0.03821 | 0.1421 |
| -12 dBm | 4 | 98.29 | 0.03720 | 0.1131 |
| -12 dBm | 19 | 99.65 | 0.03355 | 0.0300 |
| -12 dBm | 34 | 99.78 | 0.03302 | 0.0150 |
| -6 dBm | 0.75 | 99.95 | 0.04015 | 0.0309 |
| -6 dBm | 4 | 99.82 | 0.04030 | 0.0307 |
| -6 dBm | 19 | 100 | 0.03894 | 0.0009 |
| -6 dBm | 34 | 100 | 0.03892 | 0.0004 |
| 0 dBm | 0.75 | 100 | 0.04979 | 0.0190 |
| 0 dBm | 4 | 100 | 0.05009 | 0.0234 |
| 0 dBm | 19 | 100 | 0.04885 | 0 |
| 0 dBm | 34 | 100 | 0.04885 | 0 |

| **Distance = 24 meters** | | | | |
|---|---|---|---|---|
| **Number of Walls (Type I) between transmitter and receiver = 5** | | | | |
| **Power levels** | **Delay between retries (ms)** | **PSR (%)** | **Avg. cost per successful transmission (mJ)** | **Average number of retries** |
| -6 dBm | 0.75 | 32.18 | 0.40526 | 2.305 |
| -6 dBm | 4 | 33.96 | 0.40427 | 2.281 |
| -6 dBm | 19 | 50.53 | 0.21600 | 1.748 |
| -6 dBm | 34 | 51.78 | 0.21165 | 1.704 |
| 0 dBm | 0.75 | 84.63 | 0.09909 | 0.705 |
| 0 dBm | 4 | 84.93 | 0.10003 | 0.680 |
| 0 dBm | 19 | 90.68 | 0.07440 | 0.372 |
| 0 dBm | 34 | 91.34 | 0.07195 | 0.328 |
| **Distance = 20 meters** | | | | |
| **Number of Walls (Type I) between transmitter and receiver = 2**<br>**Number of Walls (Type II) between transmitter and receiver = 2** | | | | |
| -6 dBm | 0.75 | 7.78 | 1.96201 | 2.865 |
| -6 dBm | 4 | 7.48 | 2.17504 | 2.870 |
| -6 dBm | 19 | 18.78 | 0.77348 | 2.646 |
| -6 dBm | 34 | 20.15 | 0.73038 | 2.610 |
| 0 dBm | 0.75 | 94.96 | 0.06603 | 0.279 |
| 0 dBm | 4 | 96.78 | 0.06430 | 0.252 |
| 0 dBm | 19 | 98.78 | 0.05314 | 0.073 |
| 0 dBm | 34 | 98.727 | 0.05278 | 0.063 |

## 4.8 Analytical understanding of the relationship between average cost of successful transmission and the average number of retries

The average energy consumption ($C_{avg}$) of a wireless sensor when N number of transmission is allowed can be mathematically represented by equation (18) [98].

$$C_{avg} = C_P * (1 + PER + PER^2 + PER^3 + \cdots + PER^{N-1}) + C_{RD} * (PER + PER^2 + PER^3 + \cdots + PER^{N-1}) \quad (18)$$

Where

$C_{avg}$ = average energy consumption (mJ)
$C_p$ = transmission energy cost per transmission of packet (mJ)
$C_{RD}$ = Retransmission delay cost (mJ)
$PER$ = Packet error rate for individual transmission

Equation (18) can be simplified as

$$C_{avg} = = \ C_P * \left(\frac{1 - \ PER^N}{1 - PER}\right) + \ C_{RD} * (\frac{1 - \ PER^N}{1 - PER} - 1) \tag{19}$$

If the PER are assumed to be independent during each transmission, then substituting $PSR = 1\text{-}\ PER^N$ in Equation (19)

$$C_{avg} = = \ C_P * \left(\frac{PSR}{1 - PER}\right) + \ C_{RD} * (\frac{PSR}{1 - PER} - 1) \tag{20}$$

Equation (20) represents the average energy consumption when a certain number of retries are allowed and in each retry the PER values are considered to be independent and uniformly distributed. In this thesis, the PSR is the packet success rate after 1, 2, 3 or 4 transmission. A comparison of $E_{TX}$ and $E_{RD}$ values from Nordic chip is presented in Table 10.

**Table 10. Comparison of Transmission Cost and Delay Cost At Different Power Levels**

| Transmission Power | Transmission cost ($E_{TX}$) mJ | Delay cost ($E_{RD}$) mJ |
|---|---|---|
| -18 dBm | 0.030261 | 0.0008 to 0.0042 |
| -12 dBm | 0.032422 | 0.0008 to 0.0042 |
| -6 dBm | 0.038907 | 0.0008 to 0.0042 |
| 0 dBm | 0.048849 | 0.0008 to 0.0042 |

It can be observed from the table that $E_{TX} >> E_{RD}$ (~10 to 40 times higher). Therefore if $E_{RD}$ is ignored, then equation (20) can be rewritten as

$$C_{avg} = = \ C_P * \left(\frac{PSR}{1 - PER}\right) \tag{21}$$

Hence, the average energy consumption of a successful transmission is represented by equation

$$C_{S\_avg} = \ C_P * \left(\frac{1}{1 - PER}\right) \tag{22}$$

All cost or energy consumption units are in mJ.

The energy consumption values from experimental data at different power level are compared with the analytical cost values in equation (22). For the plot in Figure 36, experimentally obtained energy consumption per successful transmission values corresponding to the 19 ms delay have been used.

### 4.8.1 Validation of the mathematical model of energy consumption with the measured data

Figure 36 shows the plots of the energy consumption per successful transmission values of calculated ( from equation (22)) and experimentally obtained data. A data correlation value of 0.9998 strongly validates the mathematical model.

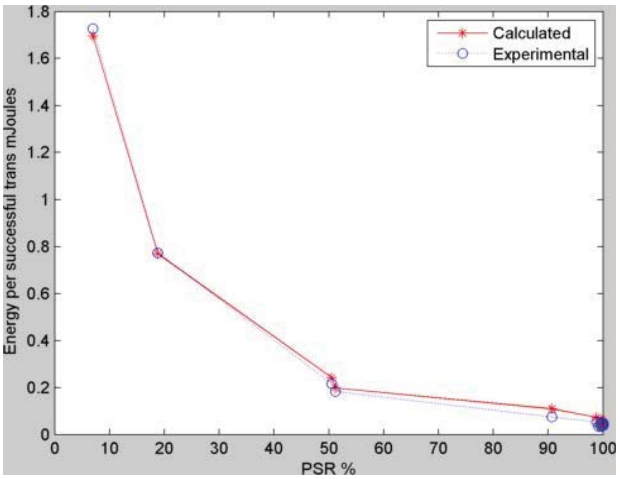


**Figure 36.** *The **energy cost per successful transmission** of the calculated and measured data is plotted against the PSR. A high correlation of 0.9998 validates the mathematical model. The measured or the experimental values correspond to the software delay between retry of 19 ms when packets are assumed to be independently affected by fading channel condition.*

Even when the energy consumption values at low hardware delay of 0.75 ms and 4 ms are compared, the correlation between the experimental values and analytical values are high.

The plots in Figure 36 also suggest that when the PSR values are quite high (~99%), the difference in the energy per successful transmission values due to different delay between retries are almost negligible. This can be observed in the plots of figure 25, figure 30, figure 31 and figures 26-28 that the average reduction of energy consumption per successful transmission is approximately 10%.

However when the PSR values are in the lower range (30% to 90%), the energy savings due to higher delay between retry values can be as high as 50%. This is due to steeper change in the energy consumption values as indicated by the plots of Figure 36.

## 4.9 Other low power wireless transceivers

This section looks into the current rating of CC2420 from Texas Instruments which is considered as one of the most popular and widely used radio transceiver for low power wireless communication [38]. Table 11 shows the current ratings of output power levels and other modes of operation. CC2420 has total of 32 output power levels. Some of them are listed in Table 11.

It can be observed that similar to nRF24L01p, the difference in the current consumption during active transmit modes and idle modes are high. The ratio of the current consumptions in transmission modes and idle mode ranges between 20 and 40.

**Table 11. Operational Modes and Current Consumptions of CC2420**

| Operational mode | Current consumed mA |
|---|---|
| Transmission @ 0 dBm output power | 17.4 |
| Transmission @ -1 dBm output power | 16.5 |
| Transmission @ -3 dBm output power | 15.2 |
| Transmission @ -5 dBm output power | 13.9 |
| Transmission @ -7 dBm output power | 12.5 |
| Transmission @ -10 dBm output power | 11.2 |
| Transmission @ -15 dBm output power | 9.9 |
| Transmission @ -25 dBm output power | 8.5 |
| Reception/Listening | 19.7 |
| Power down mode | 0.02 |
| Idle mode | 0.426 |

Other low power wireless transceivers like the Si446X series from Silicon Lab also have similar current ratings in their different operational mode. The ratio of the current consumption in transmission mode and sleep mode is in the order of 20:1 [99].

## 4.10 Discussion

It can be observed from the experimental results that the proper choice of delay between retries can impact the overall energy efficiency and therefore the operating lifetime of a battery powered wireless sensor node working in an indoor radio environment. The contribution of energy reduction can range between 10% and 50% depending on the channel condition. This is primarily because of block-fading effect of slow fading channel that is typical of indoor radio environment. The proper choice of the delay between retry increases the probability of successful packet transmission and therefore reduces the number of retries. Coupled with this improvement in PSR, the overall energy expenditure per successful transmission can be significantly reduced over the long run.

# Chapter 5 S-APC protocol and comparison with fixed power transmission

The fundamental difference between the proposed power control protocol and the existing ones is that the current power control protocols use the RSSI information to evaluate the link quality and determine the next power level. The thesis presents a link layer communication protocol that uses both power control and the number of retransmissions to control errors and save energy. The idea is to ramp up power using the available power levels when the link quality gets poor in order to meet PSR requirement. At the same time, it looks for every opportunity to reduce the energy consumption by stepping down the transmission power level as and when the channel condition improves. In order to decide the power level at which the next packet transmission should start, the adaptive algorithm uses the power level of the most recent transmission at which the packet transmission was either successful or failed. At the same time, it is important to ramp down power when the present power level is considered more than enough for successful transmission. In order to make this transition, the adaptive algorithm counts the number of successes in the current power level. After each success, the probability of transiting to the lower power level is increased using an exponential drop-off algorithm. In this manner, these two components of the adaptive algorithm work in tandem.

## 5.1 Description of the adaptive protocol

The basis of this lightweight adaptive protocol is the states and is represented by a state transition diagram in Figure 37 [100] [101].

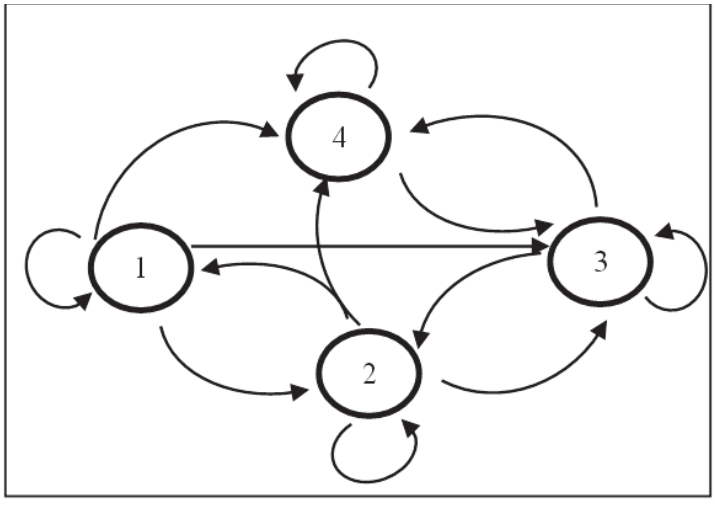


**Figure 37.** *State transition diagram of the adaptive algorithm.*

It is lightweight because it has few simple rules. In each state there are output power levels in increasing order which can be used by the transmitter. Table 12 shows the available power levels based in these states.

**Table 12. States, power levels and retry limits**

| State | 1 | 2 | 3 | 4 |
|---|---|---|---|---|
| **Available power levels** | Minimum (M) | | | |
| | Low (L) | Low (L) | | |
| | High (H) | High (H) | High (H) | |
| | Maximum (X) | Maximum (X) | Maximum (X) | Maximum (X) |
| Number of retries | 3 | 2 | 1 | 3 |

At any point of time during packet transmission, the transmitter is allowed to use only the available power levels in the current state. Transmission starts at the lowest available power level of that particular state. When all the power levels are exhausted in a given state, the process of a particular packet transmission is completed. State transition occurs depending on the power level at which the transmission is successful or failed. There are two separate algorithms that determine the state transitions, one from a lower state to higher state and the other from a higher to lower states. The logic to transit to lower states also includes situations when it remains in the same state or transit to a lower state.

The objective of S-APC is to respond to the packet error rate and move to a new state with different retry limits. The adaptive algorithm is designed in such a way that it takes into account the performance in each state. Each state has a different retry limit. Increasing state number indicates poorer channel quality. When the system is in state 4, it is considered the worst channel condition and three retries are allowed. The retry limit of state 1 is three. However, the retry limit of states 2 and 3 have been set at 2 and 1 respectively. The asymmetry is because the increase in the retry limit in states 2 and 3 can increase the current consumption while only marginally improving the packet success rate.

Table 13 describes the state transition matrix when state level goes up. All the state transition decisions take into account the success or failure of the packet being transmitted to the destination hub.

S-APC does not allow retransmissions in the same power level except for state 4 when the channel condition is considered worst and the transmitter is allowed to retry up-to 3 times to meet the PSR requirement. It also brings parity with the state 1 that is considered best channel condition where the transmitter is allowed to retry at consecutive higher power levels.

**Table 13. State transition matrix when state levels go up**

| | | Next State | | | |
|---|---|---|---|---|---|
| | | 1 (MLHX) | 2 (LHX) | 3 (HX) | 4 (X) |
| Current State | 1 (MLHX) | Succeed at level M | Succeed at level L | Succeed at level H | Failed or Succeed at level X |
| | 2 (LHX) | Not applicable | Not applicable | Succeed at level H | Failed or Succeed at level X |
| | 3 (HX) | No transition | Not applicable | Not applicable | Failed or Succeed at level X |
| | 4 (X) | No transition | No transition | Not applicable | Not applicable |

Table 14 describes the state transition logic when state level goes down. The primary objective of the adaptive protocol is to save energy by transmitting at a power level that is enough to send the packet through the channel.

**Table 14. State transition matrix when state levels go down**

| | | Next State | | | |
|---|---|---|---|---|---|
| | | 1 (MLHX) | 2 (LHX) | 3 (HX) | 4 (X) |
| Current State | 1 (MLHX) | Succeed at level M | Not applicable | Not applicable | Not applicable |
| | 2 (LHX) | Probabilistic model that depends on the number of successes in level L | Probabilistic model that depends on the number of successes in level L | Not applicable | Not applicable |
| | 3 (HX) | Not applicable | Probabilistic model that depends on the number of successes in level H | Probabilistic model that depends on the number of successes in level H | Not applicable |
| | 4 (X) | Not applicable | Not applicable | Probabilistic model that depends on the number of successes in level X | Probabilistic model that depends on the number of successes in level X |

For example, when the system is in state 4, it is transmitting at the maximum power. With time, the channel condition can improve and packet can be successfully transmitted at a lower power level. If the system drops down to state 3, the transmission starts at a

lower power level. This drop-off from a higher state to a lower state is determined by a drop-off algorithm which is probabilistic in nature.

In the proposed adaptive protocol, the drop-off or the back-off process is dependent on the number of successes (S) in the higher power level and a drop-off factor (R). By default, the drop-off factor is 1. The probability of the system to drop-off to a lower power level is represented by equation (23).

$$P_{drop-off} = 1 - e^{(-RS)} \tag{23}$$

Here,

$P_{drop\_off}$ = probability of drop-off
$S$ = the number of successes in that power level of the higher state
$R$ = drop-off factor

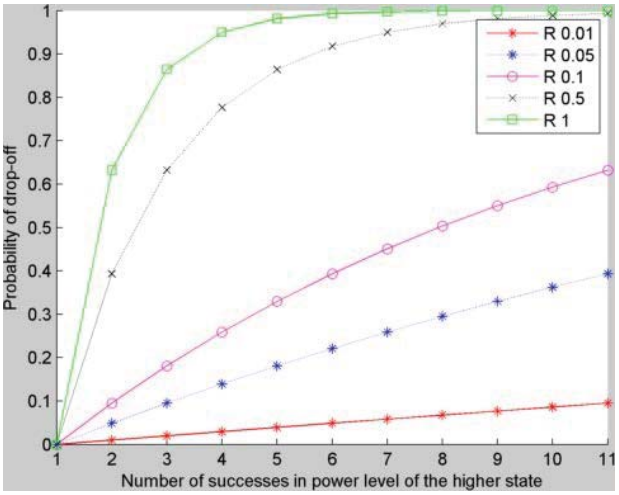


**Figure 38.** *The curves behave differently depending on the value of R. Low R value indicates slow back off while high R indicates fast back off. When the number of successes is 0, the probability of transition is 0. This drop-off algorithm takes into account of all the previous successes indicating that it uses memory information while dropping-off as well.*

Overall, the value of R indicates as to how fast the system will fall from a higher state to a lower state. When there is no success, the probability of state transition is 0. It means that there will be no state transition. When the number of successes increases, the probability converges to 1. The plots in Figure 38 show the state transition probability based on different values of R. When there is a state change, the value of S is reset to 0.

Back-off algorithms are extensively used in data communication (both wired and wireless) by MAC protocols to resolve contention among transmitting nodes to acquire channel access. In a MAC protocol, the back-off algorithm chooses a random value from the range [0, CW], where CW is the contention window size. The contention window is usually represented in terms of time slots.

The number of slot times to delay before the $n^{th}$ retransmission attempt is chosen as a uniformly distributed random integer r in the range $\mathbf{0 < r < 2^k}$
where
$k = \min(n, Max_r)$, $Max_r$ is the maximum number of retries allowed and depends on the type of application.

The $n^{th}$ retransmission attempt also means that there have been n collisions. For example, after the first collision, it has to retransmit. Based on the back-off algorithm, the sender will choose between 0 or 1 slot times for the retransmission. After the second collision, the senders will wait anywhere from 0 to 3 slot times (inclusive). After the third collision, the senders will wait anywhere from 0 to 7 slot times (inclusive), and so forth. As the number of retransmission attempts increases, the number of possibilities for delay increases exponentially [102] [103].

On the similar concept, an exponential operator is used in this thesis to decide to switch from a higher state to a lower state. The drop-off algorithm is dynamic as it re-evaluates at every successful transmission. It gets reset to 0 when it leaves the state and jumps to a lower state and starts a new packet transmission at a lower power level.

In each state there are output power levels in increasing order which can be used by the transmitter. There is no direct transition from state 4 to state 1 or 2. Direct state transition from 4 to 3 is only allowed. Similarly there is no direct transition from state 3 to state 1. The system can transit to state 2 from 3. The drop-off factor R determines as to how fast this transition will happen. In this thesis, R values of 0.01, 0.05, 0.1, 0.5 and 1 are used. Higher value of R means higher rate of drop-off or the system will switch to a lower state faster. When R is 1, the probability of switching to a lower state increases rapidly with the number of successes (from no probability of transition at single success to 90% probability after three successes in Figure 38). Whereas, when R is set at 0.01, the change in probability is slow. The probability of transition or switch changes from 0 to less than 5% after three successes.

The state based model is a general model and can be applied to any RF (radio frequency) platform. Depending on the number of available and configurable output power levels, the number of states and the number of retransmissions in each of the states will change.

The drop-off algorithm can also be designed based on

- Fixed probability for switching
- Fixed number of success counts for switching

## 5.2 Comparison of energy consumption: Fixed probability against exponential probability that takes into account the number of successes (S)

Figures 39 to 41 compare the energy consumptions when the average $E_b/N_0$s are 30 dB, 15 dB and 10 dB respectively. In these simulations using Matlab, the channel condition is varied by using different $E_b/N_0$ values (30 dB, 16 dB and 10 dB). The probability of staying in the higher state is set at 1, 0.75, 0.5 and 0.25.

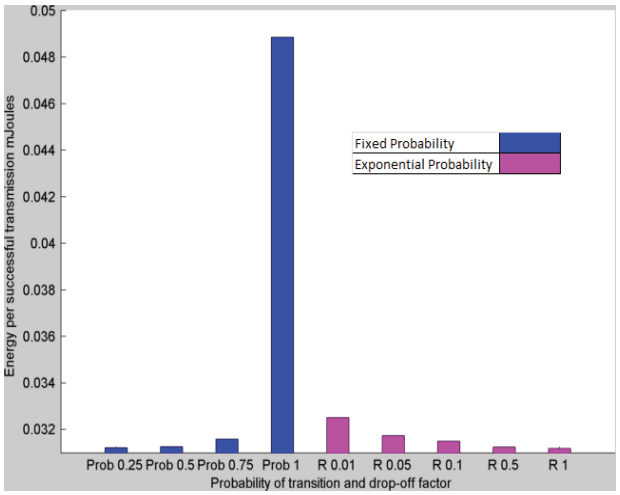


**Figure 39.** *At an average $E_b/N_0$ value of 30 dB, comparison shows that energy efficiency-wise, both fixed probability and exponential drop-off approaches are comparable.*

An average $E_b/N_0$ of 30 dB means that channel condition is good. A high fixed probability value implies that the state will switch to a lower state slowly even when the channel condition has turn to good. A fixed probability of 1 means that the system always stays in a higher state and never drops down. Therefore, a low fixed probability value will be more energy efficient because it can come back to a lower state rapidly. On the other hand, high R value indicates that drop-off will be fast (Figure 38). Therefore, the system will be more energy efficient when R = 1 as compared to when R = 0.01. The PSR and protocol efficiency values are comparable and therefore not included in this chapter.

When the channel link quality changes ($E_b/N_0$ < 20 dB), the nature of the curves start to change (Figure 40). At low $E_b/N_0$, fixed probability of 0.25 is no longer the most energy efficient option. In fact, the fixed probability = 0.75 can save more energy. Similarly, the energy consumption can be lowered when R = 0.01.

As channel link quality gets poorer ($E_b/N_0$ < 15 dB), minimum energy consumption starts to settle around fixed probability = 0.75 (Figure 41). At the same time, the value of R in exponential drop-off approach also hovers around 0.05 as the minimum energy consumption region. Interestingly, the nature of both the plots in figure 40 is unimodal with one minimum point. It implies that in order for the adaptive protocol to be efficient,

there has to be a balance between the system going up the states and falling down the states. Figures 40 and 41 also shows that the adaptive power control protocol with exponential drop-off rates is more energy efficient than fixed probability approach.
The PSR and efficiency values are comparable and therefore not included in this chapter.

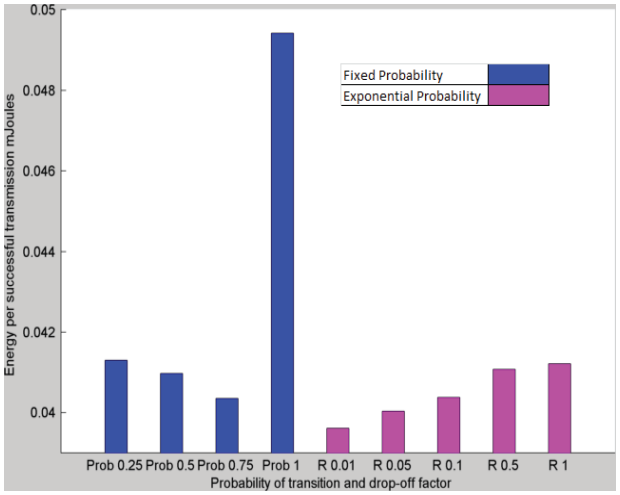


**Figure 40.** *At an average $E_b/N_0$ value of 15 dB, comparison shows that dynamic probability approach can be more energy efficient if proper choice of R value is made.*

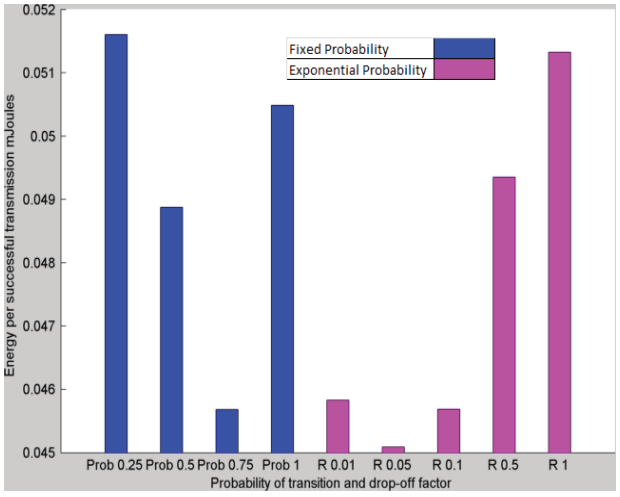


**Figure 41.** *At average $E_b/N_0$ of 10 dB, the channel condition/ link quality is poor. The more energy efficient option is to stay in higher power state which is achieved by a high fixed probability of 75% or at a slow back-off value of R 0.05.*

## 5.3 Comparison of energy consumption: Fixed count against exponential probability that takes into account the number of successes (S)

Figures 42-44 compare the energy consumptions when the average $E_b/N_0$s are 30 dB, 15 dB and 10 dB respectively. In fixed count approach, the state transition from a higher state

to a lower state occurs after a fixed number of successes. Figures 42-44 shows that this approach is even less energy efficient when compared with the fixed probability approach. Figure 42 shows that when the channel condition is good ($E_b/N_0$ ~ 30 dB), a long wait for transition in terms of the number of successes to a lower state is more energy consuming. This is because the momentary link quality fluctuation can switch the system to a higher state, but the system should be able to come back to a lower state rapidly. A low count means that the system waits less in the high level states. Overall, the adaptive power control approach with exponential drop off is more energy efficient that the fixed count approach.

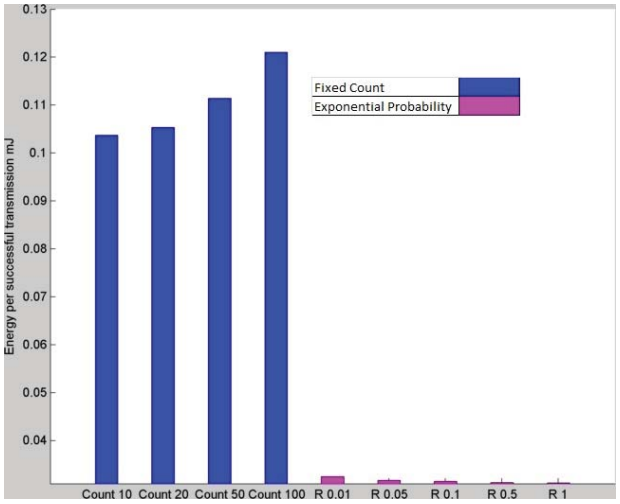


**Figure 42.** *At average $E_b/N_0$ of 30 dB, the channel condition/ link quality is good. The use of exponential probability while transiting to a lower state has outperformed the fixed count for transition by a huge margin.*

Figures 43 and 44 also show that the energy consumption will be less if the system uses a low count number.

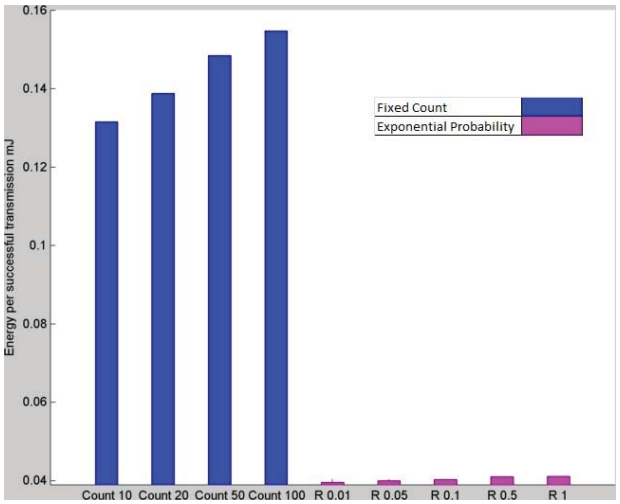

**Figure 43.** *At average $E_b/N_0$ of 15 dB, the channel condition/ link quality is average. The use of exponential probability while transiting to a lower state has outperformed the fixed count for transition by a huge margin.*

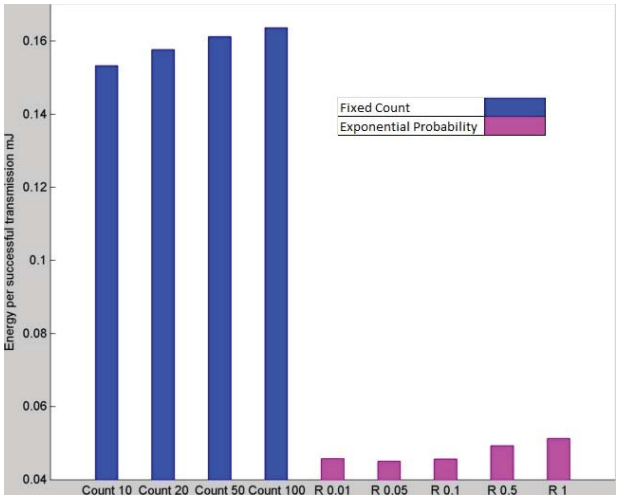


**Figure 44.** *When channel condition is poor ($E_b/N_0$ <10 dB), the use of exponential probability while transiting to a lower state has outperformed the fixed count for transition by a huge margin.*

Over-all, the adaptive communication protocol that is proposed in this thesis controls output power and decides the state at which a new packet transmission would start. The choice of state is important as that also controls the probable number of retries. This adaptive protocol can work best in terms of saving energy when sensors transmit quite frequently. It can also be effective energy saving solution when sensors are mobile and link quality changes frequently and there is a need to adjust the output power.

## 5.4 Performance comparison of adaptive protocol with the fixed power transmission

This section compares the performance criteria of adaptive protocol with the fixed power transmission using experimental data when the distance between the transmitter and the receiver is fixed. At each distance between the sensor and the hub, there is a fixed power level which provides the most energy efficient solution. This power level value is bounded by the available output power levels of a given transceiver. The energy consumption or the average cost per successful transmission value is compared with that of the adaptive power control protocol. It can be observed that the minimum energy consumption corresponding to the power level is at least 25% more than the adaptive protocol when they have comparable PSR and protocol efficiency values.

### 5.4.1 Experimental setup

The objective of the experiments is to compare the performance parameters of S-APC with fixed power transmission in indoor radio environment by fixing the distance

between the transmitting node and the hub. At different positions, the PSR, the protocol efficiency and the average energy expenditure are evaluated and compared. Experiments were conducted inside a University building and in a house where a gathering of people was held. Experiments 1 to 4 and 6 were conducted during the busy hours. Experiment 5 was conducted during the non-busy hours.

In general, the radio signal suffers from fading because of multipath propagation where the radio signal from the transmitter arrives at the receiver through multiple paths. During the busy hour, there are lots of movement of people in between the hub and the transmitting sensor. These movements induce a time varying Doppler shift on multipath components. Fading effect due to frequency shift of the radio signal cannot be ignored when the sensor is stationary. Besides, there can be temporary signal attenuation because of absorption if people have gathered around in between a transmitter and a receiver. All these affect the radio link quality over time. During the non-busy hours of the University, fading effect due to movement is minimal while the multipath effect still exists **[72]**. The objective of the experiments was also to observe how busy hour performances are different from non-busy hour performances.

The nRF24L01p module has four discrete power levels. They are -18 dBm, -12 dBm, -6 dBm and 0 dBm. In order to compare the performance criteria of adaptive protocol with the fixed power transmission, during each transmission instance, a total of nine packets were sent. They are:

- Four packets at power levels -18 dBm, -12 dBm, -6 dBm and 0 dBm
- The number of retries are set at 3 in each of the power levels to keep it at per with the allowed number of retries in adaptive protocol that is set at 3 in state 1 and 4
- Five packets at power levels determined by the drop-off rates (R) 0.01, 0.05, 0.1, 0.5 and 1 of the proposed adaptive protocol

The code for the adaptive protocol and the fixed power transmissions are all written in C and downloaded in the nRF24L01p modules and the sensors.

Before the performance parameters are compared, it is important to understand the factors that influence the cost in fixed power mode.

### 5.4.2Factors affecting the average cost in fixed power mode and trend analysis

The average cost of successful transmission is determined by three factors as shown in equation 24.

$$C_{S\_avg} = C_P \left(\frac{1 + Ret_T}{P_S}\right) \tag{24}$$

Therefore the three factors are:

- The energy used to transmit one packet
- Average number of retries
- The PSR

The energy used per packet transmission increases with the output power level. Table 7 summarises the current rating in each of these power levels of nRF24L01p. On the other hand, the average retries in each of these levels decreases and PSR increases with the increase in power level. The unimodal nature of the cost values in fixed power transmission in is understood from the fact that there are two competing factors that are working on the cost value. The number of successfully transmitted packet (PS) increases and the number of retry ($Ret_T$) decreases as the power level changes from -18 dBm to 0 dBm. But from Table 7 it can be observed that the cost of energy consumption per packet transmission ($C_p$) increases in terms of current drawn (from 7 mA to 11.3 mA at the same time). The 1st component of the product ($C_p$) in equation (24) increases as the power level increases. The 2nd component decreases as the power level increase because $Ret_T$ decreases and $P_S$ increases. Due to the competing nature of the components, the overall graph of the average cost of successful transmission takes the shape of a unimodal graph. This phenomenon can be observed in all the other plots in figures 46-51.

### 5.4.3 Experimental result and analysis

***Experiment 1***

The primary reason to include the two wall types is that a radio signal suffers different levels of attenuation when it passes through these walls in an indoor environment. The wall type I accounts for 3.4 dB signal loss per wall, while the wall type II accounts for 6.9 dB loss per wall.

| Distance between the sensor and the Hub | Number of Wall type I: Light internal walls (Plasterboards) | Number of Wall type II: internal walls (Concrete, bricks) |
|---|---|---|
| 14 m | 5 | 0 |

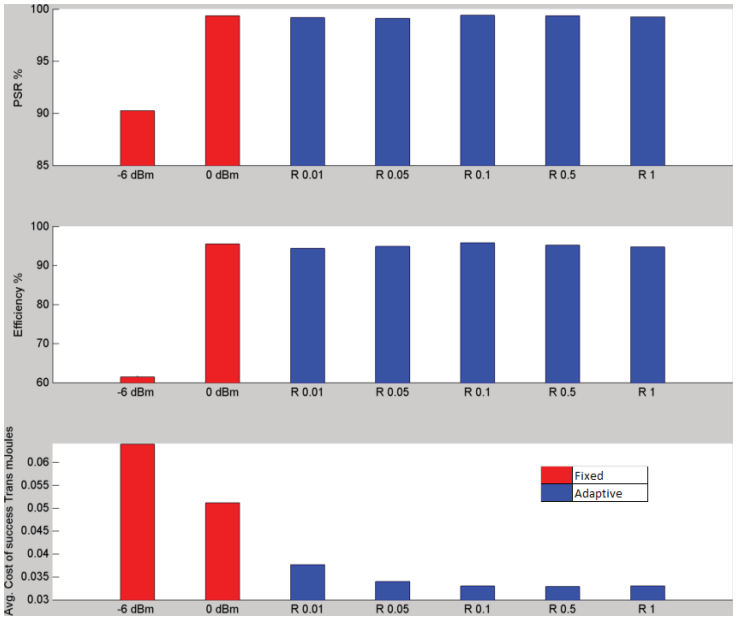


**Figure 45. Distance 14 m. Number of partition type I = 5.** *Comparison of the PSR, efficiency and average cost of successful transmission. The minimum cost at fixed power is achieved at 0 dBm. The PSR of fixed power at 0 dBm is almost similar to the PSRs of the adaptive protocol. The adaptive protocol consumes 55% less energy than at 0 dBm when value of R is 0.5.The efficiency of the fixed power transmisison (0 dBm) is a touch higher than the adaptive protocol at R = 0.5.*

Figure 45 shows that the proposed adaptive protocol can save 55% energy as compared to fixed power transmission when the value of R is 0.5. The minimum cost fixed cost was achieved at 0 dBm. However there is not much difference in the costs with other R values. The PSR of -18 dBm and -12 dBm are not included in the plot as they are too low. The indoor radio propagation mechanism is complex as it has multipaths, fading effects and propagation of radio wave through walls.

### *Experiment 2*

| Distance between the sensor and the Hub | Number of Wall type I: Light internal walls (Plasterboards) | Number of Wall type II: internal walls (Concrete, bricks) |
|---|---|---|
| 18 m | 4 | 0 |

Figure 46 plots the PSR, efficiency and cost values when the distance is 18 m. The optimal cost at fixed power transmission is at -6 dBm. This is because of almost similar PSR and efficiency values as at 0 dBm. There are four wooden partitions in between the transmitter and receiver. The adaptive protocol consumes 30% less energy than the fixed power transmission at -6 dBm when R = 1. Although the distance in experiment 1 is less than that in experiment 2, due to an extra partition in experiment 1, the average signal attenuation is more and contributed to a lower PSR than that in experiment 2.

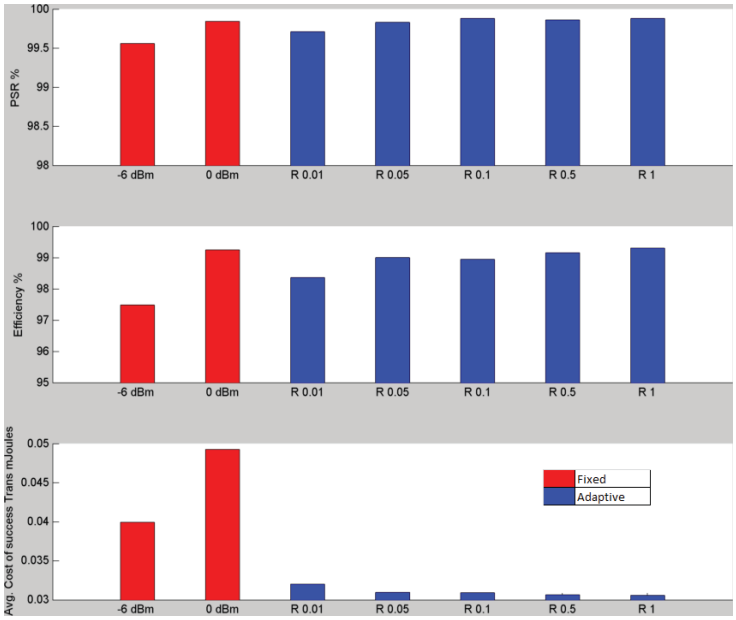


**Figure 46. Distance 18 m. Number of partition type I = 4.** *Comparison of the PSR, efficiency and average cost of successful transmission. The minimal cost of fixed power transmission is achieved at – 6 dBm. The minimum energy consumption is at -6 dBm, primarily because of similar PSR and efficiency as at 0 dBm. In terms of energy efficiency, the adaptive protocol consumes 30% less energy than the fixed power transmission at -6 dBm when R is 1. The efficiency of the adaptive protocol at R = 1 is higher than fixed power transmission at – 6 dBm.*

## *Experiment 3*

| Distance between the sensor and the Hub | Number of Wall type I: Light internal walls (Plasterboards) | Number of Wall type II: internal walls (Concrete, bricks) |
|---|---|---|
| 20 m | 4 | 0 |

Figure 47 shows that the application of adaptive protocol can consume up-to 55% less energy than when fixed power transmission is used. There are four wooden partitions in between the transmitter and receiver.

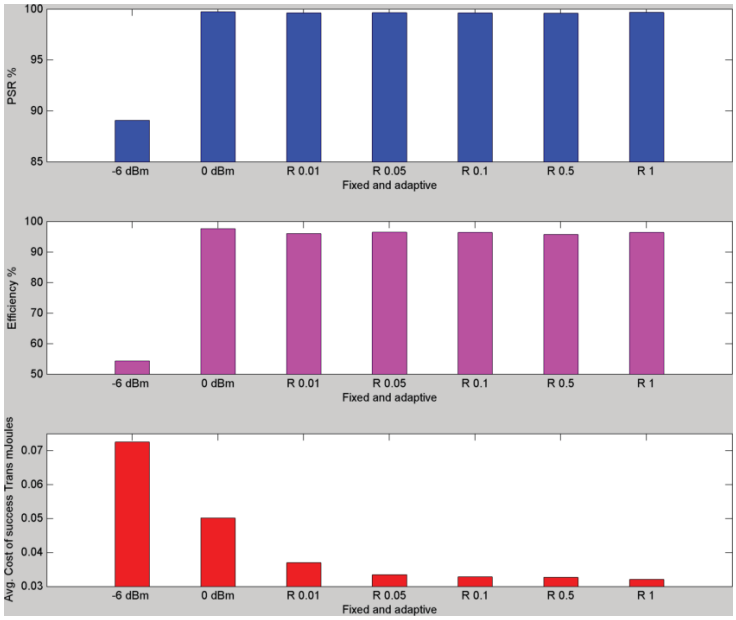


**Figure 47. Distance 20 m. Number of partition type I = 4.** *Comparison of the efficiency and average cost of successful transmission based on the PSR. The minimal cost of fixed power transmission is achieved at 0 dBm. In this case the PSR of fixed power at 0 dBm is same as the PSRs of adaptive protocol. In terms of energy efficiency, the adaptive protocol consumes 55% less energy than the fixed power transmission at 0 dBm when R =1. The efficiency of the fixed power transmisison is a touch higher than that of adpative protocol at R = 1.*

Although the current consumption at -6 dBm is less than that at 0 dBm, due to lower PSR, it is not able to compensate for the cost. The efficiency of the adaptive protocol is touch higher than fixed power transmission. The minimum energy consumption of fixed power is achieved at 0 dBm, primarily because it has much higher PSR and efficiency than at -6 dBm. In terms of energy efficiency, the adaptive protocol consumes 55% less energy than the fixed power transmission at 0 dBm.

### *Experiments 4 and 5*

| Distance between the sensor and the Hub | Number of Wall type I: Light internal walls (Plasterboards) | Number of Wall type II: internal walls (Concrete, bricks) |
|---|---|---|
| 24 m | 5 | 0 |

In these experiments, two sets of data were collected by fixing the position of the transmitter and the receiver during the busy hour and the non-busy hours of the University respectively

### Experiment 4 : busy hour data

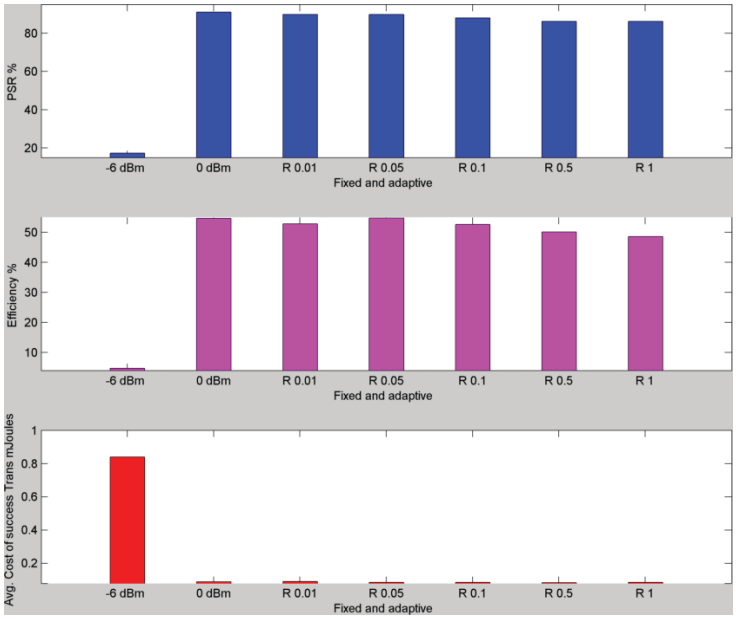


**Figure 48. Distance 24 m. Busy hour. Number of partition type I = 4.** *Comparison of the efficiency and average cost of successful transmission based on the PSR. The minimum energy consumption of fixed power is achieved at 0 dBm, primarily because it has much higher PSR and efficiency than at -6 dBm. The adaptive protocol consumes 6% less energy than the fixed power transmission at 0 dBm when R = 0.5. The efficiency of the fixed power transmission at 0 dBm is a touch higher than that of adaptive protocol at R = 0.5.*

Figure 48 shows that the minimum energy consumption of fixed power is achieved at 0 dBm, primarily because it has much higher PSR and efficiency than at -6 dBm. The adaptive protocol consumes 6% less energy than the fixed power transmission at 0 dBm when R = 0.5. The efficiency of the fixed power transmission at 0 dBm is a touch higher than that of adaptive protocol at R = 0.5.

The minimum energy consumption of fixed power is achieved at 0 dBm, primarily because it has much higher PSR and efficiency than at -6 dBm.

### Experiment 5 : Non-busy hour data

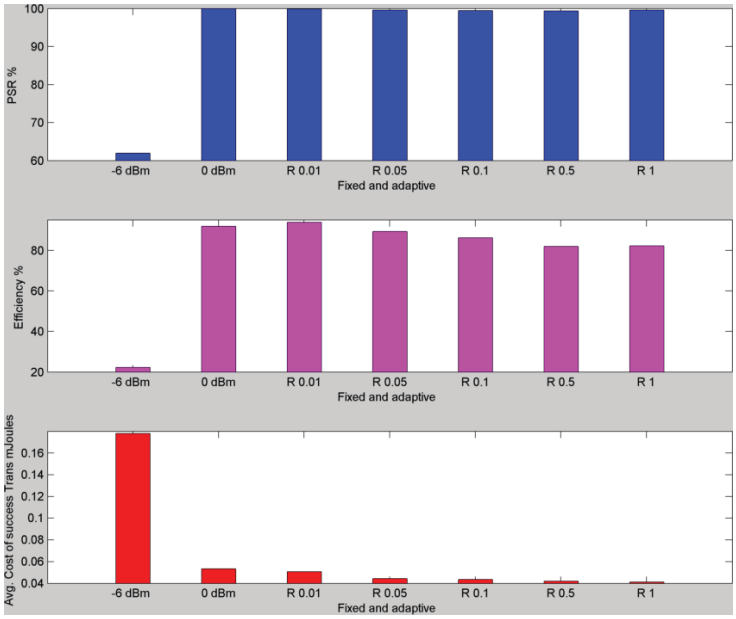


**Figure 49. Distance 24 m. Non-busy hour. Number of partition type I = 4.** *Comparison of the efficiency and average cost of successful transmission based on the PSR. The minimum energy consumption of fixed power is achieved at 0 dBm The adaptive protocol consumes 29% less energy than the fixed power transmission at 0 dBm when R = 1 The efficiencies of the adaptive protocol (at R = 1) and fixed power transmission (0 dBm) are comparable.*

Figure 49 shows the comparison of the efficiency and average cost of successful transmission based on the PSR when the distance between the sensor and the hub is 24 m and collected during non-busy hour. The minimum energy consumption of fixed power is achieved at 0 dBm The adaptive protocol consumes 29% less energy than the fixed power transmission at 0 dBm when R = 1 The efficiencies of the adaptive protocol (at R = 1) and fixed power transmission (0 dBm) are comparable.

It can be observed from the results of figures 48 and 49 that there is a significant difference in performances between busy and non busy hours of a day. It also demonstrate the fact that radio link quality can widely vary over time. The adaptive protocol is able to track the variation in link quality and save energy, thereby extending the operational lifetime of the battery.

### *Experiment 6: Data collected from house with a large gathering of people*

| Distance between the sensor and the Hub | Number of Wall type I: Light internal walls (Plasterboards) | Number of Wall type II: internal walls (Concrete, bricks) |
|---|---|---|
| 15 m | 3 | 1 |

There were around 20 people and lot of movements, mainly because of the children around. This is a also a busy hour scenario when the radio signal suffers from time-varying attenuation and wide flucation of signal over a short period of time.

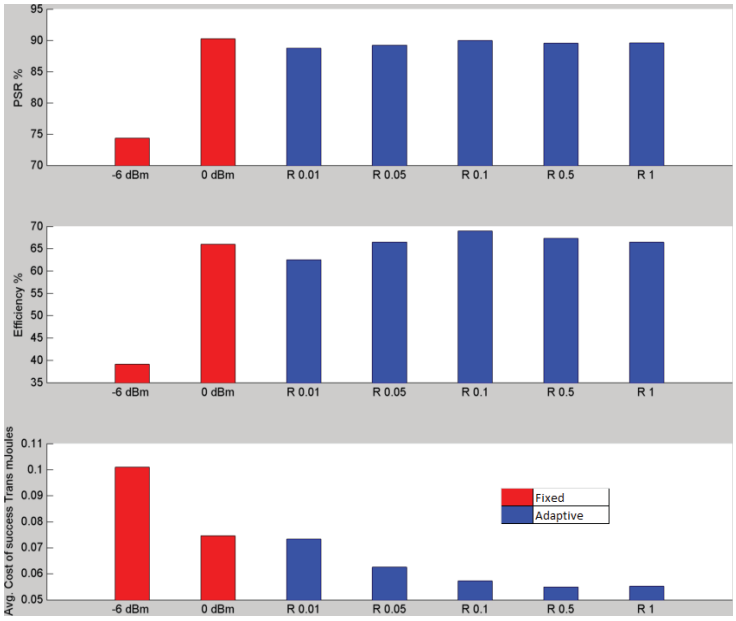


**Figure 50. Distance 15m. Large gathering of people. Number of partition type I = 3, Number of partition type II = 1.** *Comparison of the efficiency and average cost of successful transmission based on the PSR and data collected during a gathering in a house. The minimum energy consumption of fixed power is achieved at 0 dBm. In terms of energy efficiency, the adaptive protocol consumes 26% less energy than the fixed power transmission at 0 dBm when R = 0.5.The protocol efficiencies of both fixed (at 0 dBm) and adaptive R = 0.5) are the same.*

The overall energy saving is 26% when the adaptive protocol is used. The adaptive protocol has fared better because it has the ability to track the link quality even without any RSSI side information and switch to different states in response to packet lossses. At the same time, the intelligent design of the protocol also allows it to switch back to a lower level state and transmit a new packet at a low power level.

## 5.4 Computational time of the proposed S-APC protocol

The computational complexity of the proposed protocol is calculated based on the time it takes for the protocol to execute in a given hardware platform. It can also be measured in terms of the number of CPU cycles. The time for execution is calculated based on three scenarios.

- **Best case**: The distance between the transmitting sensor and the receiver is within 1 meter.
- **Worst case**: The distance between the transmitting sensor and the receiver is so large that the receiver cannot receive any data packets.

- **Average case**: Communicable distance maintained between the transmitter and the receiver (distance ~ 20 meters)

Table 15 represents the execution time of the proposed protocol under different conditions. The size of the code is approximately 10 kB.

**Table 15. Execution time of code under different scenarios**

| **Arduino MEGA 2560 with 16 MHz microcontroller** | | | |
|---|---|---|---|
| | Best case | Average case | worst case |
| Execution time (ms) | 2.45 | 71.56 | 260 |
| No. of CPU cycle | 3924 | 1144960 | 4160000 |

From [104], it is known that the primary three kinds of micro-controllers used by wireless sensor nodes are PIC microcontrollers, AVR series microcontroller and MSP430 from Texas Instruments. All these are 8-micro-controllers with 8-16 MHz processors and at-least 128 kB in-system programmable flash memory. These specifications show that the proposed adaptive protocol can efficiently be implemented in wireless sensor nodes without any performance degradation

## 5.6 Discussion

The results of experiments 1 to 6 have shown the ability of the adaptive protocol to make use of all the available power levels to successfully transmit a packet with fewer number of retries. Since in fixed power transmission there is no scope of output power level maneuvering, a large amount of energy may be wasted.

The results of this paper demonstrate that the non-RSSI based adaptive power control protocol can achieve significant energy savings as compared to fixed power solution. The drop-off factor (R) is an important parameter in the adaptive protocol as it determines how fast the system will switch back to a lower state to transmit at a lower power. The experimental data show that the value of R can be set in between 0.5 and 1 to achieve minimum energy consumption. A low value of R means that the system will switch back to a lower power level slowly. Therefore in scenarios when the system has switched to a higher state level in response to momentary drop in signal level, a low R value means that even if the channel condition improves, the system will come down to lower state level slowly. Hence, the energy cost may rise. On the other hand, if R is set at 1, it will drop fast. But if the link quality change is not transient, the system will oscillate between the states. The experiments that were conducted have covered some common indoor radio channel scenarios. Overall, the results that are presented in this paper show that it is possible to track link quality without regular channel scanning and avoiding probe packets for link quality estimation.

# Chapter 6 Applicability of S-APC protocol in mobile sensor scenarios

Mobile robots play a pivotal role in making information available anytime and anywhere. This is because robots can be used for applications that involve delicate, heavy, and repetitive or labour intensive. They can be used in assembly lines, in moving stacks of containers in warehouses, asset tracking, cleaning industrial floors etc. In process monitoring and control, process data such as pressure, humidity, temperature, flow, level, viscosity, density and vibration intensity measurements can be collected through sensing units and transferred wirelessly to a control system for operation and management. Wireless sensor equipped mobile robots can also help in reducing the "blind spots" by their ability to collect measurement values on rotating or moving equipment and in remote locations.

In healthcare, traditionally human intervention is required to transport medical equipment, samples, and meals for patients, getting rid of medical waste etc. Mobile robots can eliminate the need for manual transport of laboratory specimens, medications, supplies and other materials, allowing healthcare technicians to focus on patient-related tasks. Body sensor networks are a key technology to use different sensor data from patients and help in long term health monitoring. This technology is also used to prevent the occurrence of myocardial infarction and epileptic seizures, monitoring episodic events or any abnormal condition. These sensors are constantly in touch with the wireless gateway or the access point. Most sensors are non-invasive and therefore a patient is allowed to move freely. Therefore, the distance between the transmitting nodes and the access point also changes constantly. Power control can reduce the energy consumption and increase the lifetime of the body wearable sensors.

## 6.1 The need for control power for wireless mobile sensor nodes

When a sensor is mobile, it means that its communicating distance from the base station is changing with time. The energy loss is primarily dependent on distance. Unwanted obstructions can also lead to signal degradation due to absorption. There are also effects of fading and multipath propagation of radio signal in indoor wireless communication.

For acceptable performance, the average received $E_b/N_0$ at the base station should be above a threshold value. If that value is maintained on average, then it means that the performance will be satisfactory. Since most of these mobile wireless sensors are battery powered, they have limited energy resources. Therefore, if a mobile node is near to a base station and the received $E_b/N_0$ far exceeds the required threshold, then there is waste of energy. Similarly, when the same sensor node is far from the base station, the node is required to pump in more power than the present value. It may also happen that due to an

obstruction between the transmitting node and the base station, the node is transmitting at a power level that is enough to deliver packets. If that obstruction is removed or the node moves to a position in which the obstruction is cleared, then it should adjust its transmitting power accordingly.

## 6.2 Simulation design, preliminary investigation and observations

As part of the initial investigation to observe the effect of mobility on the communication protocol, five sets of simulation were conducted. A mobile sensor means that its distance from the hub or base station is changing with time. At different positions from the hub, the sensors can transmit data. The design of the simulation is to emulate these real world scenarios when the distance between the mobile sensor and the hub is varying with time. Since the received signal strength varies with distance [105], the different positions of the mobile sensor yield different $E_b/N_0$ values. The five random walks are simulated and the performance parameters of fixed power transmission and a general non-RSSI based adaptive power control protocol are compared with the non-RSSI based adaptive protocol that is proposed in this thesis. The walks that are simulated are one dimensional (1-D) random walks which takes a forward or a backward step with equal probability [106] [107]. In simulation, the range of distance that the walk can cover has been restricted between -40 m and 40 m with the starting point set to 0 m. Based on the Cost231 path loss model that includes 4 Type-I wall partitions in between the sensor and the hub, the minimum $E_b/N_0$ is approximately 0 dB at -18 dBm. In each position, the sensor transmits 20 times. Figure 51 shows the plot of the distances of five random walks in one dimension that are generated using MATLAB simulation.

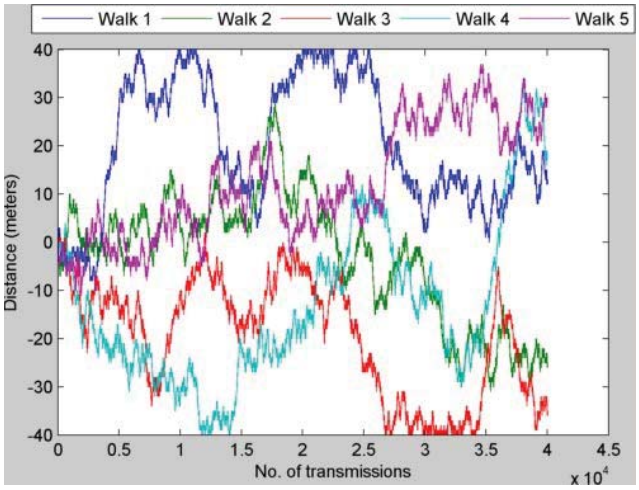


**Figure 51.** *The 5 1-D random walks are plotted with the maximum distance between the sensor the hub set to 40 m.*

As usual, the number of retries in fixed power transmission are set at 3 in each of the power levels to keep it at per with the allowed number of retries in adaptive protocol that is set at 3 in state 1 and 4. The results of the random walks are presented in section 6.2.2.

The detail of the existing general non-RSSI based adaptive power control protocol that is inspired by P-ATPC [55] has been presented in the next section.

### 6.2.1 Existing non-RSSI based adaptive power control protocol

Practical-TPC is a receiver oriented protocol that is considered robust in dynamic wireless environments and uses packet reception rate (PRR) values to compute the transmission power that should be used by the sender in the next attempt. It is to be noted that in simulation, we made no distinguish between PSR and PRR. PRR is the term used in the paper related to P-ATPC. However, no formal definition was provided.
The receiver monitors all incoming packet and counts the successes and failures of the packet transmission within the current sampling window. After the sampling window period is over, the P-TPC protocol computes the next transmission power level and sends to the transmitter. This new power level will be used during the next sampling window.
P-ATPC runs two feedback loops. The inner loop adapts the transmission power based on the PRR measurement. The outer loop adjusts the parameters based on the updated power model that defines the relationship between the PRR and transmission power. P-ATPC also initializes the power model parameters before the feedback loops kick in. In this initial phase, each link is set to transmit a sequence of probe packets using highest to lowest power level to build the transmission power model. The outer loop is designed to handle significant variation in the relationship between the transmission power and the PRR. The inner loop adapts the changes in PRR over a short term. In P-ATPC, the inner and outer loops were run every 5 mins and 150 minutes respectively.

The simulation that has been conducted has fixed the inner loop after 50 transmissions, whereas, the outer loop is varied from 100 to 1000. The required PRR is set at 99%. The P-ATPC has been tested in the random walk setup and the results are presented in this section. The outer loop involves the transmission of beacon packets at different power level and builds the model between the PRR and the transmission power. The variation of the PSR with the outer feedback window is shown in Figure 52. It can be observed from Figure 52 that the PSR values actually drop with the increase in the size of the feedback window. This is because the larger window size decreases the accuracy of the power vs. PRR model. However, the average cost of transmission decreases with the increase in the size of feedback window but does not improve after a certain window size. It is to be noted that the protocol efficiency (Equation 9) that is defined in this thesis for P-ATPC is 100% as there in no scope of retransmission.

The increase in the size of the inner feedback window has nominal effect on the PSR or the energy cost values. Therefore, results related to that are not presented in the thesis.

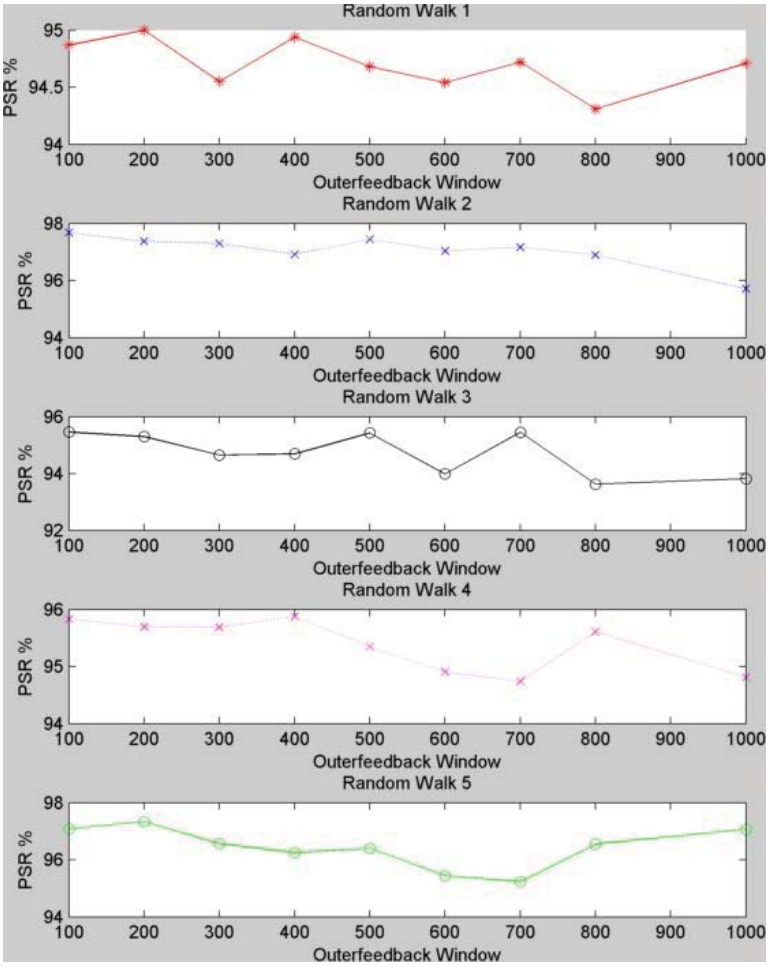


**Figure 52. Variation of PSR with the outer feedback window in different ransom walks**

### 6.2.2 Results from random walk 1 simulation

The results of this section compares the fixed power transmission are based on the random walk that is marked in deep blue in Figure 51.

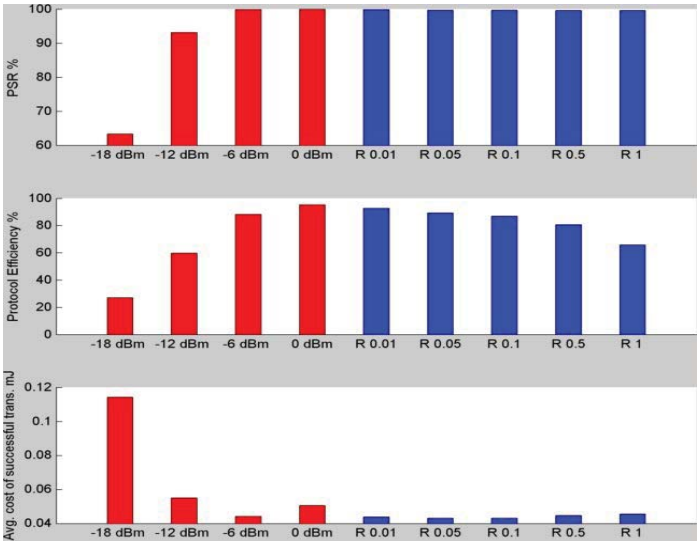


**Figure 53. Random Walk 1.** *The PSR as the constraint parameter shows that both fixed power (above power level -12 dBm) and adaptive transmission strategy have comparable values (~100%). The cost comparison shows that the adaptive protocol consumes less energy for a successful transmission on average. The power level for optimal energy consumption in fixed power mode is -6 dBm. The protocol efficiency at -6 dBm is a touch less than the adaptive protocol.*

The unimodal nature of the average energy cost of successful transmission has been explained in section 4.2 of chapter 5.

Due to the competing nature of the components, the overall graph of the average cost of successful transmission takes the shape of a unimodal graph. This phenomenon can be observed in all the other plots in figures 53, 55, 57 and 59.

In general, the results of random walk 1 demonstrate the usefulness of the adaptive protocol in terms of saving energy. The energy saving is not significant (2.5%), but it provides enough indication that the adaptive power control can be an effective method of increasing the battery lifetime in the long run. The results of the random walks 2 to 5 also shows that adaptive power control method can fare better than fixed power transmission in terms of energy consumption while maintains a comparable PSR and protocol efficiency.

There is also direct correlation among the cost and efficiency curves of adaptive protocol. The protocol efficiency decreases with the drop-off factor (R) indicating that the number of retries has increased. It has led to the increase in energy consumption cost per successful transmission as R value increases. Similar characteristics are also observed in the results of the random walks 2 to 5.

Figure 54 compares the PSR and protocol efficiency based on the minimum average cost of successful transmission of fixed power, adaptive power control proposed in this thesis and P-ATPC. The energy consumption per successful transmission can be reduced by

approximately 4% if the proposed adaptive protocol is used over the existing general PRR based protocol.

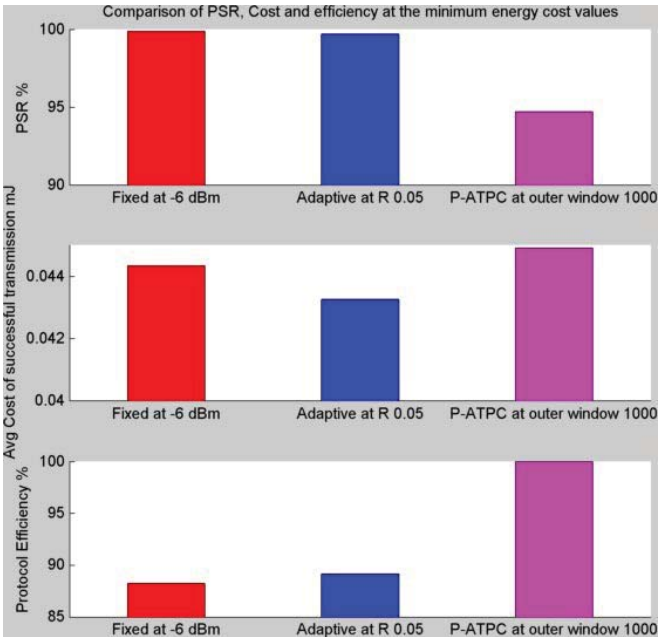


**Figure 54. Random Walk 1:** *Comparison of the PSR, protocol efficiency based on the minimum average cost of successful transmission*

### 6.2.3 Results from random walk 2 simulation

The results of this section are based on the random walk that is marked in green in Figure 51.

The minimum power level has changed from -6 dBm in **random walk 1** to -12 dBm because in **random walk 1** the distance between the sensor and the hub has been more towards the extreme ends (40 m), while in **random walk 2**, the distances are closer to the initial value (0 m). Therefore, more energy was required in random walk 1 than random walk 2 to achieve the similar PSR. There is practically no difference in the cost values (~1%) because the minimum power level is lower than in random walk 1.

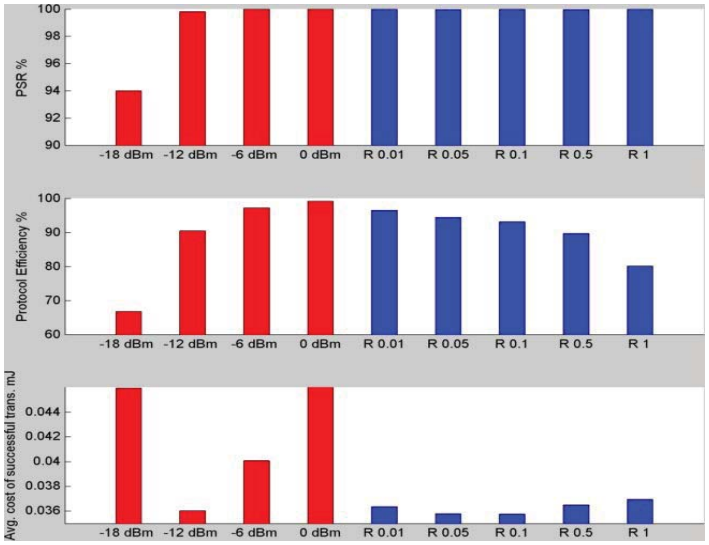


**Figure 55. Random Walk 2.** *The PSR as the constraint parameter shows that both fixed power (above power level -18 dBm) and adaptive transmission strategy have comparable values (above 95%). The cost comparison shows that the adaptive protocol consumes less energy for a successful transmission on average. The power level for optimal energy consumption in fixed power mode is -12 dBm. The protocol efficiency of the adaptive protocol is 5.5% higher than at -12 dBm.*

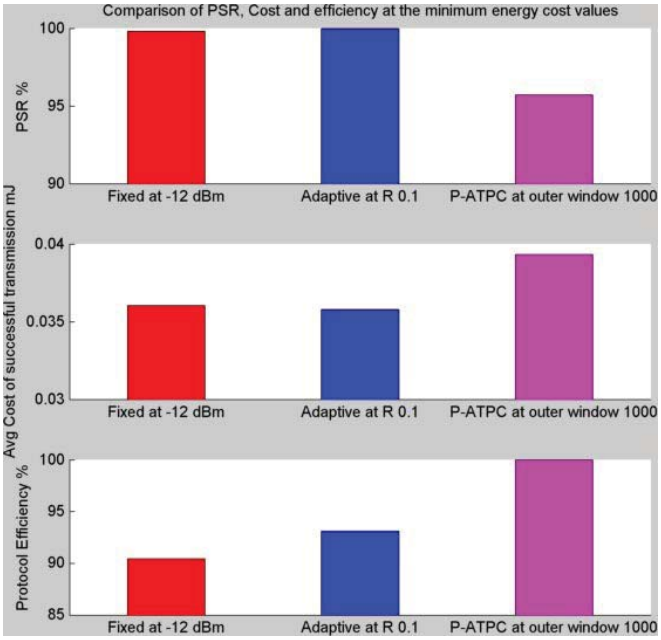


**Figure 56. Random Walk 2:** *Comparison of the PSR, protocol efficiency based on the minimum average cost of successful transmission*

Figure 56 compares the PSR and protocol efficiency based on the minimum average cost of successful transmission of fixed power, adaptive power control proposed in this thesis and P-ATPC. The energy consumption per successful transmission can be reduced by

approximately 10% if the proposed adaptive protocol is used over the existing general PRR based protocol.

### 6.2.4 Results of random walk 3 simulation

The results of this section are based on the random walk that is marked in red in Figure 51.

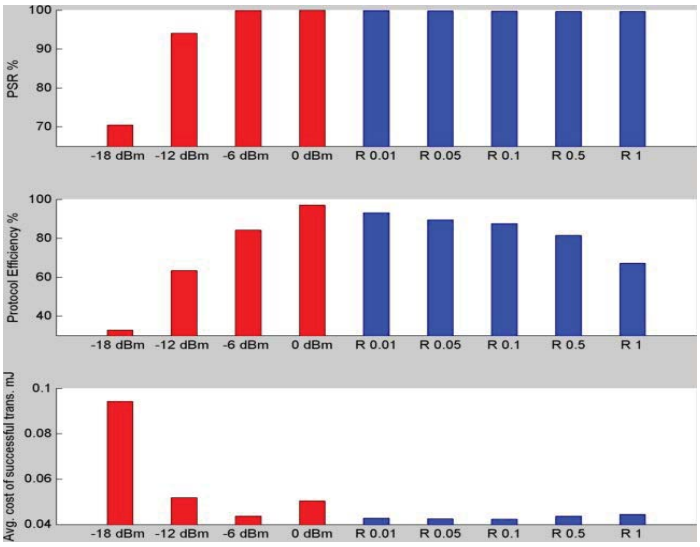


**Figure 57. Random Walk 3.** *The PSR as the constraint parameter shows that both fixed power (above power level -12 dBm) and adaptive transmission strategy have comparable values (above 95%). The cost comparison shows that the adaptive protocol consumes approximately 3% less energy for a successful transmission on average. The power level for optimal energy consumption in fixed power mode is -6 dBm. The protocol efficiency of the adaptive protocol is a touch higher than the minimum fixed power level at -6 dBm.*

The cost comparison in Figure 57 shows that the adaptive protocol is roughly 3% more energy efficient than transmission at fixed power of -6 dBm.

Figure 58 compares the PSR and protocol efficiency based on the minimum average cost of successful transmission of fixed power, adaptive power control proposed in this thesis and P-ATPC. The energy consumption per successful transmission can be reduced by approximately 5% if the proposed adaptive protocol is used over the existing general PRR based protocol.

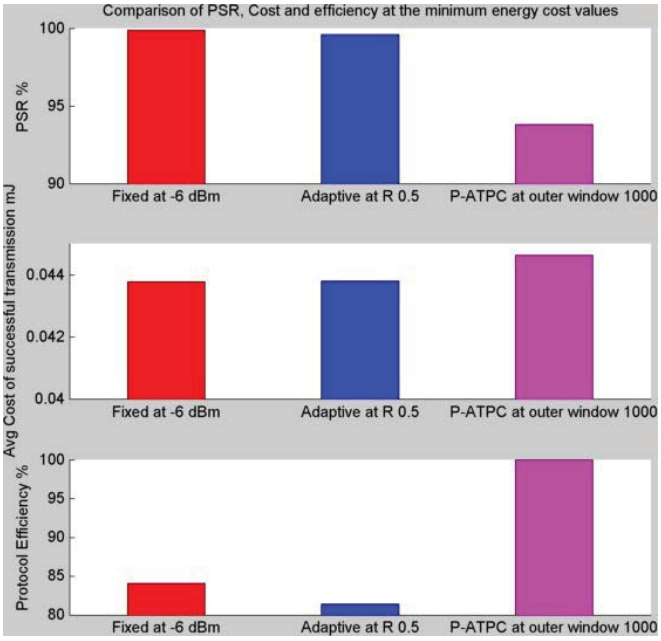


**Figure 58. Random Walk 3:** *Comparison of the PSR, protocol efficiency based on the minimum average cost of successful transmission*

### 6.2.5 Results from random walk 4 simulation

The results of this section are based on the random walk that is marked in light blue in Figure 51.

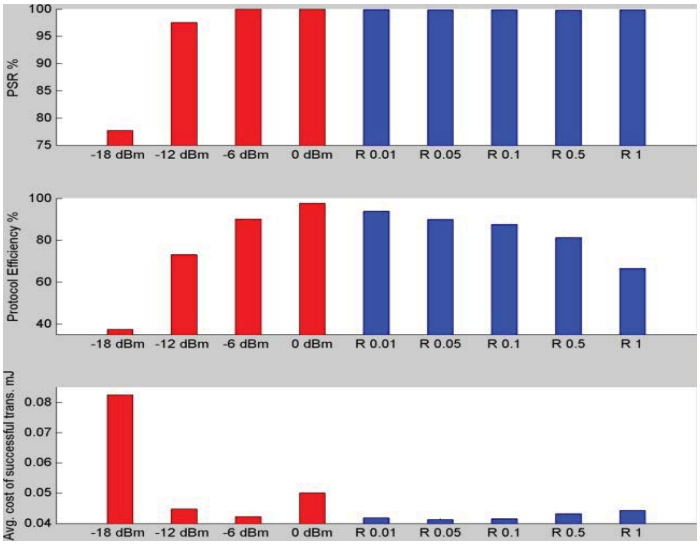


**Figure 59. Random Walk 4.** *The PSR as the constraint parameter shows that both fixed power (above power level -12 dBm) and adaptive transmission strategy have comparable values (above 95%). The cost comparison shows that the adaptive protocol consumes less energy for a successful transmission on average. The power level for minimum energy consumption in fixed power mode is -6 dBm. The protocol efficiency of the adaptive protocol is comparable with the power level at -6 dBm.*

The energy savings in random walk 4 is not significant and is around 2.3%.

Figure 60 compares the PSR and protocol efficiency based on the minimum average cost of successful transmission of fixed power, adaptive power control proposed in this thesis and P-ATPC. The energy consumption per successful transmission can be reduced by approximately 13% if the proposed adaptive protocol is used over the existing general PRR based protocol.

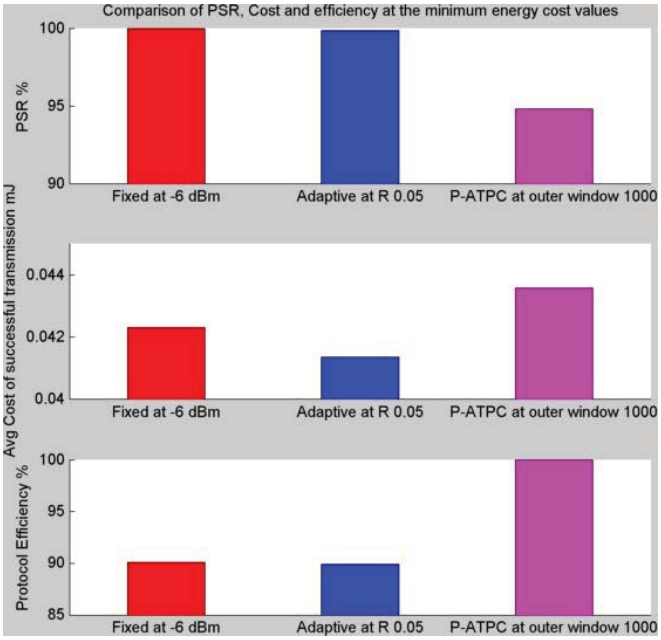


**Figure 60. Random Walk 4:** *Comparison of the PSR, protocol efficiency based on the minimum average cost of successful transmission*

### 6.2.6 Results from random walk 5 simulation

The results of this section are based on the random walk that is marked in purple in Figure 51. The energy savings in random walk 5 is approximately 6% based on Figure 61.

Figure 62 compares the PSR and protocol efficiency based on the minimum average cost of successful transmission of fixed power, adaptive power control proposed in this thesis and P-ATPC. The energy consumption per successful transmission can be reduced by approximately 10% if the proposed adaptive protocol is used over the existing general PRR based protocol.

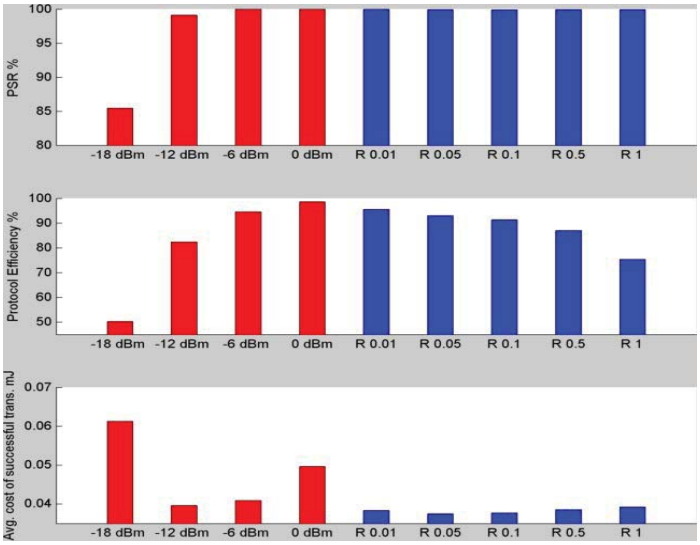


**Figure 61. Random Walk 5.** *The PSR as the constraint parameter shows that both fixed power (above power level -18 dBm) and adaptive transmission strategy have comparable values (above 95%). The cost comparison shows that the adaptive protocol consumes less energy for a successful transmission on average. The power level for optimal energy consumption in fixed power mode is -12 dBm. The protocol efficiency of the adaptive protocol is 15% more than that at optimal fixed power level of -12 dBm.*

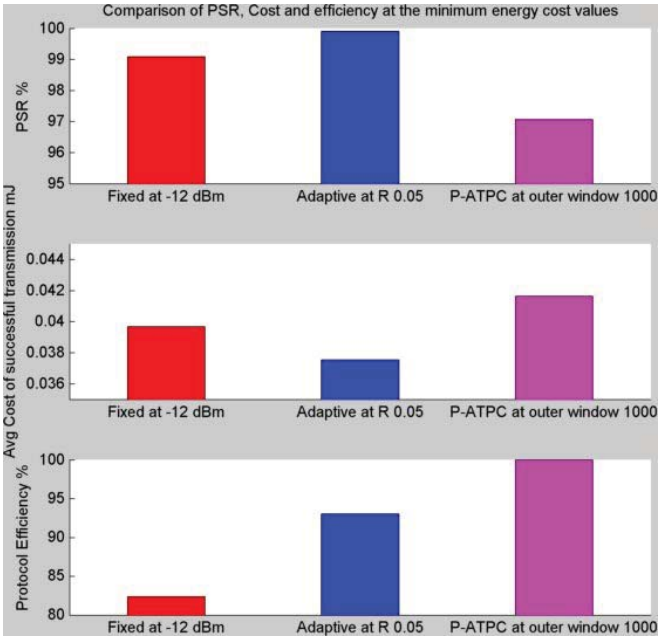


**Figure 62. Random Walk 5:** *Comparison of the PSR, protocol efficiency based on the minimum average cost of successful transmission*

## Random walk conclusion

The aim of the simulations with random walk was to investigate and verify if the adaptive power control protocol can be more energy efficient than fixed power transmission when the sensors are mobile. From figures 53 to 62 it is observed that the proposed adaptive

protocol can save more energy than either fixed power transmission or the PRR based adaptive power control protocol that is in existence. However, that also depends on the value of the drop-off factor R. Results show that at R value of 0.05, the energy efficiency can be achieved. These results provide the motivation to implement the adaptive protocol in hardware and test in real world environment.

## 6.3 Determining the sensitivity of the drop-off factor R

It is important to understand the behaviour of the state transitions based on R when distance between the sensor and the hub changes. In order to understand how the system behaves when the sensor changes its position continuously, a sample random walk with the transmitting sensor was conducted within a University building. The traversal path of the sensor is shown in Figure 63.

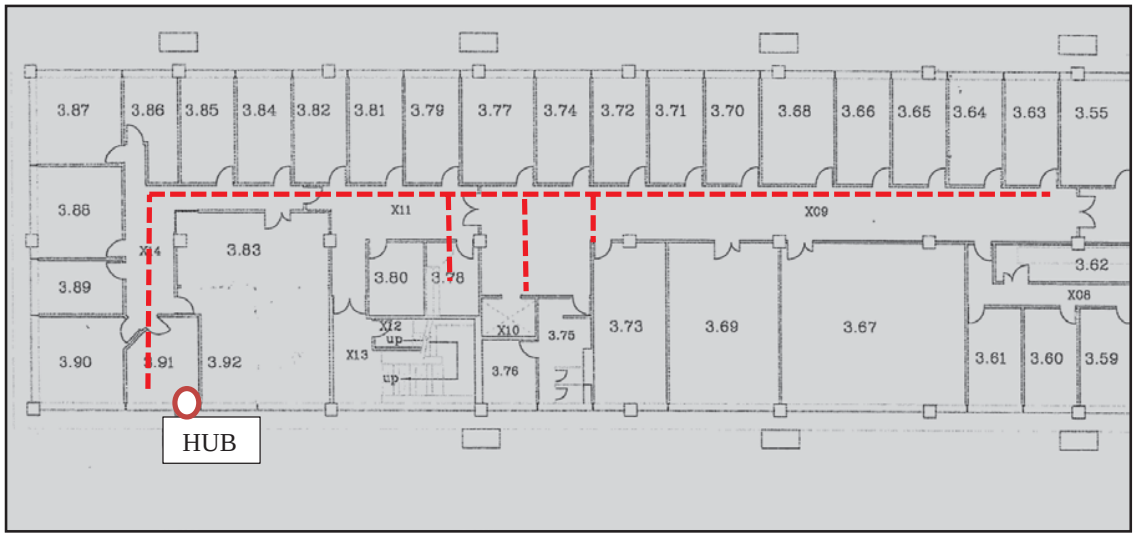


**Figure 63.** *Traversal path of the sensor is shown in dotted red line. The distance between the sensor and the hub is not constant*

Figure 64 to 68 plot the states of the system when the distance between the transmitting sensor node and the base station is made to vary. The radio features of the transmitting sensor and the hub are available in Table 5 of chapter 3. The sensor was made to transmit every 5 seconds. Therefore, essentially the snapshot duration is 25 minutes. The cluttered radio environment can also be well understood from some sample pictures of the radio environment in appendix B.1.

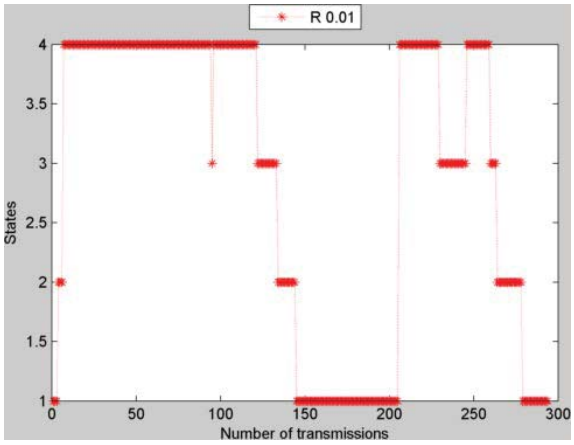


**Figure 64.** *State traversal with the number of transmission when exponential drop-off rate is 0.01. The system toggles between different states less frequently even when link quality decreases (by increasing the distance between the sensor and the hub).*

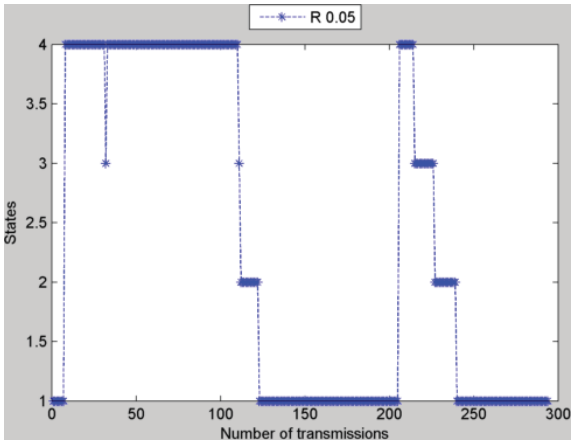


**Figure 65.** *State traversal with the number of transmission when exponential drop-off rate is 0.05. The state drops are faster as compared to R =0.01.*

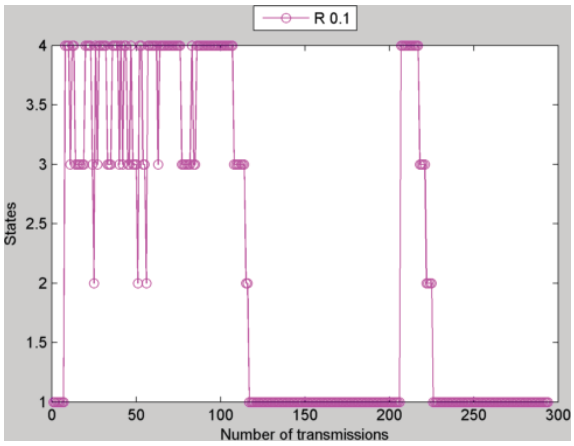


**Figure 66.** *State traversal with the number of transmission when exponential drop-off rate is 0.1. The state drops are now very frequent and system stays in the lower state (1 and 2) more often as compared to R 0.01 and R 0.05.*

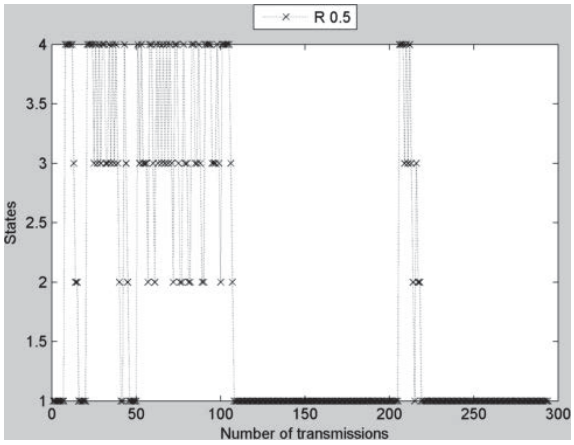


**Figure 67.** *State traversal with the number of transmission when exponential drop-off rate is 0.5. Even less time spent in higher states.*

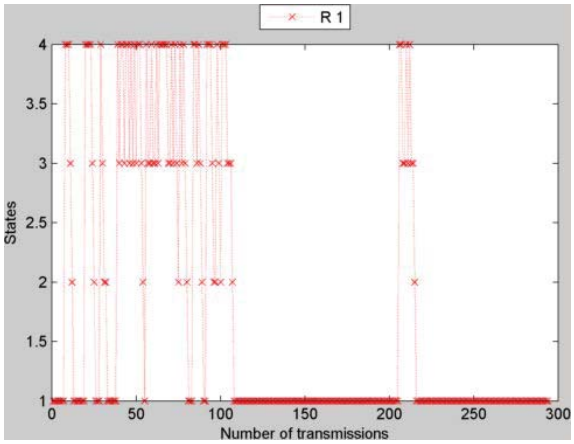


**Figure 68.** *State traversal with the number of transmission when exponential drop-off rate is 1. The system has spent most of the time in lower states.*

The state change responses show that depending on the value of R the states will change more or less rapidly. When the distance increases, the path loss value increases and the system stay more often in a higher state. The value of R determines as to how frequently the states will switch. When R is 0.01, the system hardly ever changes state when the distance between the sensor and hub is large, as shown in Figure 64. On the other hand, when R is set at 1, the system bounces between the states more frequently (Figure 68). It is the ability of the system to switch to a lower state to start transmitting at a lower power that makes it energy efficient in the long run.

## 6.4 Initial test run with mobile sensors in a cluttered radio environment

During the initial design and development phase of the adaptive communication protocol the retry limit of state 4 is set at 0 in order to avoid retries and keep the communication

cost low. A super market environment was chosen as it will offer different kinds of RF attenuation and reflection due to variety of structures like metal shelves, cans and freezers and movements of people in between the sensor and the hub. The experiments were conducted twice during the weekend from 11:30 till 12 noon. The choice of time was deliberately made to coincide with busy hour of the supermarket and provides an RF environment that exhibits time varying frequency deviation due to Doppler shift (resulting in fading). The pictorial representation of the sample radio environment is shown in appendix B.2.1.

On day 1, the drop-off factor R = 1 was not used. On day 2, the drop-off factor R =1 was used.

### 6.4.1 Experimental setup

The receiver is placed inside the car that is parked just outside a supermarket. The transmitting sensor is placed inside the shopping bag. With the shopping bag placed in the trolley, the sensor is moved along the aisles of the supermarket that emulates a random walk. The transmitter transmits 9 packets during each transmission cycle. The first four packets are transmitted at output power levels of -18 dBm, -12 dBm, -6 dBm and 0 dBm. The remaining 5 packets are transmitted at the power levels that are determined by the adaptive power control protocol using the four drop-off rates of 0.01, 0.05, 0.1 and 0.5 and 1. In this adaptive protocol, the transmitter is allowed to transmit only once in the state 4 (the highest power state). That implies that in this design of the adaptive protocol, the probability of successful packet transmission in state 4 is the minimum of all states. Table 16 shows the states and the available power levels to retry in case the first one is not successful. Unlike in Table 12, it has only one transmission allowed in state 4. The retry limit of states 1, 2, 3, 4 are respectively 3, 2, 1 and 0. The primary reason to use no retries in state 4 was to avoid repeated energy consumption at the highest power level. In fixed power transmission, the maximum retry limit set for each output power level is 3. It means that the probability of success is the highest when fixed power at 0 dBm is used. The state transition logics remain the same as mentioned in Table 13 and Table 14.

**Table 16. States, power levels and number of retries allowed**

| State | 1 | 2 | 3 | 4 |
|---|---|---|---|---|
| Available power levels | Minimum (M) | | | |
| | Low (L) | Low (L) | | |
| | High (H) | High (H) | High (H) | |
| | Maximum (X) | Maximum (X) | Maximum (X) | Maximum (X) |
| Number of retries | 3 | 2 | 1 | 0 |

The frequency of transmission is 5 seconds. Therefore the total number of samples is roughly 400 that are collected over a period of 30 minutes. The idea is to change the distance between the transmitter and the receiver and observe as to how the adaptive protocol adjusts its transmitting power in an energy efficient manner. Results of the experiments are presented in subsection 6.4.2.

### 6.4.2 Analysis based on data collected from super market

***Day 1 Supermarket***

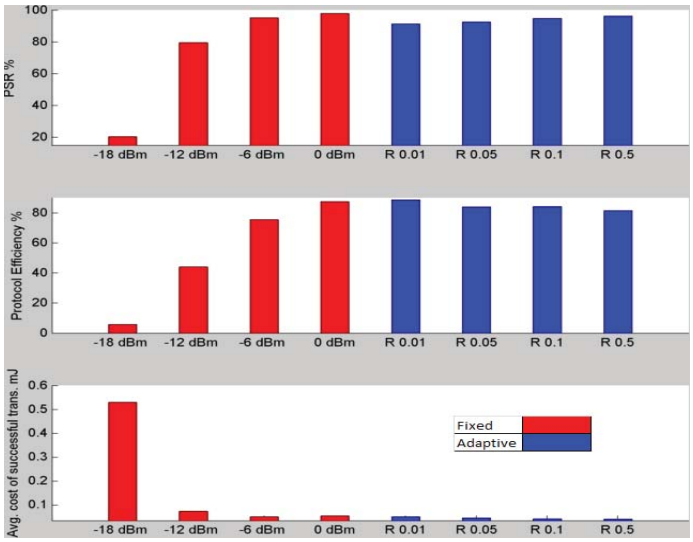


**Figure 69.** *Performance comparison of fixed and adaptive protocol. As expected, the PSR at fixed power of 0 dBm is the maximum but adaptive protocol at R value of 0.5 has comparable PSR. The efficiencies of adaptive and fixed power are comparable. The adaptive protocol saves almost 20% energy at R = 0.5.*

Figure 69 shows that the maximum PSR is achieved when the power of the transmitter is set at maximum level of 0 dBm. The PSR of the adaptive system gradually increases from R 0.01 to R 0.5. A high value of R means that the adaptive protocol has a slow drop-off rate from high state to a lower state. It implies that it will spend more time in the higher state. That, in turn, will affect the PSR in an adverse manner. Since the retry limit in state 4 is turned off, the PSR of the adaptive protocol at different R values could not exceed the PSR of fixed power transmission at -0 dBm Therefore, as expected the PSR with R 0.5 is higher than R 0.01.

The protocol efficiency of the adaptive protocol at lowest drop-off is highest because a low drop-off rate means that system stays more often in higher state which has a lower retry limit.

The minimum cost of successful transmission in fixed power transmission is achieved at -6 dBm. The adaptive protocol with drop-off factor R 0.5 can consume 20% less energy

than the fixed power transmission (-6 dBm). Figure 69 shows that at R 0.5, the PSR values of adaptive protocol are comparable with that of fixed power transmission at -6 dBm. However, the efficiency of the adaptive protocol is better (at R = 0.5) is better than fixed power transmission (at -6 dBm).

***Day 2 Supermarket***

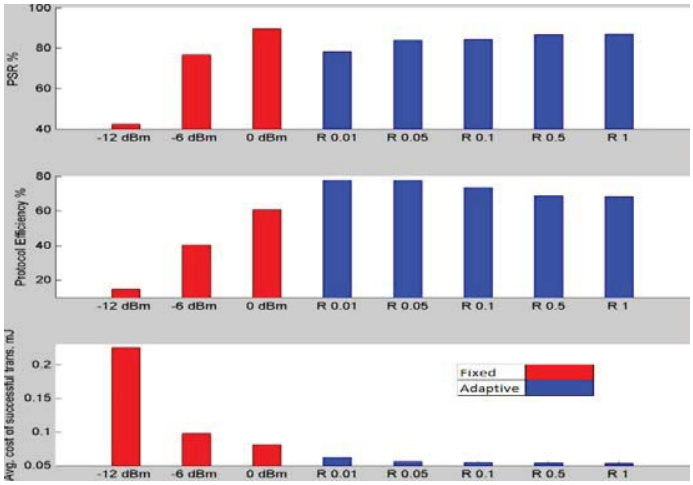


**Figure 70.** *Performance comparison of fixed and adaptive protocol. As expected, the PSR at fixed power of 0 dBm is the maximum but adaptive protocol at R value of 1 approaches that of 0 dBm. The efficiencies of adaptive and fixed power are comparable. The adaptive protocol at R = 1 consumes approximately 35% less energy than fixed power transmission (0 dBm)***.**

Figure 70 shows that the adaptive protocol at R = 1 consumes almost 35% less energy than the fixed power transmission (0 dBm) which is the minimum consumption power level.

Figure 70 shows similar results to the first set of data. Compared to the first set, the channel condition has deteriorated and that is reflected in the overall PSR values.

These preliminary experiments have given an overview as to how the adaptive protocol reacts to mobility in terms of PSR, efficiency and cost. However, in order to improve the PSR of the adaptive protocol when the sensor is at the fringe of the communicable link, the number of retry in state 4 should be set at higher values. In the next set of experiments that were conducted within University campus building, the retry limit in state 4 is set to 3 (Table 12).

## 6.5 Experimental results to compare performance of the adaptive system with fixed power system when sensors are mobile

In this section, the experimental results of the adaptive and fixed power transmission systems are presented. The primary objective of the experiment is to compare the energy costs and efficiencies of the adaptive protocol with that of the optimal power level of

fixed power transmission when they have a comparable packet success rate. The distance between the sensor and hub is changed with time. It has been a random walk during the busy hours inside the University campus building and repeated 5 times.

The design of the experiment is tabulated in Table 17.

**Table 17. Experimental design to test the performance when sensors are mobile**

| | | | |
|---|---|---|---|
| Number of packets sent during each transmission cycle | 9 packets | 4 packets at power levels -18 dBm, -12 dBm, -6 dBm and 0 dBm with retry limit set to 3 in each power level | 5 packets that follows the adaptive protocols at drop-off factors R 0.01, 0.05, 0.1, 0.5 and 1 |

Figures 71 to 75 compare the performance parameters.

### *Walk 1 Experimental data*

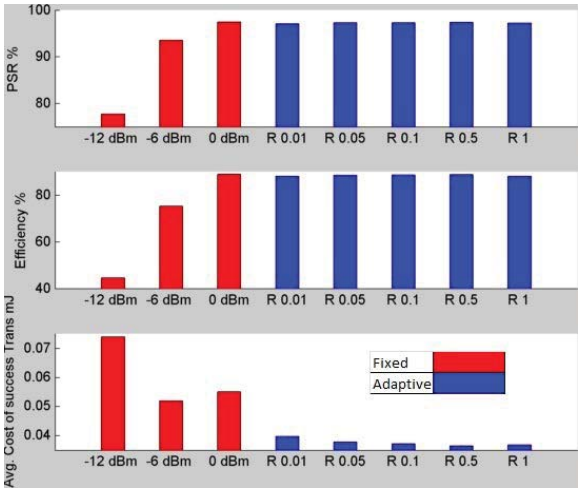


**Figure 71.** *PSR, Efficiency and cost per successful transmission plots based on random walk in University campus. For a PSR > 97%, the % efficiency is comparable at 88% while using 42% less power.*

The results of walk 1 are presented in Figure 71. The PSR values for -18 dBm are too low to be included in these plots. The minimum cost in fixed power transmission occurs at – 6 dBm. The PSR values of fixed power transmission (at -6 dBm) is comparable with that of the adaptive protocol when R = 0.5. The protocol efficiency at R =0.5 is comparable to that at -6 dBm. But, the adaptive protocol can save (up to) 42% energy as compared to fixed power transmission.

### *Walk 2 Experimental data*

The results of walk 2 are presented in Figure 72. The minimum cost in fixed power transmission occurs at -6 dBm. The PSR and the efficiency values of fixed power transmission (at -6 dBm) is comparable with that of the adaptive protocol when R = 0.1.

But, the adaptive protocol can save upto 27% energy as compared to fixed power transmission.

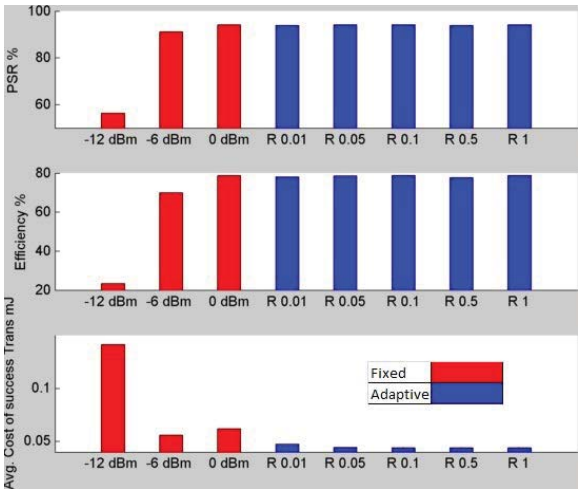


**Figure 72.** *PSR, Efficiency and cost per successful transmission plots based on random walk in University campus. For a PSR > 95%, the % efficiency values are same at 78% while the cost per successful transmission is reduced by 20% when adaptive power control at R = 0.1 is used over fixed transmission at -6 dBm.*

### *Walk 3 Experimental data*

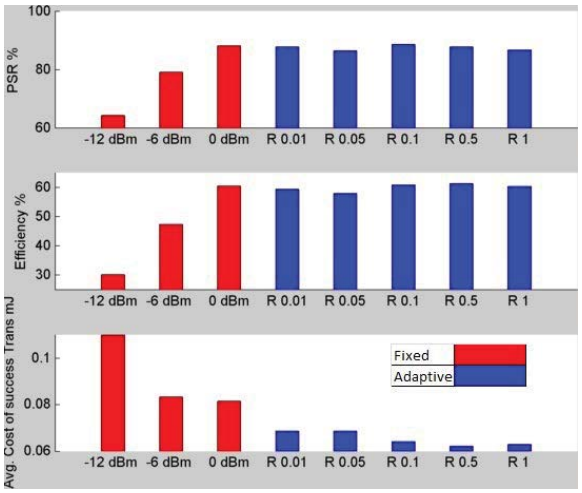


**Figure 73.** *PSR, Efficiency and cost per successful transmission plots based on random walk in University campus. For a PSR > 85%, the % efficiency values are same at 60% while the there is a reduction of approximately 25% in the cost.*

In walk 3, the minimum energy consumption at fixed power is achieved at -6 dBm (Figure 73). The PSR and the efficiency values of fixed power transmission (at -6 dBm) is comparable with that of the adaptive protocol when R = 0.1. But, the adaptive protocol can save upto 27% energy as compared to fixed power transmission.

### *Walk 4 Experimental data*

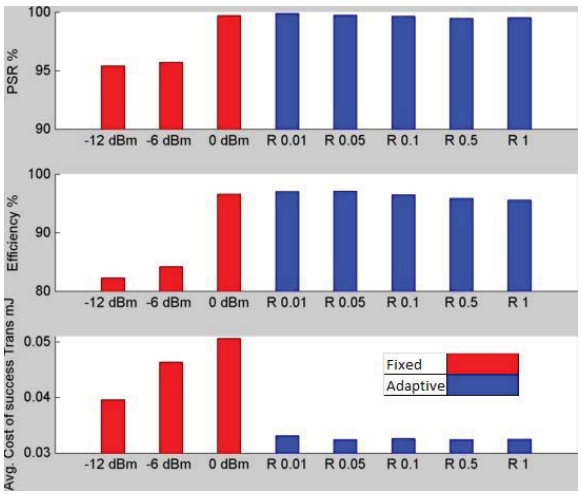


**Figure 74.** *PSR, Efficiency and cost per successful transmission plots based on random walk in University campus. For a PSR > 99%, the % efficiency values are same at 96% while using 22% less power when adaptive protocol is used at R = 0.5.*

The results of walk 4 are presented in Figure 74. The minimum cost in fixed power transmission occurs at -12 dBm. But, the adaptive protocol can save energy upto 22% at R = 0.5 as compared to fixed power transmission. The PSR and the efficiency values of the adaptive protocol when R = 0.5 are higher than the fixed power transmission at -12 dBm.

### *Walk 5 Experimental data*

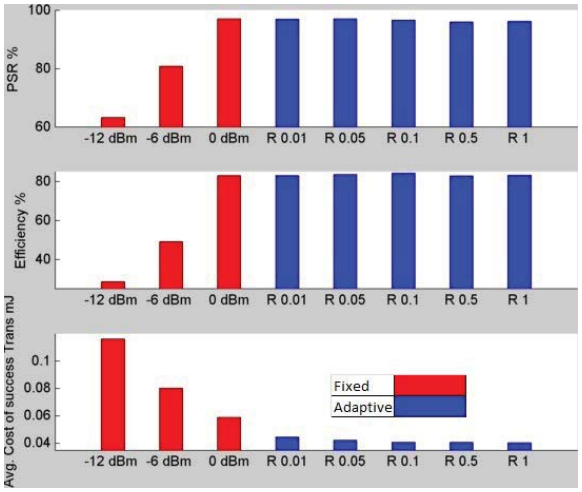


**Figure 75.** *PSR, Efficiency and cost per successful transmission plots based on random walk in University campus. For a PSR > 96%, the % efficiency values are more than 80%, while the there is a reduction of more than 45% in cost when adaptive protocol with R = 1.*

In walk 5, the minimum energy consumption at fixed power is achieved at 0 dBm (Figure 75). The adaptive protocol can save upto 45% energy as compared to fixed power transmission (at 0 dBm) when R = 1. The PSR and efficiency values are comparable.

Table 18 has tabulated the PSR, cost and protocol efficiency of fixed and adaptive protocol when used in mobile sensors.

**Table 18 Tabulated PSR, cost and protocol efficiency of fixed and adaptive protocol when used in mobile sensors**

| **Walk 1 Experimental data** | | | |
|---|---|---|---|
| **Transmission protocol** | **PSR (%)** | **Avg. cost per successful transmission (mJ)** | **Protocol efficiency (%)** |
| Fixed (-18 dBm) | 46.04 | 0.190302 | 16.34 |
| Fixed (-12 dBm) | 77.81 | 0.073918 | 44.61 |
| Fixed (-6 dBm) | 93.53 | 0.052041 | 75.25 |
| Fixed (0 dBm) | 97.46 | 0.055077 | 88.90 |
| S-APC ( R 0.01) | 97.06 | 0.039871 | 88.00 |
| S-APC ( R 0.05) | 97.28 | 0.037862 | 88.48 |
| S-APC ( R 0.1) | 97.30 | 0.037309 | 88.59 |
| S-APC ( R 0.5) | 97.38 | 0.036539 | 88.78 |
| S-APC ( R 1) | 97.26 | 0.036869 | 88.11 |
| **Walk 2 Experimental data** | | | |
| **Transmission protocol** | **PSR (%)** | **Avg. cost per successful transmission (mJ)** | **Protocol efficiency (%)** |
| Fixed (-18 dBm) | 25.64 | 0.398559 | 7.82 |
| Fixed (-12 dBm) | 56.45 | 0.141515 | 23.44 |
| Fixed (-6 dBm) | 91.18 | 0.056142 | 69.84 |
| Fixed (0 dBm) | 94.08 | 0.062348 | 78.69 |
| S-APC ( R 0.01) | 93.79 | 0.047747 | 77.96 |
| S-APC ( R 0.05) | 94.08 | 0.044786 | 78.56 |
| S-APC ( R 0.1) | 94.2 | 0.044175 | 78.80 |
| S-APC ( R 0.5) | 93.89 | 0.044369 | 77.66 |
| S-APC ( R 1) | 94.2 | 0.044175 | 78.80 |

| Transmission protocol | PSR (%) | Avg. cost per successful transmission (mJ) | Protocol efficiency (%) |
|---|---|---|---|
| **Walk 3 Experimental data** | | | |
| Fixed (-18 dBm) | 46.5 | 0.18669 | 16.65 |
| Fixed (-12 dBm) | 64.27 | 0.10993 | 30.12 |
| Fixed (-6 dBm) | 79.1 | 0.08336 | 47.29 |
| Fixed (0 dBm) | 88.125 | 0.081489 | 60.44 |
| S-APC ( R 0.01) | 87.75 | 0.068673 | 59.31 |
| S-APC ( R 0.05) | 86.425 | 0.068702 | 57.91 |
| S-APC ( R 0.1) | 88.6 | 0.064204 | 60.84 |
| S-APC ( R 0.5) | 87.75 | 0.062184 | 61.29 |
| S-APC ( R 1) | 86.72 | 0.063002 | 60.35 |
| **Walk 4 Experimental data** | | | |
| Fixed (-18 dBm) | 47.18 | 0.170793 | 18.18 |
| Fixed (-12 dBm) | 95.42 | 0.039617 | 82.29 |
| Fixed (-6 dBm) | 95.72 | 0.046395 | 84.19 |
| Fixed (0 dBm) | 99.69 | 0.050616 | 96.59 |
| S-APC ( R 0.01) | 99.87 | 0.033189 | 97.03 |
| S-APC ( R 0.05) | 99.72 | 0.032436 | 97.05 |
| S-APC ( R 0.1) | 99.63 | 0.032633 | 96.48 |
| S-APC ( R 0.5) | 99.45 | 0.032475 | 95.88 |
| S-APC ( R 1) | 99.51 | 0.032551 | 95.54 |
| **Walk 5 Experimental data** | | | |
| Fixed (-18 dBm) | 27.00 | 0.369136 | 8.44 |
| Fixed (-12 dBm) | 63.27 | 0.116138 | 28.53 |
| Fixed (-6 dBm) | 80.82 | 0.080218 | 49.13 |
| Fixed (0 dBm) | 96.97 | 0.059114 | 82.95 |
| S-APC ( R 0.01) | 96.87 | 0.044806 | 82.94 |
| S-APC ( R 0.05) | 970.. | 0.042459 | 83.62 |
| S-APC ( R 0.1) | 96.55 | 0.041010 | 84.27 |
| S-APC ( R 0.5) | 95.90 | 0.040928 | 82.92 |
| S-APC ( R 1) | 96.12 | 0.040506 | 83.22 |

## 6.6 Discussion

The results based on practical experiments are promising and demonstrates the usefulness of employing power control to achieve energy efficiency when sensor nodes are mobile. Overall, the energy consumption per successful transmission can be reduced by atleast 25%. This saving can go (up to) as much as 45% depending on the radio channel condition and the mobility of the sensor.

These experimental results also verify the initial findings using simulation. The advantage of the adaptive protocol is that it does not uses RSSI values for packet transmission. There are two distinct sections in the adaptive protocol. One section guides the system to move up in the state when channel condition deteriorates so that high output power is required. The other section set the rule for dropping-off to a lower state using back-off algorithm. It is able to adapt to link quality changes that are transient or long term. The proper choice of the drop-off parameter R can optimize energy efficiency. The experimental results indicate that optimal energy consumption can be achieved if the R value is set at in between 0.5 and 1. Simulation results gave the preliminary indication that the adaptive protocol can help in saving energy. The simulations have their limitations because they are conducted in controlled environment. All the experiments were conducted both during the busy and non-busy hour of the University. Therefore the radio environment is not typically controlled. Rather, the radio link is more dynamic, both temporally and spatially. The adaptive protocol is designed in such a fashion that it can make use of every opportunity to save energy. It is not a memory-less system and therefore Markovian mathematics cannot be applied to analytically calculate the costs and efficiencies. On the other hand, it is simple and light weight and can be applied to any type of wireless network that uses adaptive power control.

# Chapter 7 Performance comparison of RSSI based and proposed S-APC

In this chapter, simulations with MATLAB are used to compare the performance of RSSI-based output power control with non-RSSI based adaptive power in terms of saving energy and extend battery powered wireless sensor nodes. A general approach has been adopted for RSSI based power control protocol where the sensor node sends beacon packets to the base station at different power levels and builds the neighbourhood table that maps the output power levels with the RSSI values that it receives in the feedback path. This adaptive approach also uses RSSI information during run time when it is transmits data packets. The proposed non-RSSI based approach in this thesis uses information of successful packet transmissions to choose the appropriate power level. It also has drop-off algorithm that enables it to come back from higher to lower power level when deemed necessary. The contribution of this chapter is twofold. It shows that the non-RSSI based approach is more energy efficient than the RSSI based adaptive power control, primarily because it does not use beacon packets before data transmission and therefore has minimum overhead cost. In fact, the proposed protocol can save up-to 20% energy. This chapter also demonstrates that in an indoor multipath fading environment, a single value of RSSI is not sufficient to assess the link quality and accurately predict the output power level. A sufficient number of sample RSSI values are required, which can significantly increase the cost of total transmission.

## 7.1 Radio link quality estimators

In traditional link quality estimation, the transceiver sends probe packets to the destination nodes, either in unicast or broadcast modes, and senses the channel for feedback packets before the actual transmission commences. The first adaptive power control protocol for low power wireless communication was proposed by Shan Lin and et.al in [49]. That paper has introduced Adaptive Transmission power control (ATPC) that maintains a neighbour table at each node and a feedback loop for transmission power control between each pair of nodes. The general simulation model for RSSI based adaptive power control in this chapter has used the ATPC algorithm.

## 7.2 General approach to RSSI based adaptive power control

The basic principle behind the RSSI based adaptive power control system is guided by closed loop control between the transmitting node and the receiving base station mechanism. The general steps are described below:

- The transmitter sends packet at an updated power level to the receiver
- Receiver measures the RSSI

- If the RSSI is below the threshold required for faithful packet delivery, then the receiver sends the control packet with the new transmission power level.
- At the transmitter, the control packet is received and the current power level is updated for subsequent packet delivery

During initialization phase, the transmitter needs to know the power level at which it should transmit to successfully deliver the packet. In this phase, the transmitter sends several packets at all its available power levels. In return, it receives RSSI values for each power levels. Based on the mapping of the RSSI and the received $E_b/N_0$ value that is evaluated prior, the transmitter selects the required power level

- There is an initial overhead cost for building up the RSSI vs. Power level table.
- If the sensor is mobile, the refreshing frequency of the table becomes crucial and that also adds to the cost.

### 7.2.1 Validation of theoretical RSSI value using simulation

RSSI is a measurement of signal power and which is averaged over 8 symbols of each incoming packet [49].

The value of RSSI is dependent on the received power, the channel data rate and the noise spectral density ($N_0$).

If the received average bit energy is denoted by $E_b$ and channel data rate as R, then by definition, in linear scale,

$$RSSI = E_b * R \tag{25}$$

If this expression is rearranged to include the effect of noise floor ($N_0$)

$$RSSI = \left(\frac{E_b}{N_0}\right) * (N_0 * R) \tag{26}$$

In dBm,

$$RSSI = \frac{E_b}{N_0} + Noise\ Power \tag{27}$$

If the noise floor is assumed to be constant, the RSSI value will depend on the average bit energy and channel data rate.

In dBm scale, the relationship between the RSSI and $E_b/N_0$ is linear with intercept of -119.9978 dBm at x-axis when $E_b/N_0$ and RSSI are plotted on x-axis and y-axis respectively. Different data rates will have different intercept values when the noise floor level is kept constant.

The value of -119.9978 is derived from the value of $N_0$ and channel data rate set at 250 kbps for simulation.

$$Noise\ Power = KTR \tag{28}$$

where,

K = Boltzmann's constant (1.28 x $10^{-23}$ Joules/Kelvin)

T = Noise temperature in Kelvin (290) and

R = 250 kbps

Therefore the linear relationship between RSSI and $E_b/N_0$ takes the following form in equation (29) which is derived from equation (27).

$$RSSI = \frac{E_b}{N_0} - 119.9978 \tag{29}$$

In simulation, the RSSI values are plotted against the $E_b/N_0$ and the results are presented in figures 76-78. At different distances, the average RSSI values are calculated using a MATLAB simulation. The first 8 symbols of the FSK modulated signal are used to calculate the RSSI. The simulation parameters are presented in Table 19.

**Table 19. Simulation parameters to find relationship between RSSI and average $E_b/N_0$**

| | |
|---|---|
| Modulation technique | BFSK |
| Channel data Rate | 250 kbps |
| Maximum Doppler spread | 20 Hz |
| Packet size | 41 bytes |
| Cyclic redundancy check | CRC-16 |
| Multi-path Fading channel model | UMTS Indoor Office Test Environment [76] |
| Output power range | 0 to -25 dBm with step size of 1 dB |
| Number of samples of RSSI per transmission power level taken to calcuate the average RSSI value for the particular power level and distance | 100 |
| Path loss model used to calculate the average $E_b/N_0$ | Cost 231 indoor path loss model [76] |

The plots show the relationship between the RSSI and the average received $E_b/N_0$ at distances of 10, 20 and 30 m when the channel data rate is set at 250 kbps.

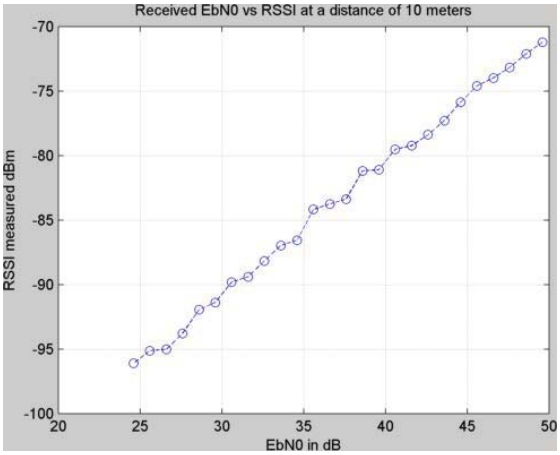


**Figure 76.** *A linear relationship is observed between RSSI and received $E_b/N_0$, both in log scale at distance of 10 m between the transmitter and the receiver with data rate of 250 kbps.*

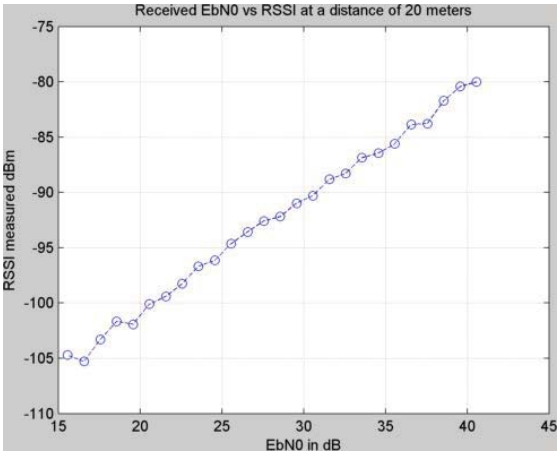


**Figure 77.** *A linear relationship is observed between RSSI and received $E_b/N_0$, both in log scale at distance of 20 m between the transmitter and the receiver with data rate of 250 kbps.*

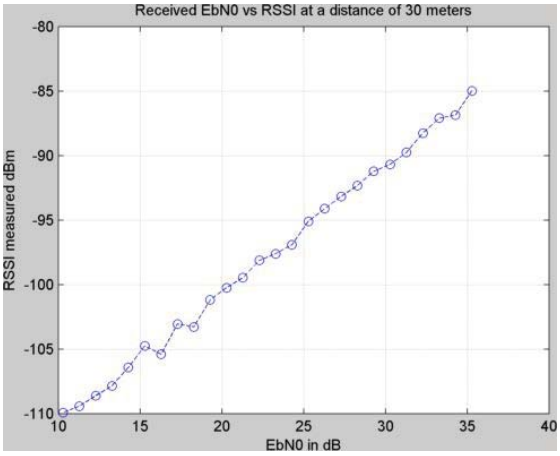


**Figure 78.** *A linear relationship is observed between RSSI and received $E_b/N_0$, both in log scale at distance of 30 m between the transmitter and the receiver with data rate of 250 kbps.*

In all these figures (76-78), the $E_b/N_0$ values are calculated using the Cost231 path loss model.

MATLAB curve fitting tool suggests the relationship between the values on x and y axes as

$$RSSI = 0.9987 * \frac{E_b}{N_0} - 120.45 \tag{30}$$

Equation (30) describes the relationship between the RSSI and the average $E_b/N_0$ values that is derived from simulation. This relationship closely matches the theoretical equation (29) validating the use of simulation result to compare the RSSI-based adaptive protocol with the proposed non-RSSI based adaptive protocol in the next section.

In fading radio environment, it is required to take enough samples of RSSI for every transmitted power level to ascertain the link quality. A small number of samples will give an inaccurate picture of the link quality as can be seen from the plot in Figure 79 that uses just 1 sample of RSSI.

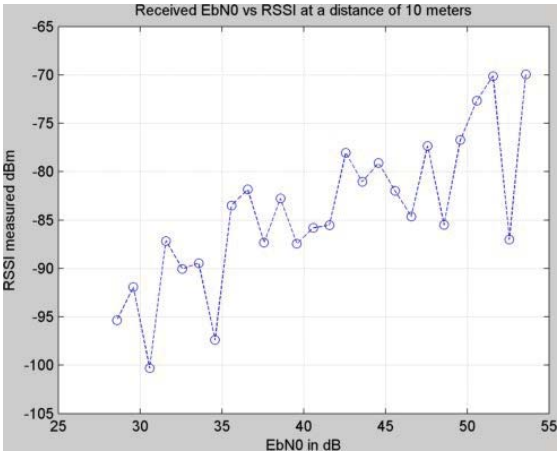


**Figure 79.** *A comparatively patchy or incomplete relationship between RSSI and $E_b/N_0$ is achieved when one sample of RSSI per output power level are plotted.*

## 7.3 Determining the threshold RSSI value for consistently high (> 95%) packet success rate based on its relationship with the average received $E_b/N_0$

In single hop wireless communication it is important to determine the output transmission power for high packet success rate. The transmission range can be defined by three regions that may have regular shape, dynamic bounds and specific features. They are generally determined by the average packet success rate. Table 20 shows the regions of the transmission range and corresponding PSR.

**Table 20. Transmission regions, PSR and features [37] [108]**

| Regions | PSR % | Features |
|---|---|---|
| Connected region | > 90% | Link with good quality and stable |
| Transition region | Between 10% and 90% | Unstable |
| Disconnected | < 10% | Link with poor quality and inadequate for communication |

It makes sense that a transmitting node must stay in the connected region by adjusting its transmission power so that a PSR of more than 90% is achieved. The plot of the $E_b/N_0$ vs. the PSR in Figure 80 from simulation shows that below 30 dB, the PSR value falls sharply from approximately 98% to 10% within a gap of 25 dB Therefore, in order for a wireless link to be in the connected region, the average $E_b/N_0$ should be above 30 dB.

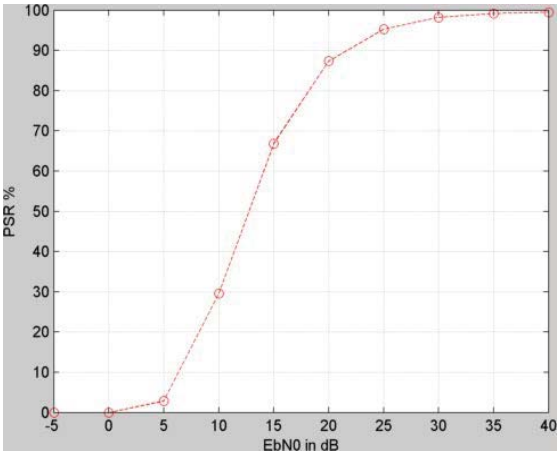


**Figure 80.** *Plot of PSR vs the average received $E_b/N_0$ with FSK modulation and channel data rate 250 kbps shows that in order to achieve a high PSR (>98%), the average received $E_b/N_0$ should be around 30 dB.*

From figures 76 to 78, it is can be found out that the RSSI value corresponding to $E_b/N_0$ of 30 dB is -90 dBm. From [48-49], it is known that in order to achieve high PSR of 99%, the threshold RSSI value should be around -87 dBm The simulated threshold RSSI value of -90 dBm closely matches with the findings of [48-49] in order to achieve a high PSR (>95%). Therefore, this RSSI value is used as the threshold for simulation with RSSI based adaptive power control algorithms.

Simulations with data rate of 100 kbps and 500 kbps have been conducted and plots of figures 81-84 show that the RSSI threshold should be around -90 dBm.

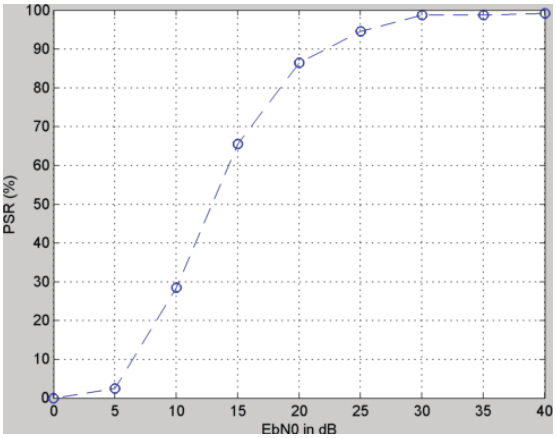


**Figure 81.** *Plot of PSR vs the average received $E_b/N_0$ with FSK modulation and channel data rate 100 kbps shows that in order to achieve a high PSR (>98%), the average received $E_b/N_0$ should be around 30 dB.*

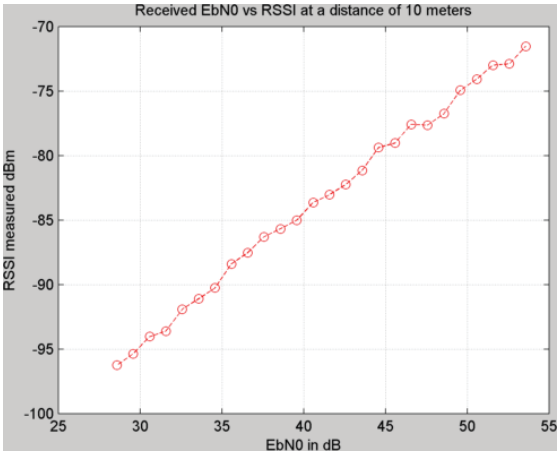


**Figure 82.** *A linear relationship is observed between RSSI and received $E_b/N_0$, both in log scale at distance of 10 m between the transmitter and the receiver when data rate of 100 kbps is set.*

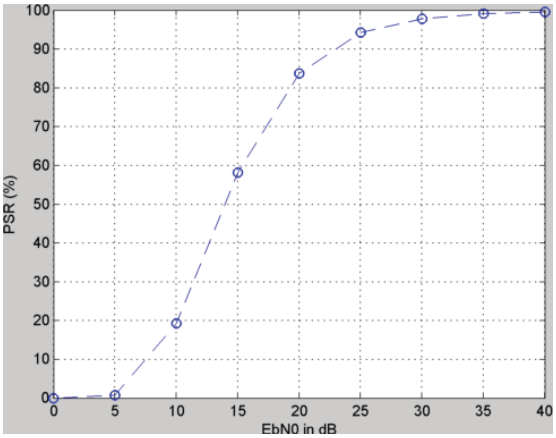


**Figure 83.** *Plot of PSR vs the average received $E_b/N_0$ with FSK modulation and channel data rate 500 kbps shows that in order to achieve a high PSR (>98%), the average received $E_b/N_0$ should be around 30 dB.*

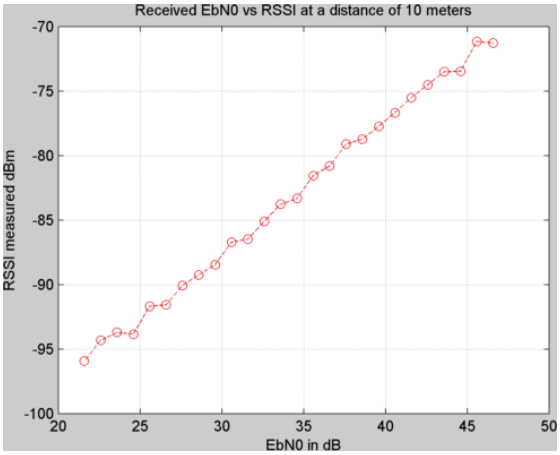


**Figure 84.** *A linear relationship is observed between RSSI and received $E_b/N_0$, (using log scales) at distance of 10 m between the transmitter and the receiver when data rate of 500 kbps is set.*

The next section discusses the ATPC protocol in details and the methodology used to simulate it.

## 7.4 ATPC: Adaptive transmission power control for wireless sensor networks

As mentioned earlier, the first adaptive power control protocol for wireless sensor network was proposed in [49]. Results show that the ATPC only consumes 53% of the transmission energy of the maximum transmission power solutions and 78.8 % of that of network level transmission power solutions [41]. In ATPC, the sensor nodes build a model for each of its neighbouring nodes that describe the correlation between the transmission power and the link quality. The radio link quality varies over time and with change in the environment. The objective of the ATPC protocol is to find out the minimum transmission power level to maintain a good quality link (~PSR > 98%) and dynamically change the transmission power level over time to address the time varying nature of the wireless channel. Each node sends beacon packets at different transmission power level to the neighbouring node and makes note of the RSSI value that it receives on the feedback path. Based on this information, the node builds a predictive model and uses least square approximation method to calculate the desired transmission power level.

In run time, it also monitors the link quality by using the information of RSSI and set the upper and the lower limits to the link quality estimator. As long as the RSSI value is steady and within the range, the transmitter is not required to adjust the power level. Therefore the upper and lower limits of RSSI are critical design parameter to make ATPC energy efficient. The other important parameters of ATPC protocol are the link quality threshold, the frequency of transmission power control and the number of beacon packets in the setup phase. Based on the empirical findings regarding the temporal variation of

the link quality, the paper proposed that one packet per hour would maintain the freshness of the predictive model [49].

However, the research work in this thesis is dealing with indoor radio environment that is temporally and spatially dynamic so that it is not predictable about when and how the link quality will change. There are three kinds of application areas that are being targeted. They are

- Industrial environments where link quality can be unexpected plagued by external noise and temperature and movements of objects and people
- Town shopping malls where there are peak hours and non-peak hours in terms of foot traffic and that can dynamically alter the radio link quality
- Mobile sensors used in industrial automation where there will be effect of distance dependent path loss on the radio link

Section 7.5 compares the general beacon based adaptive protocol with the proposed power control protocol in this thesis.

## 7.5 Simulation results analysis of the beacon based adaptive protocol

Taking the cue from ATPC protocol, this section considers a general beacon-based adaptive protocol that uses RSSI information for link quality assessment. It compares the cost function with the proposed non-RSSI based adaptive protocol that does not use beacon packets for channel estimation. The performance parameters are based on equations (5) and ().

### 7.5.1 Simulation design

In this research the cost calculation during transmission is considered only because the reception current is the same for all. The formula for cost calculation is given by equation (7). In simulation the minimum packet length is used for sending the beacon packets by the transmitter to receive the RSSI value that is embedded in the notification packet from the neighbouring node. It contains the overheads of 1 byte preamble, 5 byte address, 1 byte packet control value, 2 byte CRC and one byte of payload to carry the RSSI value. Therefore this is the minimum packet size that can be transmitted.

### 7.5.2 Simulation results for comparison of cost and efficiency between the ATPC and non-RSSI based adaptive power control

In ATPC mode, the transmitter periodically scans the radio link by transmitting beacon packets and keeping a note of the RSSI values from the notification packets on the feedback path. These RSSI information are used to create the neighbourhood table and determine the minimum transmission power required to maintain a good radio link (PSR

> 95%). During each scan or sampling, there are 20 packets sent at each power level to build an appropriate relationship between the transmission power and the RSSI values. A sample neighbouring table is shown in Table 21.

**Table 21. Sample neighbourhood table**

| Transmission Power | Mean RSSI (dBm) |
|---|---|
| -18 dBm | -103.899 |
| -12 dBm | -99.115 |
| -6 dBm | -91.4 |
| 0 dBm | -88.86 |

The condition to choose the appropriate output power level for packet transmission is derived from the relationship between the RSSI and PSR in section 7.3 of the current chapter. For consistent high (> 95%) PSR, the RSSI value should be above -90 dBm. Based on this condition and the neighbourhood table (shown in Table 21), the output power of 0 dBm is chosen for next n transmission when the radio link is scanned again. In simulation, the values of n that are used are 1, 10, 100, 1000 and 1000. The value of n equal to 1 implies that the channel is scanned only in the beginning of transmission. The sensor transmitter sends 20 beacon packets per output power level and calculates the average of the RSSI values that are piggybacked on the notification packets by the neighbouring sensors.

**Overhead cost due to link scanning:** In the energy cost function, the transmission and reception costs of the beacon and notifications packets are included as the overhead cost. The average received $E_b/N_0$ values used in the simulations are based on the distance between the sensor and the hub and the number of wall type I between them. The number of all walls of type I in this research is taken as 4. The distances that are selected are 5 m, 10 m, 15 m, 20 m and 25 m. The calculated $E_b/N_0$ values are shown in Table 22.

**Table 22. $E_b/N_0$ values derived from the distance and number of separations using Cost231 model**

| Distance | Number of Wall type I: Light internal walls | Number of Wall type II: internal walls | Average received $E_b/N_0$ based on Cost231 path loss model at minimum (-18 dBm) output power |
|---|---|---|---|
| 5 m | 4 | 0 | 30 dB |
| 10 m | 4 | 0 | 21 dB |
| 15 m | 4 | 0 | 16 dB |
| 20 m | 4 | 0 | 12 dB |
| 25 m | 4 | 0 | ~ 10 dB |

Figures 79 to 83 compare the cost of successful transmissions at different distances with variable scanning or sampling rate of link quality for transmission power control. In each of these bar charts, the average base $E_b/N_0$ is calculated based on the path loss due to transmission at the lowest power level (-18 dBm).

From Figure 85 to Figure 89 it is seen that the average energy consumption per successful transmission is the lowest when the radio link is scanned once. This makes sense because the more often the channel quality is assessed more is the overhead cost. This scanning interval is, therefore, the optimal interval for link quality estimation with minimum cost. These cost values are compared with the adaptive protocol at different R values. In all the simulation 100% PSR is achieved. The efficiency values are all high (>97%). These values are not plotted as the primary objective is to find an energy efficient solution for a satisfactory PSR value.

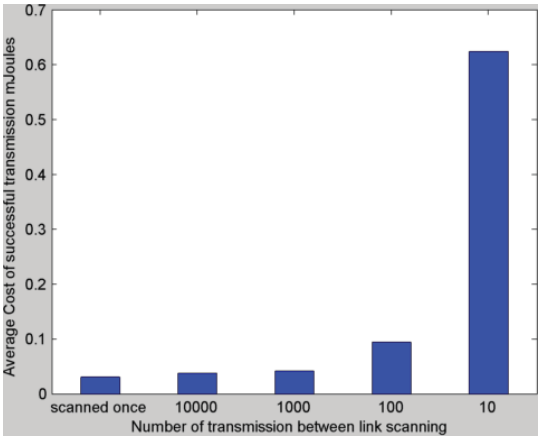


**Figure 85.** *Comparison of cost of successful transmission at different frequencies of scanning at distance of 5 m between the transmitter and receiver and 4 type-1 walls resulting in average $E_b/N_0$ of 30 dB at lowest transmission power level of -18 dBm.*

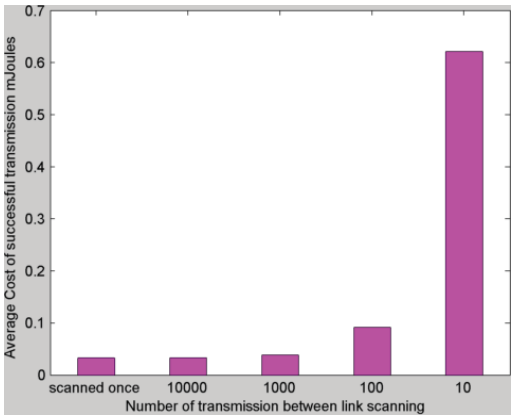


**Figure 86.** *Comparison of cost of successful transmission at different frequencies of scanning at distance of 10 m between the transmitter and receiver and 4 type-1 walls resulting in average $E_b/N_0$ of 21 dB at lowest transmission power level of -18 dBm.*

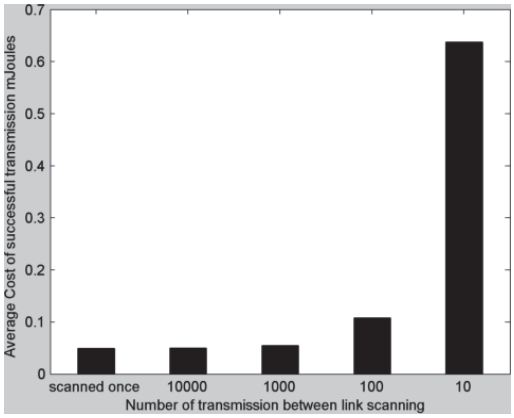


**Figure 87.** *Comparison of cost of successful transmission at different frequencies of scanning at distance of 15 m between the transmitter and receiver and 4 type-1 walls resulting in average $E_b/N_0$ of 16 dB at lowest transmission power level of -18 dBm.*

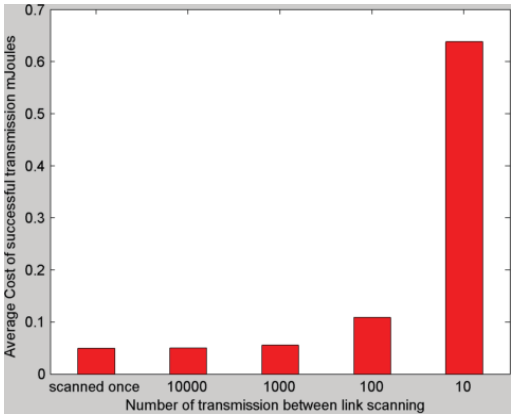


**Figure 88.** *Comparison of cost of successful transmission at different frequencies of scanning at distance of 20 m between the transmitter and receiver and 4 type-1 walls resulting in average $E_b/N_0$ of 12 dB at lowest transmission power level of -18 dBm.*

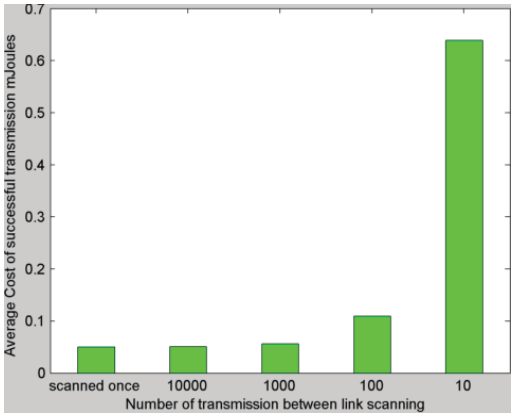


**Figure 89.** *Comparison of cost of successful transmission at different frequencies of scanning at distance of 25 m between the transmitter and receiver and 4 type-1 walls resulting in average $E_b/N_0$ of 10 dB at lowest transmission power level of -18 dBm.*

## 7.6 Comparison of the energy cost of beacon-based (uses RSSI measurement) power control algorithm with S-APC

Figures 90 to 94 compare the minimum energy cost value of RSSI-based power control with the energy cost values of non-RSSI based adaptive power control at different drop-offs rates (R). In each of these bar charts, the average base $E_b/N_0$ is calculated based on the path loss due to transmission at the lowest power level (-18 dBm). The number of beacon packets that are sent per output power level is equal to 20.

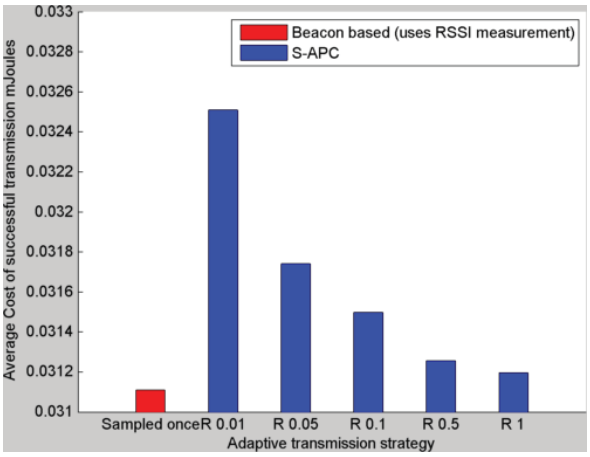


**Figure 90. Distance 5 m. Average $E_b/N_0$ = 30 dB at Transmission power = -18 dBm.** *Comparison of average cost per successful transmission shows that beacon based power control scheme (using RSSI information) with single scanning only saves 0.5% energy as compared to S-APC at R = 1.*

Figure 90 shows that beacon based power control scheme (using RSSI information) with single channel scanning is nominally better than the proposed S-APC protocol in terms of saving energy consumption.

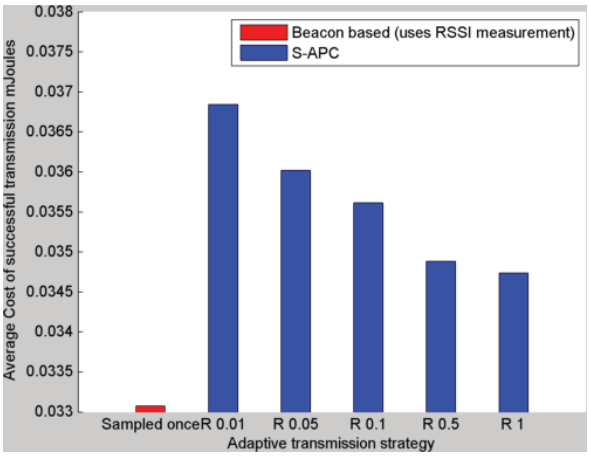


**Figure 91. Distance 10 m. Average $E_b/N_0$ = 21 dB at Transmission power = -18 dBm.** *Comparison of average cost per successful transmission shows that beacon based power control scheme (using RSSI information) with single scanning saves 5% energy as compared to S-APC at R = 1.*

Figure 91 shows that beacon based power control scheme (using RSSI information) with single channel scanning saves only 5% energy as compared to the proposed non-RSSI based adaptive protocol.

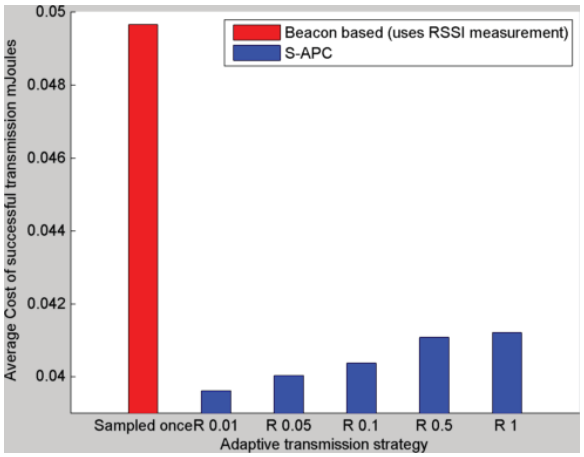


**Figure 92. Distance 15 m. Average $E_b/N_0$ = 16 dB at Transmission power = -18 dBm.** *Comparison of average cost per successful transmission shows that beacon based power control scheme (using RSSI information) with single scanning consumes 20% more energy than S-APC at R = 0.01.*

Figure 92 shows that beacon based power control scheme (using RSSI information) with single channel scanning consumes 20% more energy than the proposed non-RSSI based adaptive protocol.

This plot shows that as the channel link quality degrades in terms of average $E_b/N_0$ (from 30 dB to 16 dB), the proposed adaptive protocol can prove to be more energy efficient as compared to the beacon-based adaptive power control using RSSI.

In figures 90 to 92, the bar graphs demonstrate the useful of using a non-RSSI based adaptive power control protocol. The percentage energy reductions in these scenarios are 15% and 10% respectively. This is expected because the link quality has deteriorated further and packets will be dropped more often. This will lead to the increase in energy consumption in both beacon-based and non-beacon based adaptive protocols. Therefore, a big reduction in energy consumption is not possible.

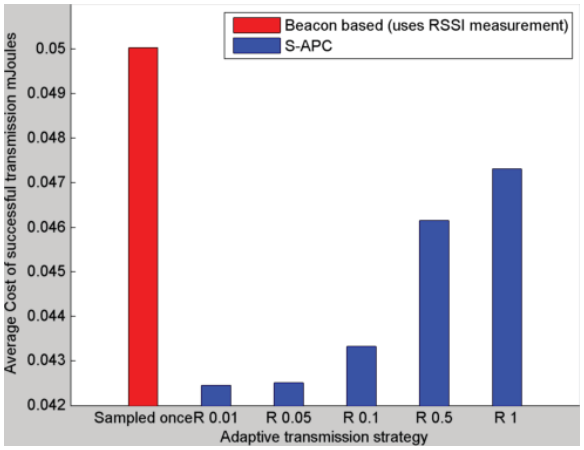


**Figure 93. Distance 20 m. Average $E_b/N_0$ = 12 dB at Transmission power = -18 dBm.** *Comparison of average cost per successful transmission shows that beacon based power control scheme (using RSSI information) with single scanning consumes 15% more energy than S-APC at R = 0.05.*

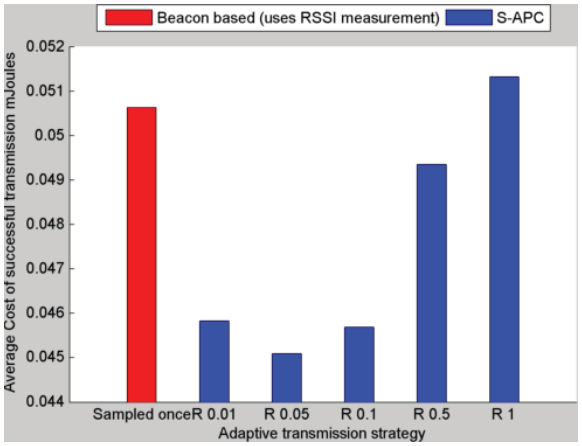


**Figure 94. Distance 25 m. Average $E_b/N_0$ = 10 dB at Transmission power = -18 dBm.** *Comparison of average cost per successful transmission shows that beacon based power control scheme (using RSSI information) with single scanning consumes 10% more energy than S-APC at R = 0.05.*

In figure 93 and 94, the beacon-based adaptive protocol performs better than the proposed S-APC protocol. This is because the channel link quality is good (average $E_b/N_0$ > 20 dB at -18 dBm transmission power) and any adaptation will not contribute to tangible energy savings. When the average $E_b/N_0$ ~ 15 dB (at -18 dBm transmission power), S-APC proves to be more energy efficient than the RSSI based protocols. In fact, the RSSI-based protocol can consume up to 20% more energy. However, as link quality deteriorates further ($E_b/N_0$ < 15 dB), the energy savings get reduced because packets will be dropped more often. This will lead to the increase in energy consumption in both beacon-based and non-beacon based adaptive protocols

The choice of drop-off rate (R) is important in saving energy. However, the bar graphs in Figures 84-88 shows that any of the R values can be used to save energy.

## 7.7 Trade-off between the accuracy of predicting the transmission power and cost

In the beacon based adaptive power control protocol, the channel is scanned to evaluate the link quality after a certain number of transmissions. This is referred to as the channel scanning or sampling rate. It is the number of transmission after which the transmission power control is invoked. After each scanning, the current output power level may be altered to meet the link quality requirement. The sampling rate and the number of sample packets during each scan can influence the accurate prediction of transmission power and the overall energy consumption. A high sampling rate and sample packets will help to accurately track link quality change. However that adds to the overhead cost. The step size of output power level can also influence the adjustment of transmission power. However, real world RF modules have finite and discrete power levels. In our simulation, the available output power levels are -18 dBm, -12 dBm, -6 dBm and 0 dBm with a step size of 6 dB.

The feedback sampling rate will depend on how fast the link quality changes over time and the data traffic. Higher the link quality dynamics change, higher is the sampling rate required to ascertain the appropriate power level. When the data traffic is higher than the sampling rate, the notification packets can be sent as and when required. An indoor radio environment is considered dynamic and a reasonable sampling rate must be maintained irrespective of the data traffic.

The number of packets per transmission power level is also important to evaluate the RSSI values. A single value is unlikely to be accurate enough while too many packets will increase the overhead cost.

## 7.8 Simulation results with different beacon packets sent per output power level

In the section, more simulation results of RSSI based adaptive protocol are presented to demonstrate the effect of using different number of packets for accurate RSSI estimation using the same range of sampling rates. In simulation, two different values of beacon packets are selected that will be used for RSSI calculation. They are 1 and 10. The aim of these simulations is to find out if a lower value of the number of beacon packet can save energy consumption by reducing the amount of overhead energy cost that is incurred when they are transmitted.

### 7.8.1 Simulation results with 10 beacon packets sent per output power level

Figures 90 to 94 plot and compare the energy expenditure of beacon based adaptive protocol with the non-RSSI based adaptive power control when the RSSI is measured from one sample of RSSI value.

They show that a small sample value of RSSI can actually lead to more expenditure because of its less accurate measurement of RSSI and prediction of the output power level as compared to a large sample value per output power level.

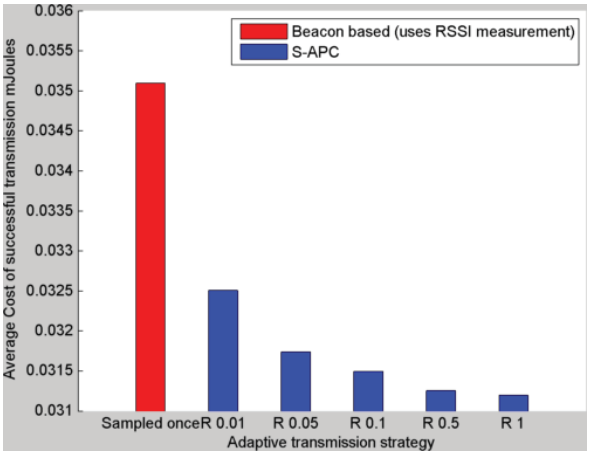


**Figure 95. Distance 5 m. Average $E_b/N_0$ = 30 dB at Transmission power = -18 dBm** *Comparison of average cost per successful transmission shows that beacon based power control scheme (using RSSI information) with single scanning consumes 12.5% more energy than S-APC.*

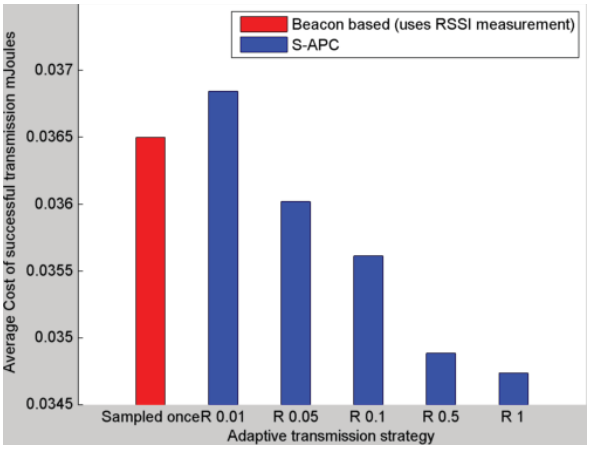


**Figure 96. Distance 10 m. Average $E_b/N_0$ = 21 dB at Transmission power = -18 dBm** *Comparison of average cost per successful transmission shows that beacon based power control scheme (using RSSI information) with single scanning consumes 5% more energy than S-APC.*

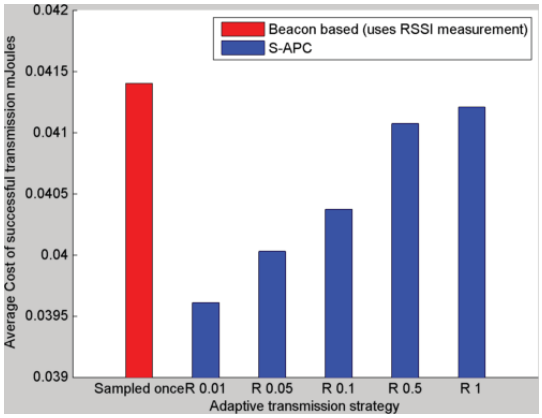


**Figure 97. Distance 15 m. Average $E_b/N_0$ = 16 dB at Transmission power = -18 dBm** *Comparison of average cost per successful transmission shows that beacon based power control scheme (using RSSI information) with single scanning consumes 4.5% more energy than S-APC.*

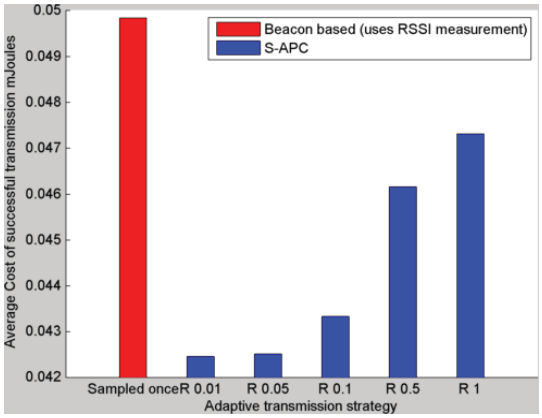


**Figure 98. Distance 20 m. Average $E_b/N_0$ = 12 dB at Transmission power = -18 dBm** *Comparison of average cost per successful transmission shows that beacon based power control scheme (using RSSI information) with single scanning consumes 17% more energy than S-APC.*

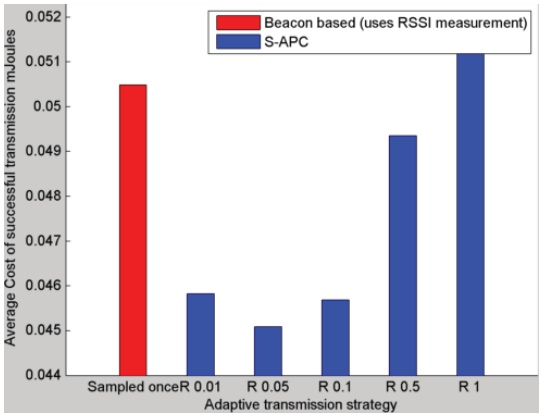


**Figure 99. Distance 25 m. Average $E_b/N_0$ = 10 dB at Transmission power = -18 dBm** *Comparison of average cost per successful transmission shows that beacon based power control scheme (using RSSI information) with single scanning consumes 12% more energy than S-APC.*

Overall, it can be concluded from the results of the plots in figures 95-99 that when the number of beacon packet sent per output power level is 1, the beacon based channel estimation and power control protocol consumes (atleast) 10% more energy than the proposed non-RSSI based adaptive power control protocol.

### 7.8.2 Simulation results with 1 beacon packet sent per output power level

Figures 94 to 98 compare the optimal average cost of successful transmission of RSSI-based protocol with the proposed adaptive protocol.

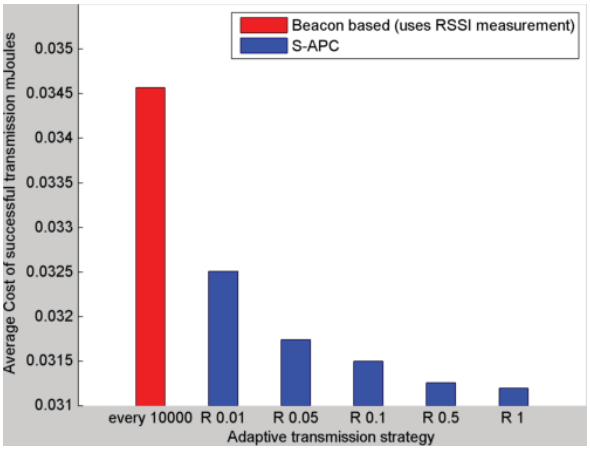


**Figure 100. Distance 5 m. Average $E_b/N_0$ = 30 dB at Transmission power = -18 dBm**. *Comparison of average cost per successful transmission shows that beacon based power control scheme (using RSSI information) with single scanning consumes 11% more energy than S-APC.*

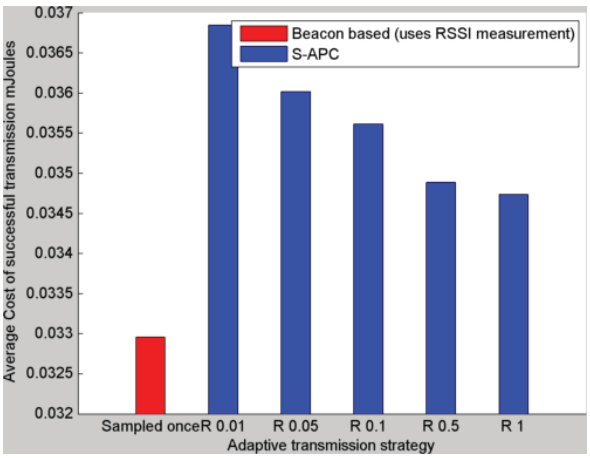


**Figure 101. Distance 10 m. Average $E_b/N_0$ = 21 dB at Transmission power = -18 dBm**. *Comparison of average cost per successful transmission shows that beacon based power control scheme (using RSSI information) with single scanning consumes 5% more energy than S-APC.*

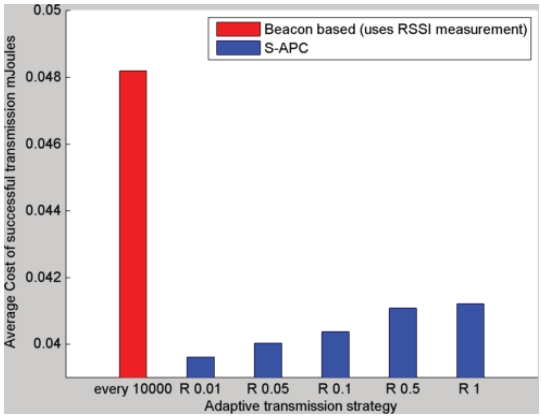


**Figure 102. Distance 15 m. Average $E_b/N_0$ =16 dB at Transmission power = -18 dBm**. *Comparison of average cost per successful transmission shows that beacon based power control scheme (using RSSI information) with single scanning consumes 21% more energy than S-APC.*

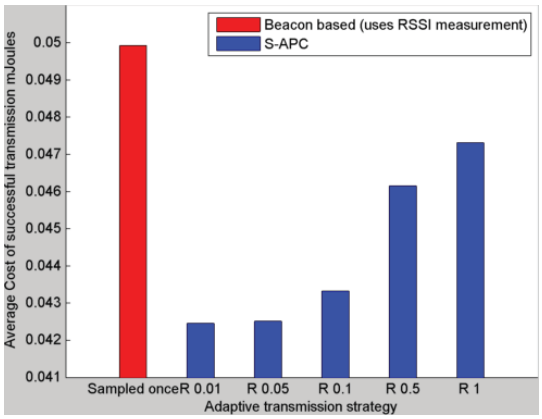


**Figure 103. Distance 20 m. Average $E_b/N_0$ = 12 dB at Transmission power = -18 dBm**. *Comparison of average cost per successful transmission shows that beacon based power control scheme (using RSSI information) with single scanning consumes 17% more energy than S-APC.*

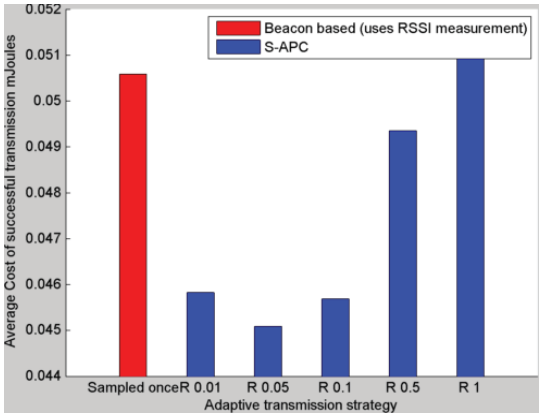


**Figure 104. Distance 25 m. Average $E_b/N_0$ = 10 dB at Transmission power = -18 dBm**. *Comparison of average cost per successful transmission shows that beacon based power control scheme (using RSSI information) with single scanning consumes 12% more energy than S-APC.*

The packet success rate and the efficiency parameters in all these cases are 100% and around 98% respectively and therefore not plotted. The results in the plots show that an inaccurate RSSI value actually increases the over-all energy consumption.

The higher cost with beacon-based scheme is due to inaccurate link quality estimation with the RSSI values that are obtained from the beacon packets. At high $E_b/N_0$ (> 20), the RSSI-based and the proposed adaptive scheme have comparable energy efficiency. At lower $E_b/N_0$, the non-RSSI based adaptive scheme saves energy as compared to RSSI-based protocol.

## 7.9 Discussions

This chapter has evaluated and compared the cost per successful transmission of a general adaptive power control protocol that uses RSSI values for power control with that of the proposed non-RSSI based power control protocol introduced in this thesis. In an indoor multipath fading radio environment, a sufficient number of RSSI values are required per output power level during initial link quality modelling that maps RSSI to the power levels. In run time, a single value of RSSI may not be enough to decide the next output power level accurately. A faulty decision can make the transmitter to radiate at a higher power than is required to successfully transmit a data packet. On the other hand, it can decide to step down power and data transmission can fail. In simulation, the number of samples per output power levels and the sampling rate of link quality to control the output power are varied to study the impact of these parameters on the energy efficiency. As expected, it costs less when there are one sample packet sent per output power level. However, the cost values of the proposed adaptive protocol at different drop-off rates are less than the cost per successful transmission when RSSI-based protocol is used.

The next chapter compares the performance of the non-RSSI adaptive power control protocol with the RSSI based ATPC protocol in run time when does not use beacon packets for channel estimation but uses the piggybacked RSSI values (emulating real world RSSI variation) that are sent in acknowledgement packets by the receiver to set the power level of subsequent packets.

# Chapter 8 Use of real world RSSI data to compare performance of S-APC with ATPC and fixed power transmission

This chapter compares the performance parameters of three different strategies of transmission in sensor network using Matlab simulation. They are

- Fixed power transmission
- RSSI based adaptive transmission (ATPC)
- Proposed non-RSSI based adaptive transmission

Since nRF24L01p does not provide RSSI information, in order to compare performance of the RSSI based adaptive transmission power control (ATPC) protocol with the proposed non-RSSI based output power control protocol in real world scenarios, instead the RSSI data of WIFI beacon packets are used by the ATPC protocol. These beacon packets are transmitted from the WIFI access points. Beacon frames are transmitted by the Access Point (AP) in an infrastructure basic service set (BSS). The beacon frame is one of the management frames in IEEE 802.11 based WLANs. It contains all the information about the network. Beacon frames are transmitted periodically to announce the presence of a wireless LAN [109] [110]. The reason to use the WIFI beacon packets is because both WIFI and nRF24L01p operate in the same frequency band (ISM 2.5 GHz) and the nature of path loss will be similar.

This RSSI values are used by the ATPC protocol when it decides to use a particular power level for a packet transmission. Since the AP transmits at a fixed power level, any variation in the RSSI value is an indication of the link quality variation. This link quality change can be transient or may have an effect over a longer period of time. Therefore the RSSI values can be used to adapt or manipulate the output power. This setup emulates the real world approach of ATPC protocol where the RSSI values from the neighbouring node in response to the beacon signal are used to setup the output power level in the initialization phase or during run time. However, the channel data rates are different. But we are interested in the variation of link quality and the corresponding RSSI values.

## 8.1 Collection of the RSSI values

The NetSurveyor tool [111] was used to collect RSSI of beacon signals from a wireless access point that are send every 5 seconds. NetSurveyor is an 802.11 (Wi-Fi) network scanning and discovery tool that gathers information about nearby wireless access points in real time. These RSSI values give a measurement of how the received $E_b/N_0$ changes over time.

In this simulation scenario, a wireless sensor receives these RSSI values in response to the acknowledgement from the neighbouring node. In the single hop topology, it is the hub that piggybacks the RSSI information to the sensor. A 5 second interval between fresh RSSI values indicates that the sensor is transmitting at a rate of 1 packet every 5 seconds and therefore has received the RSSI value as the feedback from the hub.

### 8.1.1 Data collection scenarios

There are two types of RSSI variation scenarios that are investigated. They are collected from three different environments after an interval of 5 seconds. They are

- Three sets of long term data over a period of approximately 10 hours from within University campus building. The distance between the transmitter and receiver is approximately 24 meters. They represent the long term variation of RSSI during University opening hours.
- Three sets of short term data over the busy period of the day (approximately between 90 minutes and 120 minutes) from town shopping centre. The distance between the transmitter and receiver is approximately 30 meters.
- Three set of short term data over the busy period of the day (approximately between 90 minutes and 120 minutes) from University dining hall. The distance between the transmitter and receiver is approximately 25 meters.

Images of the mentioned scenarios are added in appendix B. The mapping of the RSSI with the average received $E_b/N_0$ follows equation (27).

$$RSSI = \frac{E_b}{N_0} + Noise\ Power \tag{31}$$

### 8.1.2 Simulation parameters:

The general simulation parameters are presented in Table 23.

**Table 23. Simulation parameters for comparison of ATPC with non-RSSI based adaptive protocol in MATLAB**

| | |
|---|---|
| Modulation technique | BFSK |
| Channel data Rate | 250 kbps |
| Maximum Doppler spread | 20 Hz |
| Packet size | 41 bytes |
| Cyclic redundancy check | CRC-16 |
| Multi-path Fading channel model | UMTS Indoor Office Test Environment |
| $E_b/N_0$ | Derived from the RSSI values |
| Retry limit in fixed power transmission and ATPC | 3 |
| Retry limit to highest power level in state 4 of adaptive | 3 |

| protocol | |
|---|---|
| RSSI threshold | -90 dBm |

### 8.1.3 Working principle of ATPC

The ATPC protocol changes its output power based on the RSSI value of the most recent transmitted packet. It has four power levels to choose from and uses the decision matrix as explained in Table 24. It explains the conditions under which the ATPC will change the output power level. On the left column we have the current power levels. The 2nd top row contains the new transmission power levels. RSSI_TH is the threshold RSSI value that is required to successfully detect a packet.

**Table 24. Decision matrix table of ATPC on run time**

| | | New transmission power level | | | |
|---|---|---|---|---|---|
| | | -18 dBm | -12 dBm | -6 dBm | 0 dBm |
| **Current Power level** | -18 dBm | RSSI >= RSSI_TH | **RSSI_TH - RSSI <= 6 dB** | **6 dB < RSSI_TH - RSSI < 12 dB** | RSSI_TH - RSSI >=12 dB |
| | -12 dBm | RSSI - RSSI_TH >= 6 dB | **RSSI - RSSI_TH ~ 0 dB** | **RSSI_TH - RSSI <=6 dB** | RSSI_TH - RSSI >= 6 dB |
| | -6 dBm | RSSI- RSSI_TH >= 12 dB | RSSI- RSSI_TH <= 6 dB | **RSSI - RSSI_TH ~ 0 dB** | **RSSI_TH- RSSI <= 6 dB** |
| | 0 dBm | RSSI- RSSI_TH >= 18 dB | 6 dB < RSSI – RSSI_TH <= 12 dB | RSSI – RSSI_TH <= 6 dB | **RSSI - RSSI_TH ~ 0 dB** |

During each cycle of power control, the ATPC compares the present RSSI with the RSSI_TH. If the difference between the current RSSI and RSSI_TH is negligible or equal to 0, then the new power level is same as the old power level. These conditions are highlighted in bold brown. Only when the current power level is -18 dBm and RSSI is greater than the RSSI_TH, it sticks to -18 dBm.

***Conditions when to ramp up output power:***

When **RSSI_TH > RSSI**, it is required to ramp up power for subsequent packets.

When **RSSI_TH - RSSI ≤ 6 dB**, the output power is incremented by 6 dB. For example, when current output power is -12 dBm, then new power level will be -6 dBm. These conditions are highlighted in bold blue.

When **6 dB < RSSI_TH - RSSI < 12 dB**, then the output power level is incremented by 12 dB. For example, if the current output power is -18 dBm, then new power level will be -6 dBm. These conditions are highlighted in bold black.

When **RSSI_TH - RSSI ≥ 12 dB** and the current power level is -18 dBm, then the new power level will be 0 dBm.

When **RSSI_TH - RSSI ≥ 6 dB** and the current power level is -12 dBm, then the new power level will be 0 dBm.

***Conditions when to ramp down output power:***

When **RSSI - RSSI_TH ≥ 18 dB** and output power is 0 dBm, then power level can be decremented by 18 dB to -18 dBm as that will satisfy **RSSI ≥ RSSI_TH**.

But when **6 dB < RSSI – RSSI_TH ≤ 12 dB,** the output power level decrements to -12 dBm. When **RSSI – RSSI_TH ≤ 6 dB,** the output power level decrements by 6 dB.

When **RSSI - RSSI_TH ≥ 6 dB** and current power level is -12 dBm, then the current power level can be decremented by 6 dB to -18 dBm.

Finally when the current power level is -6 dBm and **RSSI- RSSI_TH ≤ 6 dB,** the power level decrements to -12 dBm, while if **RSSI- RSSI_TH ≥ 12 dB**, it decrements by 12 dB.

It is known that the minimum RSSI level to maintain high PSR (> 95%) is -90 dBm. Therefore -90 dBm is set as the minimum threshold. Here RSSI_TH is the RSSI threshold and RSSI is the received signal strength indicator of the transmitter packet. In this simulation, the performances of the ATPC are observed at channel sampling/scanning interval of 1, 5, 10, 50 and 100 transmissions.

## 8.2 Comparison of the minimum cost values of ATPC, S-APC and fixed power transmission using RSSI data

In section 8.2, three sets of RSSI data are collected from three different locations. They are divided into long term data and short term busy-hour data. These sets of RSSI values are used in simulation for ATPC protocol and the performance parameters are compared with the fixed power and adaptive power control protocols.

### 8.2.1 Long term RSSI data collected over a period of approximately 10 hours inside University building

Three sets of data are collected during the period of approximately 10 hours. The busy hour RSSI variation was captured by logging the data between 8:30 am till 5 pm. These RSSI values are converted to the corresponding $E_b/N_0$ using Equation 32.

$$RSSI = \frac{E_b}{N_0} - 119.9978 \tag{32}$$

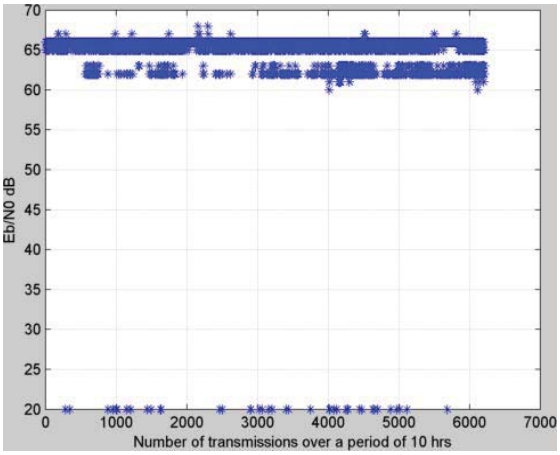


**Figure 105. University building- long term variation.** *Variation of the average $E_b/N_0$ over time. Along x-axis, the numbers of transmissions are noted. The average $E_b/N_0$ is quite high (>60 dB) and occasionally dropped to 20 dB. Since the distance between the access point and the laptop is constant, the drop in the value is attributed to human movements in between and multipath effects.*

The variation of the $E_b/N_0$ over time inside a University building is shown in Figure 105. The normalised frequency distribution plots of the average of the three data sets of $E_b/N_0$ are shown in Figure 106. The channel condition is very good with occasional drop to 35 dB.

### *Normalised frequency distribution plot of data set inside a University building*

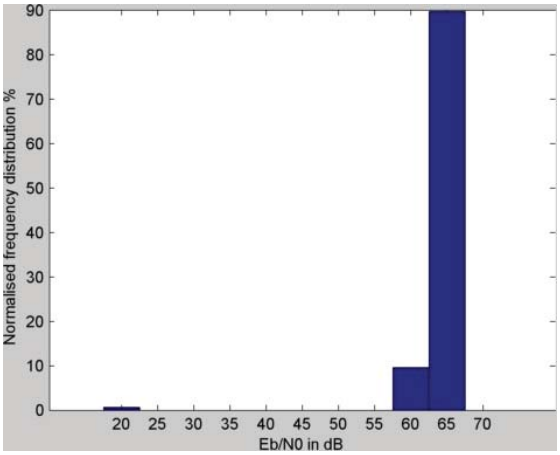


**Figure 106. University building long- term variation.** *The distribution plot of the received $E_b/N_0$ from data set 1 shows the wide variation over a range of 40 dB. The proportion of $E_b/N_0$ values at around 20 dB is appreciable. This has significantly contributed to high standard deviation.*

Plots of the average cost of successful transmission in each of the schemes are shown in figures 107 to 109. The PSR and the efficiency values in all these cases are 100% and higher than 99% respectively and their differences are negligible. Therefore they are not plotted.

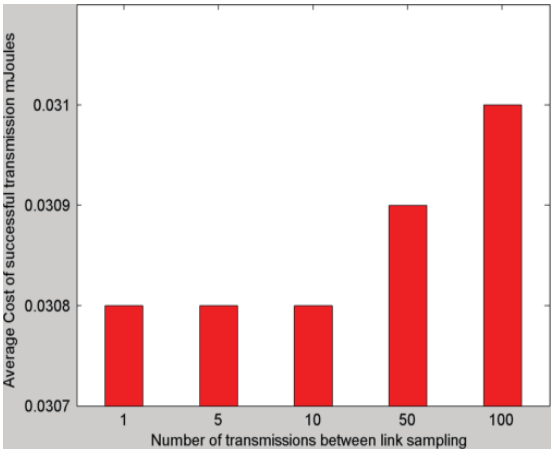


**Figure 107. University building.** *Plot of average cost of successful transmission at different link sampling rates when **ATPC** is used. There are no significant differences in the cost due to different sampling rates.*

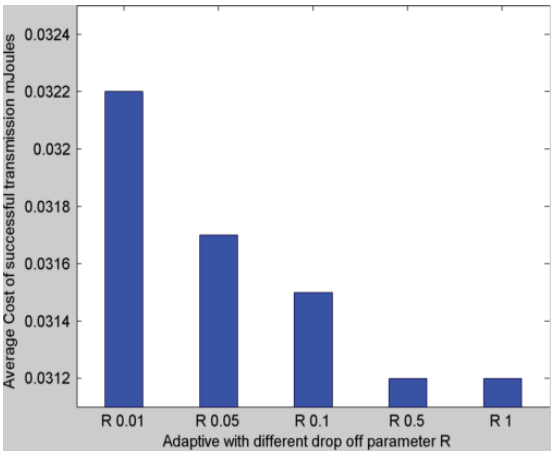


**Figure 108. University building.** *Plot of average cost of successful transmission at different drop-off rates (R) when **S-APC** is used. The change from R =0.01 to R =1 is approximately 3%.*

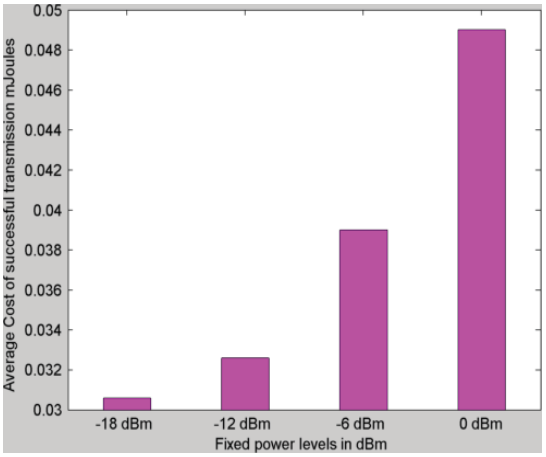


**Figure 109. University building.** *Plot of average cost of successful transmission at different output power levels when **fixed power transmissions** are used. As expected, the cost values increases with the output power level as the channel condition is generally very good ($E_b/N_0$> 60).*

Table 25 shows the average values of the performance parameters of the different transmission strategies that are compared in this thesis.

**Table 25. Average cost, PSR and protocol efficiency of data sets inside University building**

| **ATPC : RSSI based adaptive power control** | | | |
|---|---|---|---|
| **Channel scanning frequency** | **PSR %** | **Avg. Cost per successful transmission mJ** | **Protocol Efficiency %** |
| Every time the sensor transmits | 100 | 0.0308 | 99.10 |
| Every 5 transmissions | 100 | 0.0308 | 99.08 |
| Every 10 transmissions | 100 | 0.0308 | 99.07 |
| Every 50 transmissions | 100 | 0.0309 | 99.08 |
| Every 100 transmissions | 100 | 0.0310 | 99.15 |
| **S-APC : Non-RSSI based adaptive power control** | | | |
| **Drop-off factor R** | **PSR %** | **Avg. Cost per successful transmission mJ** | **Protocol Efficiency %** |
| 0.01 | 100 | 0.0322 | 98.99 |
| 0.05 | 100 | 0.0317 | 98.70 |
| 0.1 | 100 | 0.0315 | 98.63 |
| 0.5 | 100 | 0.0312 | 98.68 |
| 1 | 100 | 0.0312 | 98.57 |
| **Fixed power transmission** | | | |
| **Output power** | **PSR %** | **Avg. Cost per successful transmission mJ** | **Protocol Efficiency %** |
| -18 dBm | 100 | 0.0306 | 99.27 |
| -12 dBm | 100 | 0.0326 | 99.94 |
| -6 dBm | 100 | 0.0390 | 100.00 |
| 0 dBm | 100 | 0.0490 | 100.00 |

Figure 110 compare the minimum average cost of successful transmission based on the three data sets of University building. The minimum cost values of each of the transmission strategies are plotted. If the plot of Figure 80 is recalled, it is observed that when $E_b/N_0$ is more than or equal to 20 dB, the average packet success rate is more than 95%.

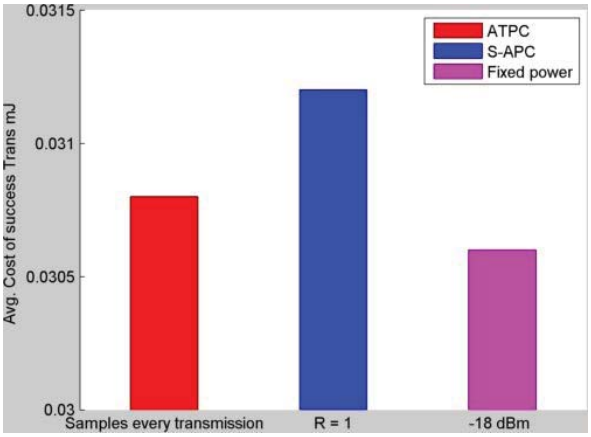


**Figure 110. University building data.** *Comparison of the cost due to different transmission strategy shows that there is hardly any difference in the cost per successful transmission.*

That explains the observations made from Figure 110 that fixed power transmission at the lowest power level (-18 dBm) provides the most energy efficient solution. Any ramping-up will always be wastage of power. The energy consumption values (average cost per successful transmission) of the proposed protocol matches closely when the value of drop-off rate is 1. It signifies that the state-based system can perform most energy efficiently under high link quality when it drops-off the fastest and rapidly moves to a state that starts transmitting at a lower power.

It can be concluded from the plots and discussions of section 8.2.1 that channel link quality is very good then fixed power transmission at the lowest power level can provide the most energy efficient solution.

### 8.2.2 Short term busy hour RSSI data collected from University dining hall between 11:30 am and 1:00 pm

Section 8.2.2 deals with short time busy hour data that are collected from a University dining hall. The reason to choose this location is to have a cluttered environment with lots of movements of people and different patterns of multipath signals due to a variety of reflective surfaces. The aim of this section is to observe as to how the different transmission strategies adapt with time dependent fading radio signals over a short period of time. This section compares the energy cost due to ATPC, adaptive power control and fixed power transmission when the RSSI data are collected over a short and busy period of the day. All the data show similar $E_b/N_0$ distribution and variation over time.
The variation of the $E_b/N_0$ and their normalised frequency distribution of one of the data sets are plotted in figure 111 and 112.

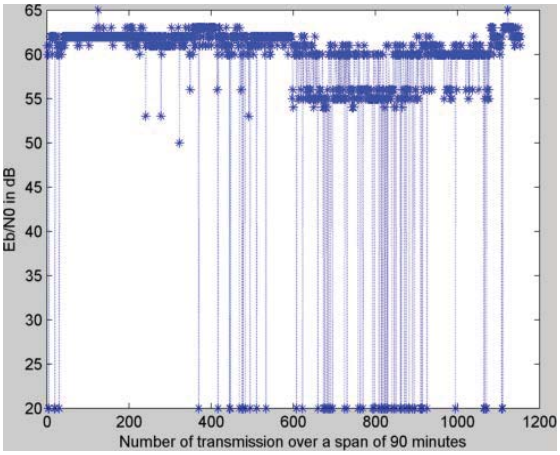


**Figure 111. University dining hall.** *It shows the variation of the average $E_b/N_0$ from University dining hall during busy hour between 11:30 am and 1:00 pm. The average $E_b/N_0$ is quite high (>55 dB) and occasionally dropped to 20 dB. The busy hour period shows that the average $E_b/N_0$ can widely fluctuate between high $E_b/N_0$ (> 55 dB) and low $E_b/N_0$ (~20 dB).*

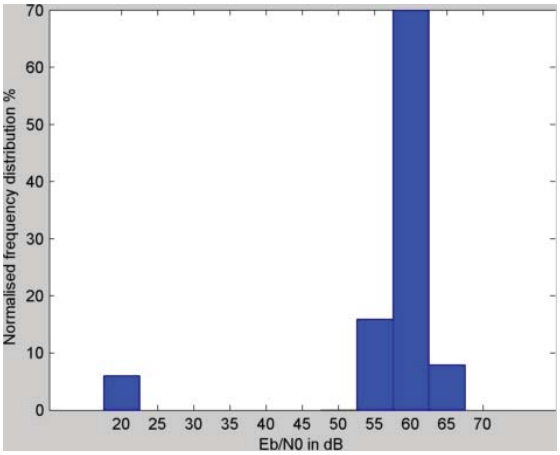


**Figure 112. University dining hall.** *The distribution plot of the received $E_b/N_0$ from University dining hall during busy hour between 11:30 am and 1:00 pm shows the wide variation over a range of 40 dB. The $E_b/N_0$ values are fairly uniformly distributed between 55 dB and 63 dB with the majority of values around 65 dB. However 6% occupancy in 20 dB indicates rapid fluctuation in the signal level caused by movements of people in between and receiver.*

The channel link quality is still good, with occasional drop to 30 dB due to multi-path fading effect.

Figures 114 to 116 plot the average cost of successful transmission based on data collected from University dining hall during the busy hour.

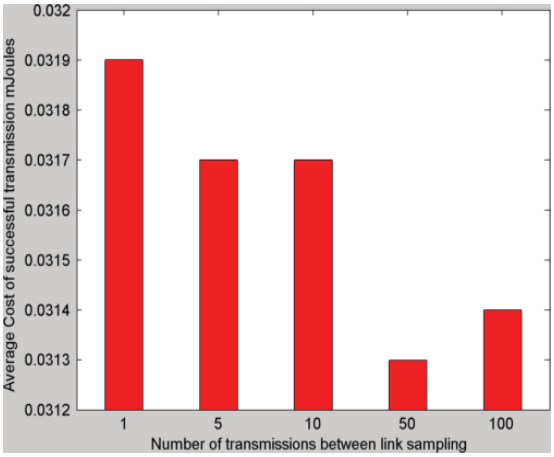


**Figure 113. University dining hall.** *Plot of average cost of successful transmission at different link sampling rates when **ATPC** is used.*

The number of transmissions between link sampling that yields the minimum energy cost is 50. However, there is hardly any difference between the costs at 50 and 100. It shows that a higher sampling rate can reduce the average cost of successful transmission.

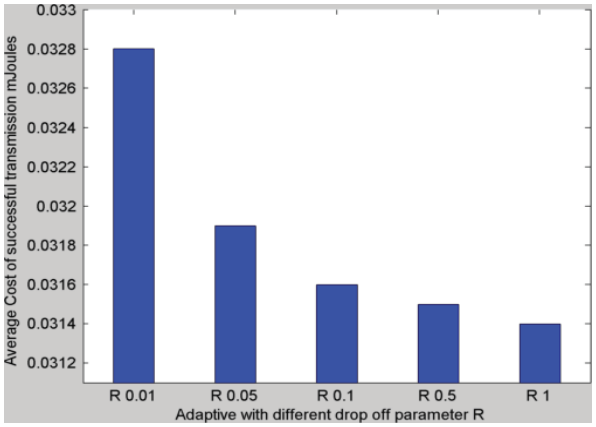


**Figure 114. University dining hall.** *Plot of average cost of successful transmission at different drop-off rates (R) when **adaptive power control protocol** is used. There is only a change of 4% savings from R 0.01 to R 1.*

Since the over-all link quality is still very good (average $E_b/N_0$ > 55 dB), the PSR and the efficiency values in all these cases are 100 and higher than 98% respectively and their differences are negligible. Therefore they are not plotted.

Figure 116 compares the cost per successful transmission when University dining hall data are used. The difference in the cost is negligible. This is due to the very good quality of link quality (average $E_b/N_0$ >55 dB) for most of the time (> 93%).

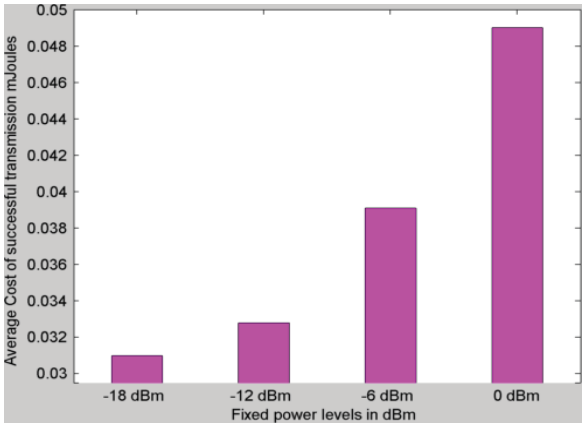


**Figure 115. University dining hall.** *Plot of average cost of successful transmission at different output power levels when **fixed power transmissions** are used. As expected, the cost values increases with the output power level as the channel condition is generally very good ($E_b/N_0$> 55).*

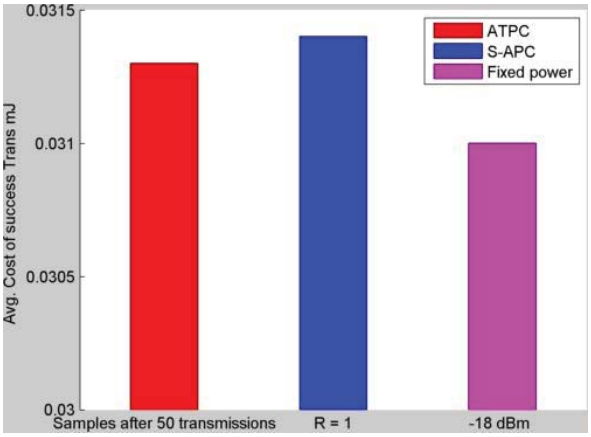


**Figure 116. University dining hall.** *Comparison of the minimum costs of the different transmission strategies shows that there is negligible difference in the cost per successful transmission.*

The tabulated data of the performance parameters averaged over the three sets of observations are presented in Table 26.

**Table 26. Average cost, PSR and protocol efficiency inside University dining hall**

| **ATPC : RSSI based adaptive power control** | | | |
|---|---|---|---|
| **Channel scanning frequency** | **PSR %** | **Avg. Cost per successful transmission mJ** | **Protocol Efficiency %** |
| Everytime the sensor transmits | 100 | 0.0319 | 98.65 |
| Every 5 transmissions | 100 | 0.0317 | 98.21 |
| Every 10 transmissions | 100 | 0.0317 | 98.14 |
| Every 50 transmissions | 100 | 0.0313 | 98.05 |
| Every 100 transmissions | 100 | 0.0314 | 97.86 |

| S-APC : Non-RSSI based adaptive power control | | | |
|---|---|---|---|
| **Drop-off factor R** | **PSR %** | **Avg. Cost per successful transmission mJ** | **Protocol Efficiency %** |
| 0.01 | 100 | 0.0328 | 98.19 |
| 0.05 | 100 | 0.0319 | 98.21 |
| 0.1 | 100 | 0.0316 | 98.15 |
| 0.5 | 100 | 0.0315 | 97.98 |
| 1 | 100 | 0.0314 | 97.85 |
| **Fixed power transmission** | | | |
| **Output power** | **PSR %** | **Avg. Cost per successful transmission mJ** | **Protocol Efficiency %** |
| -18 dBm | 100 | 0.0310 | 97.74 |
| -12 dBm | 100 | 0.0328 | 99.17 |
| -6 dBm | 100 | 0.0391 | 99.59 |
| 0 dBm | 100 | 0.0490 | 99.82 |

### 8.2.3 Short term RSSI data collected from town shopping centre between 11:30 am and 1:30 pm during weekends

RSSI data are also collected from a town main shopping centre/mall during busy hour between 11:30 am and 1:30 pm on consecutive weekends. The aim was to evaluate and compare the transmission strategies in different radio environments. A town shopping mall on a weekend during the rush hour can provide a typical indoor radio environment with lots of movement and multipath fading with occasional obstruction of the radio signal resulting in attenuation. The comparative study of the different transmission strategies based on these data is presented in section 8.2.3. The variation of the $E_b/N_0$ of one the data sets of the town shopping centre is plotted in Figure 117. This plot shows the significant variations of link quality during busy hours which is primarily due to multipath fading effect as people move around in a shopping centre. The distributions of the $E_b/N_0$ of one of the data sets can be observed in Figure 118. It can be observed that the $E_b/N_0$ remained low (~ 20 dB) a significant percentage of time.

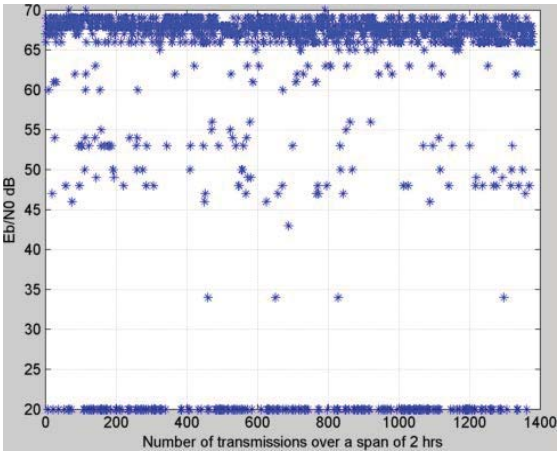


**Figure 117. Shopping centre Weekend.** *It shows the variation of the average $E_b/N_0$ from town shopping centre from data set 1 during busy hour between 11:30 am and 1:30 pm.*

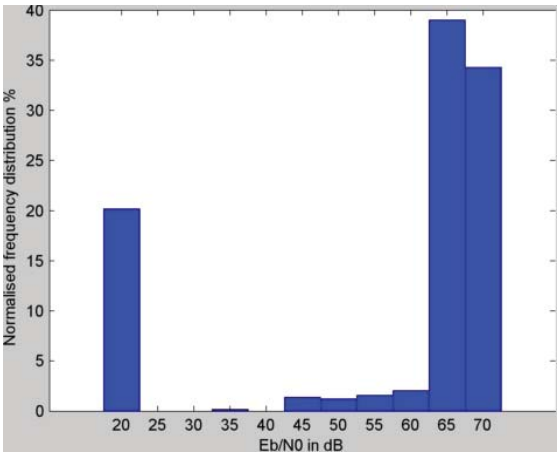


**Figure 118. Shopping centre during Weekend.** *The distribution plot of the received $E_b/N_0$ from town shopping centre data set 1 during busy hour between 11:30 am and 1:30 pm shows the wide variation of link quality. The percentage $E_b/N_0$ at 35 dB is approximately 5%, but still very good link quality.*

Figures 119-121 plot the average cost of successful transmission based on data collected from the town shopping centre during busy hour.

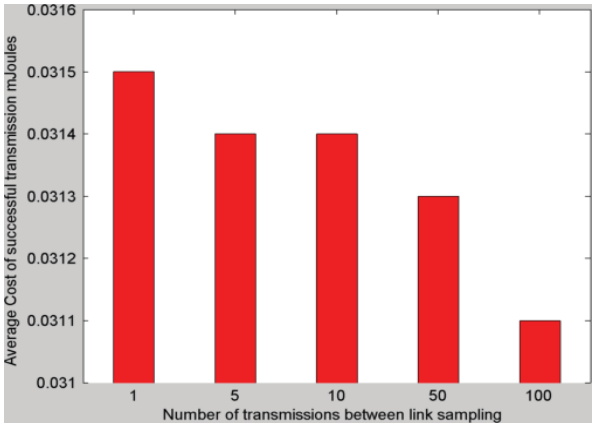


**Figure 119. Shopping centre Weekend:** *Plot of average cost of successful transmission at different link sampling rates when **ATPC** is used. There are less than 2% savings in cost when number of samples between sampling link changes from 1 to 100.*

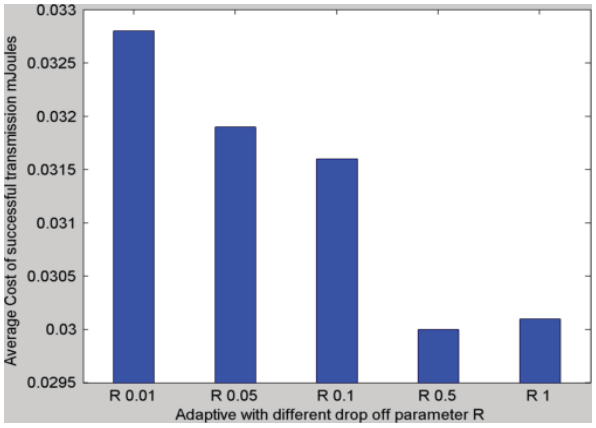


**Figure 120. Shopping centre Weekend:** *Plot of average cost of successful transmission at different drop-off rates (R) **S-APC** is used. There is 5% savings from R 0.01 to R 1.*

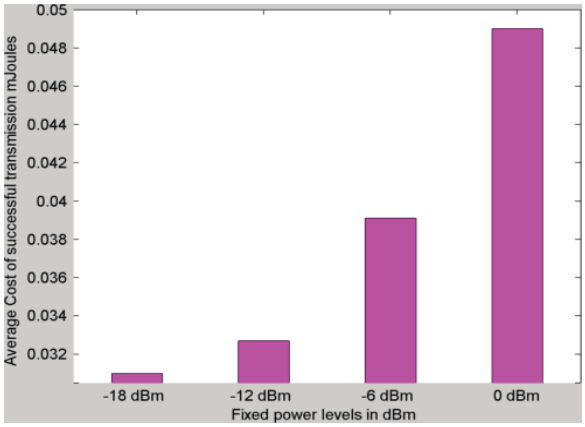


**Figure 121. Shopping centre Weekend:** *Plot of average cost of successful transmission at different output power levels when fixed power transmissions are used. As expected, the cost values increases with the output power level.*

Table 27 presents the average values the performance parameters based on the three sets of collected data.

**Table 27. Average cost, PSR and protocol efficiency inside shopping centre**

| **ATPC : RSSI based adaptive power control** | | | |
|---|---|---|---|
| **Channel scanning frequency** | **Avg. Cost per successful transmission mJ** | **PSR %** | **Protocol Efficiency %** |
| Every time the sensor transmits | 0.0315 | 100 | 98.44 |
| Every 5 transmissions | 0.0314 | 100 | 98.03 |
| Every 10 transmissions | 0.0314 | 100 | 98.02 |
| Every 50 transmissions | 0.0313 | 100 | 98.12 |
| Every 100 transmissions | 0.0311 | 100 | 97.88 |
| **S-APC : Non-RSSI based adaptive power control** | | | |
| **Drop-off factor R** | **Avg. Cost per successful transmission mJ** | **PSR %** | **Protocol Efficiency %** |
| 0.01 | 0.0328 | 100 | 98.19 |
| 0.05 | 0.0319 | 100 | 98.11 |
| 0.1 | 0.0316 | 100 | 98.12 |
| 0.5 | 0.0300 | 100 | 97.90 |
| 1 | 0.0301 | 100 | 97.74 |
| **Fixed power transmission** | | | |
| **Output power** | **Avg. Cost per successful transmission mJ** | **PSR %** | **Protocol Efficiency %** |
| -18 dBm | 0.0310 | 100 | 97.91 |
| -12 dBm | 0.0327 | 100 | 99.24 |
| -6 dBm | 0.0391 | 100 | 99.67 |
| 0 dBm | 0.0490 | 100 | 99.82 |

Figure 122 compares the cost per successful transmission in different transmission strategies. There is no significant difference observed. The average $E_b/N_0$ is around 58 dB indicating a fairly good link quality.

Over-all, it can be observed that in ATPC, the more is the number of sampling in between transmission, less is the energy consumption. This is because frequent sampling helps to make more accurate channel estimation than less frequent sampling and reduces energy consumption in the long run.

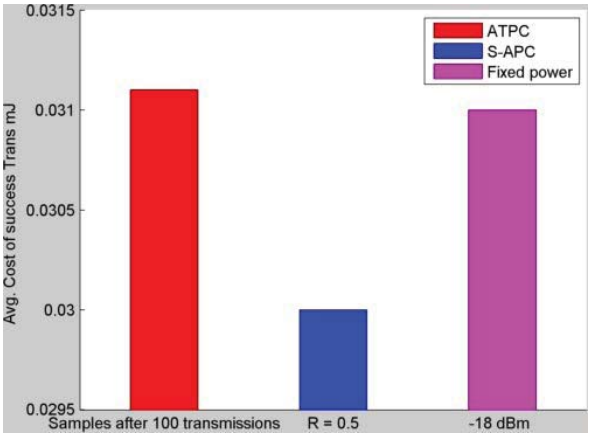


**Figure 122. Shopping centre during weekend.** *Comparison of the cost due to different transmission strategy shows that there is negligible difference in the cost per successful transmission.*

From this section it can be seen that when the average $E_b/N_0$ is high (> 55 dB), even momentary fluctuations in the order of 35-40 dB caused by movements in between the transmitter and the receiver does not seriously affect the packet success rate, the cost of successful transmission and efficiency.

In section 8.3, the mean $E_b/N_0$ is decremented by 20 dB in order to compare the costs and efficiencies in different transmission strategies. This is to emulates the situations when the distance between the sensor and the receiving hub is increased resulting in the decrease in the mean signal level.

## 8.3 Comparison of the minimum cost values of ATPC, S-APC and fixed power transmission when the mean $E_b/N_0$ value is reduced by 20 dB

This section has studied the performance of the transmission strategies when the average or mean $E_b/N_0$ is reduced by 20 dB. In indoor environments with multiple partitions in between the transmitter and receiver with variable attenuation levels through these partitions, the mean signal level can drop if new partitions get introduced in between them or the distance between them is increased. The aim of these simulations is to understand the behaviour of the transmission strategies when the mean link quality changes. With respect to each of the cases discussed in the previous section, the fluctuation of the $E_b/N_0$ is now roughly between 0 dB and 40 dB. The adaptive power control protocol (both RSSI and non-RSSI based) are now in a position to modulate the output power level when the signal level has dropped. Results in the next section shows that the optimal energy level in fixed power mode is no longer -18 dBm. This higher power level has also pushed the average cost of successful transmission high.

### 8.3.1 University building with average $E_b/N_0$ reduced by 20 dB

The distribution of the average $E_b/N_0$ is shown in Figure 123 when the mean $E_b/N_0$ is reduced by 20 dB.

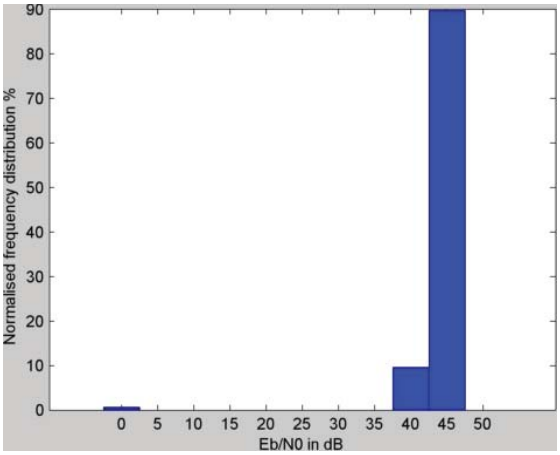


**Figure 123. University building.** *The frequency distribution plot of the received $E_b/N_0$ from University building (data set 1) is presented when it is reduced by 20 dB. The link quality is still good, with maximum time in $E_b/N_0$ above 40 dB.*

**Table 28. Average cost, PSR and protocol efficiency inside University building when $E_b/N_0$ is reduced by 20 dB**

| **ATPC- RSSI based adaptive power control** | | | |
|---|---|---|---|
| **Channel scanning frequency** | **PSR %** | **Avg. Cost per successful transmission mJ** | **Protocol Efficiency %** |
| Every time the sensor transmits | 95.68 | 0.0394 | 88.10 |
| Every 5 transmissions | 95.71 | 0.0400 | 88.27 |
| Every 10 transmissions | 95.87 | 0.0396 | 88.52 |
| Every 50 transmissions | 95.85 | 0.0402 | 88.51 |
| Every 100 transmissions | 94.96 | 0.0404 | 86.54 |
| **Non-RSSI based adaptive power control** | | | |
| **Drop-off factor R** | **PSR %** | **Avg. Cost per successful transmission mJ** | **Protocol Efficiency %** |
| 0.01 | 99.70 | 0.0376 | 94.56 |
| 0.05 | 99.70 | 0.0370 | 92.28 |
| 0.1 | 99.70 | 0.0369 | 91.16 |
| 0.5 | 99.70 | 0.0371 | 88.65 |
| 1 | 99.70 | 0.0372 | 87.91 |

| Fixed power transmission | | | |
|---|---|---|---|
| **Output power** | **PSR %** | **Avg. Cost per successful transmission mJ** | **Protocol Efficiency %** |
| -18 dBm | 93.52 | 0.0413 | 82.35 |
| -12 dBm | 94.69 | 0.0414 | 84.03 |
| -6 dBm | 99.41 | 0.0419 | 94.04 |
| 0 dBm | 99.99 | 0.0498 | 98.67 |

Table 28 shows the average of the performance parameters of the data that were collected.

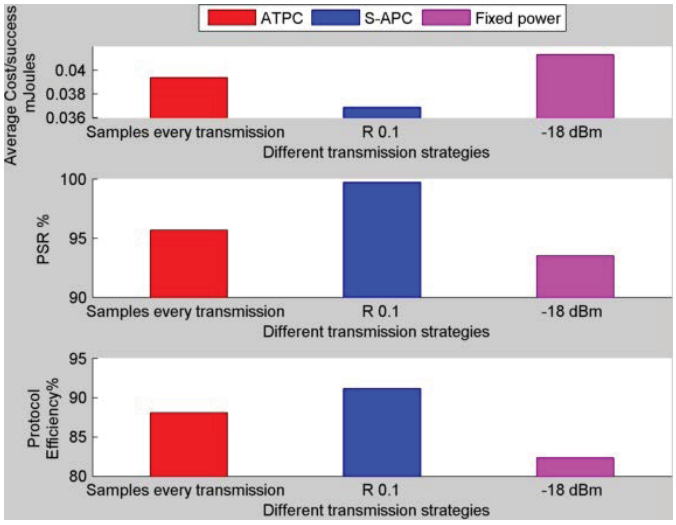


**Figure 124. University building- long term variation.** *Comparison of the minimum cost and the corresponding PSR and protocol efficiencies due to different transmission strategy shows that the adaptive protocol can save 7% and 12% energy as compared to ATPC and fixed power transmission and outperforming the others in terms of PSR and efficiency.*

Figure 124 compares the minimum cost of each of the transmission strategies. The average $E_b/N_0$ has reduced by 20 dB and present average value is around 37 dB. Figure 124 shows that the proposed adaptive protocol can work best in terms of saving energy. The adaptive protocol still maintains a high PSR and protocol efficiency values of 99% and 91% respectively at R =0.1 and better than fixed power and ATPC.

### 8.3.2 University dining hall with average $E_b/N_0$ reduced by 20 dB

Table 29 has tabulated all the performance parameter values of the data that were collected from University dining hall during busy hours.

**Table 29. Average cost, PSR and protocol efficiency inside University dining hall during busy hour**

| **ATPC : RSSI based adaptive power control** | | | |
|---|---|---|---|
| **Channel scanning frequency** | **PSR %** | **Avg. Cost per successful transmission mJ** | **Protocol Efficiency %** |
| Every time the sensor transmits | 92.44 | 0.0461 | 74.07 |
| Every 5 transmissions | 90.43 | 0.0514 | 70.45 |
| Every 10 transmissions | 89.88 | 0.0523 | 69.61 |
| Every 50 transmissions | 89.27 | 0.0534 | 68.38 |
| Every 100 transmissions | 86.62 | 0.0538 | 63.33 |
| **S-APC: Non-RSSI based adaptive power control** | | | |
| **Drop-off factor R** | **PSR %** | **Avg. Cost per successful transmission mJ** | **Protocol Efficiency %** |
| 0.01 | 99.53 | 0.0448 | 92.20 |
| 0.05 | 99.37 | 0.0431 | 89.03 |
| 0.1 | 99.16 | 0.0431 | 87.22 |
| 0.5 | 98.98 | 0.0420 | 84.25 |
| 1 | 98.97 | 0.0422 | 83.04 |
| **Fixed power transmission** | | | |
| **Output power** | **PSR %** | **Avg. Cost per successful transmission mJ** | **Protocol Efficiency %** |
| -18 dBm | 83.84 | 0.0568 | 60.59 |
| -12 dBm | 86.98 | 0.0556 | 63.56 |
| -6 dBm | 98.46 | 0.0462 | 85.42 |
| 0 dBm | 99.88 | 0.0508 | 96.34 |

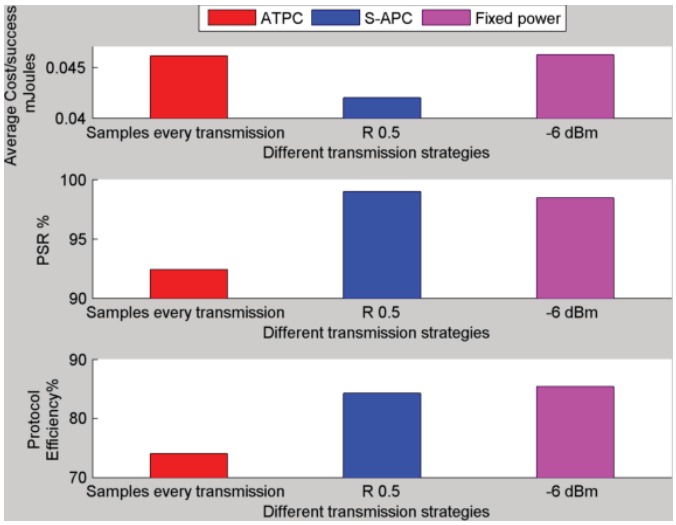


**Figure 125. University dining hall.** *Comparison of the minimum cost and their corresponding PSR and protocol efficiencies due to different transmission strategy shows that S-APC consumes 10% less energy than ATPC protocol and fixed power transmission, with comparable PSR and efficiency.*

Figure 125 shows the comparison of the minimum cost values of the different transmission strategies. It demonstrates that the proposed adaptive protocol can perform in the most energy efficient manner. The minimum average energy expenditure per successful transmission at R = 0.5 is able to save up to 10% energy as compared to ATPC (samples the channel after every transmission) and fixed power transmission at -6 dBm.

The PSR and efficiency values of ATPC and fixed power transmission are less than that of adaptive power control as evident from Figure 125. At R = 0.5, the PSR and the protocol efficiency of the adaptive protocol is higher than APTC (at channel sampling frequency of 1) by 7% and 14% respectively.

The normalised frequency distribution of $E_b/N_0$ in Figure 126 shows that the channel is in low $E_b/N_0$ for less than 10% of time. Therefore, there is scope of power adaptation and the proposed adaptive protocol has outperformed the other transmission strategies

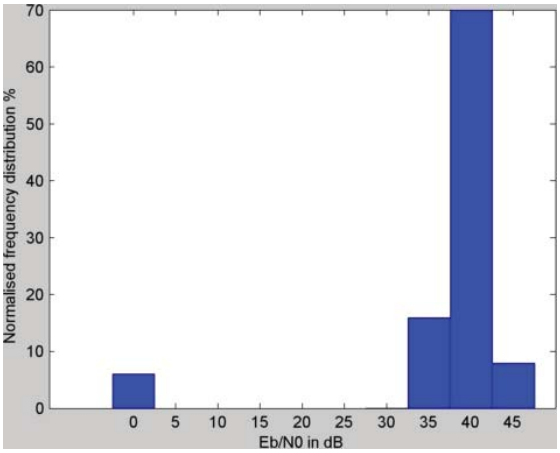


**Figure 126 University dining hall.** *The frequency distribution plot of the received $E_b/N_0$ from the University dining hall data is presented when it is reduced by 20 dB. The link quality is still good, with the maximum time in $E_b/N_0$ around 40 dB.*

### 8.3.3 Town Shopping centre with average $E_b/N_0$ reduced by 20 dB

Table 30 has tabulated all the performance parameter values of the data that were collected from town shopping centre during busy hours.

**Table 30. Average cost, PSR and protocol efficiency inside shopping centre during busy hour**

| **ATPC : RSSI based adaptive power control** | | | |
|---|---|---|---|
| **Channel scanning frequency** | **PSR %** | **Avg. Cost per successful transmission mJ** | **Protocol Efficiency %** |
| Every time the sensor transmits | 90.78 | 0.0479 | 70.73 |
| Every 5 transmissions | 90.05 | 0.0498 | 68.11 |
| Every 10 transmissions | 89.37 | 0.0508 | 65.62 |
| Every 50 transmissions | 88.9 | 0.0504 | 65.93 |
| Every 100 transmissions | 88.92 | 0.0522 | 62.25 |

| S-APC : Non-RSSI based adaptive power control | | | |
|---|---|---|---|
| **Drop-off factor R** | **PSR %** | **Avg. Cost per successful transmission mJ** | **Protocol Efficiency %** |
| 0.01 | 99.83 | 0.0438 | 92.20 |
| 0.05 | 99.83 | 0.0419 | 89.03 |
| 0.1 | 99.8 | 0.0417 | 87.22 |
| 0.5 | 99.85 | 0.0409 | 84.25 |
| 1 | 99.83 | 0.0410 | 83.04 |
| **Fixed power transmission** | | | |
| **Output power** | **PSR %** | **Avg. Cost per successful transmission mJ** | **Protocol Efficiency %** |
| -18 dBm | 83.84 | 0.0568 | 60.59 |
| -12 dBm | 86.98 | 0.0556 | 63.56 |
| -6 dBm | 98.46 | 0.0462 | 85.42 |
| 0 dBm | 99.88 | 0.0508 | 96.34 |

Table 29 suggests that the PSR and efficiency of the adaptive protocol at R = 0.5 are almost 10% and 20% higher than that of ATPC respectively when channel is scanned after every packet transmission.

Figure 127 compares the minimum average cost of successful transmission. Overall the adaptive protocol fares better than ATPC and fixed power transmission and consumes almost 13% less energy than the ATPC when sampled after every transmission.

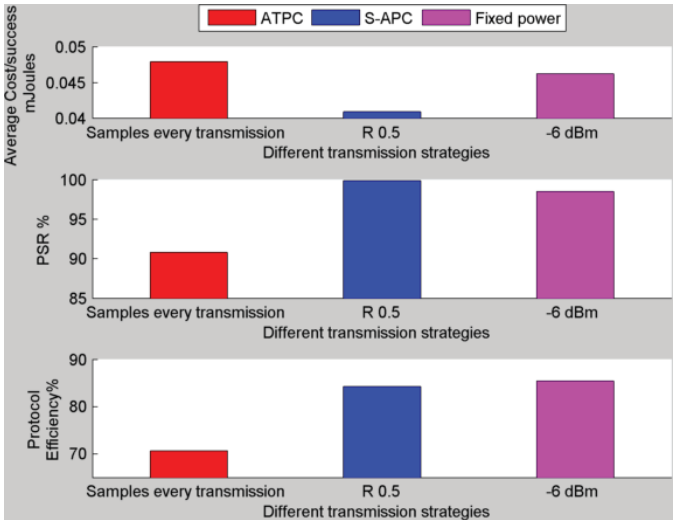


**Figure 127. Shopping centre Weekend.** *Comparison of the minimum cost and their corresponding PSR and protocol efficiencies due to different transmission strategy shows that the adaptive protocol at R =0.5 consumes 17% less energy than the ATPC protocol, outperforming the others in terms of PSR and efficiency.*

## 8.4 Comparison of the minimum cost values of ATPC, S-APC and fixed power transmission when the mean $E_b/N_0$ value is reduced by 40 dB

These simulations were conducted to observe as to how the performances change, irrespective of the transmission strategy that was adopted. If the mean $E_b/N_0$ is further reduced by 20 dB, then the behaviour of the channel is such that it oscillates between a fairly good channel state ($E_b/N_0$ = 20 dB) and a bad channel state ($E_b/N_0$ ~ -20 dB).

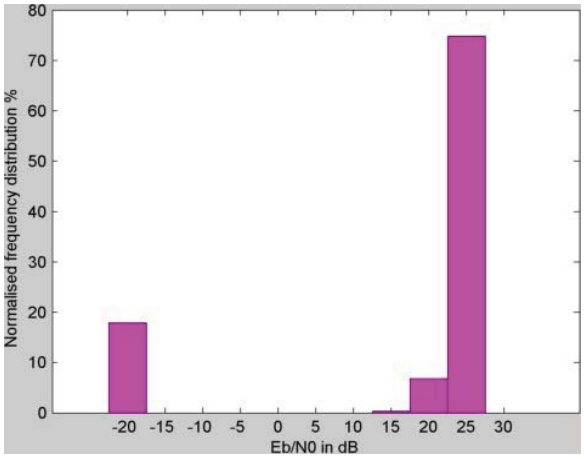


**Figure 128. University building-** *The normalised frequency distribution of the $E_b/N_0$ values suggests that channel is in bad condition for ~10% of time.*

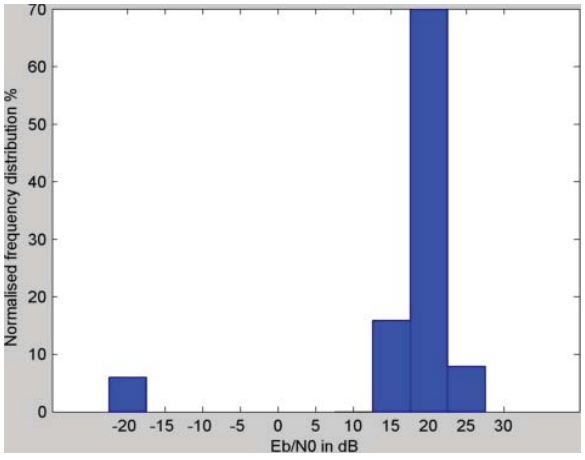


**Figure 129. University dining hall -** *The frequency distribution of the $E_b/N_0$ values in during busy hour shows that the channel quality has oscillated between good and bad.*

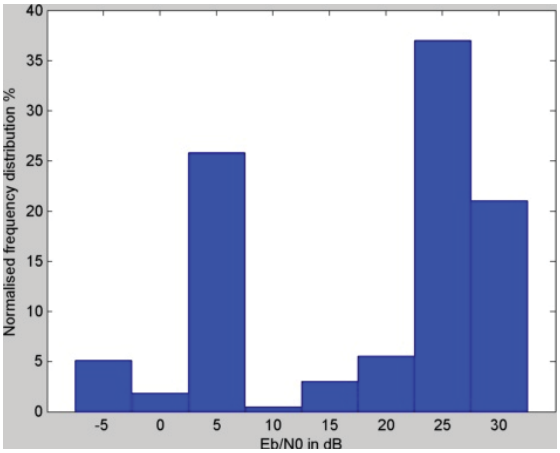


**Figure 130. Town shopping center-** *The frequency distribution of the $E_b/N_0$ values during busy hour shows that the channel quality has oscillated between good and bad*

The sample normalized frequency distributions of the $E_b/N_0$ are shown in figures 128-130. In good state most of the packets will be successfully transmitted, while in bad state almost no packet transmission will be successful

### 8.4.1 University building with average $E_b/N_0$ reduced by 40 dB

Table 31 represents the average of the performance comparison values from the three sets of data when the $E_b/N_0$ is further reduced by 20 dB. The PSR values of all the transmission strategies are approximately 93.5%. This is because of the extreme swing of the channel link quality states and the significantly longer time the channel was in good state (> 95%). When the $E_b/N_0$ drops below 0 dB, no packet could be transmitted successfully. In good channel state, it was possible to transmit almost all the packets successfully.

**Table 31. Average cost, PSR and protocol efficiency inside University building when $E_b/N_0$ is reduced by 40 dB**

| ATPC : RSSI based adaptive power control | | | |
|---|---|---|---|
| **Channel scanning frequency** | **PSR %** | **Avg. Cost per successful transmission mJ** | **Protocol Efficiency %** |
| Every time the sensor transmits | 93.50 | 0.0498 | 81.60 |
| Every 5 transmissions | 93.50 | 0.0497 | 81.57 |
| Every 10 transmissions | 93.50 | 0.0497 | 81.58 |
| Every 50 transmissions | 93.50 | 0.0494 | 81.61 |
| Every 100 transmissions | 93.50 | 0.0498 | 81.54 |

| **S-APC : Non-RSSI based adaptive power control** | | | |
|---|---|---|---|
| **Drop-off factor R** | **PSR %** | **Avg. Cost per successful transmission mJ** | **Protocol Efficiency %** |
| 0.01 | 93.74 | 0.0743 | 80.12 |
| 0.05 | 93.74 | 0.0681 | 78.45 |
| 0.1 | 93.74 | 0.0655 | 77.75 |
| 0.5 | 93.74 | 0.0613 | 75.92 |
| 1 | 93.74 | 0.0601 | 75.50 |
| **Fixed power transmission** | | | |
| **Output power** | **PSR %** | **Avg. Cost per successful transmission mJ** | **Protocol Efficiency %** |
| -18 dBm | 93.73 | 0.0420 | 78.21 |
| -12 dBm | 93.75 | 0.0435 | 81.17 |
| -6 dBm | 93.75 | 0.0517 | 82.00 |
| 0 dBm | 93.75 | 0.0647 | 82.29 |

Figure 131 has plotted the minimum average cost of successful transmission for the three different transmission strategies and their corresponding PSR and protocol efficiency. Since the channel is oscillating between the good state and the bad, it is most advantageous to stick to a fixed power level in order to save energy rather than employ output power modulation. That is why the fixed power at -18 dBm consumes the least energy among all. The minimum energy consumption for the adaptive protocol is achieved when R = 1. This makes sense because R = 1 can provide the fastest drop-off rate and the system can come down to the lowest state fast. However, the average cost of successful transmission in S-APC is higher than ATPC. The reason is that the ATPC protocol can actually track the channel more effectively.

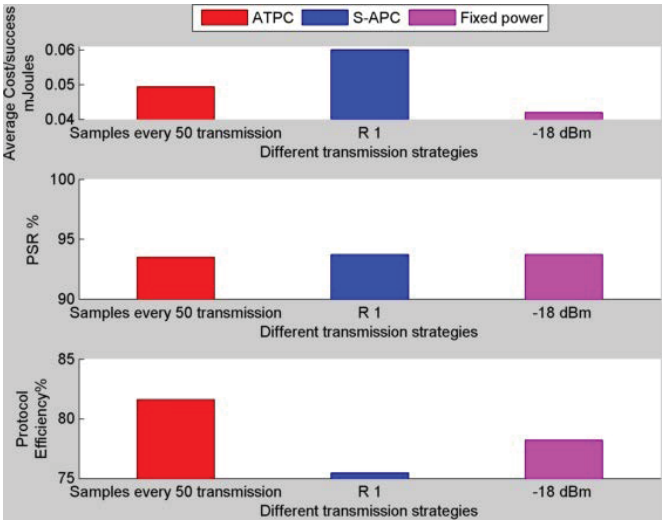


**Figure 131. University building data.** *Comparison of the **cost** due to different transmission strategy shows that S-APC consumes more energy than ATPC protocol. However, the minimum power consumption occurs if the output power level is fixed at the lowest power level (-18 dBm).*

### 8.4.2 University dining Hall with average $E_b/N_0$ reduced by 40 dB

Table 32 represents the average of the performance comparison values from the three sets of data when the $E_b/N_0$ is further reduced by 20 dB.

**Table 32. Average cost, PSR and protocol efficiency inside University dining hall when Eb/N0 is reduced by 40 dB**

| **ATPC : RSSI based adaptive power control** | | | |
|---|---|---|---|
| **Channel scanning frequency** | **PSR %** | **Avg. Cost per successful transmission mJ** | **Protocol Efficiency %** |
| Every time the sensor transmits | 83.84 | 0.0731 | 59.34 |
| Every 5 transmissions | 83.84 | 0.0724 | 59.28 |
| Every 10 transmissions | 83.84 | 0.0723 | 59.30 |
| Every 50 transmissions | 83.84 | 0.0720 | 59.19 |
| Every 100 transmissions | 83.84 | 0.0716 | 59.13 |
| **S-APC : Non-RSSI based adaptive power control** | | | |
| **Drop-off factor R** | **PSR %** | **Avg. Cost per successful transmission mJ** | **Protocol Efficiency %** |
| 0.01 | 83.84 | 0.1373 | 59.60 |
| 0.05 | 83.84 | 0.1263 | 58.76 |
| 0.1 | 83.84 | 0.1218 | 58.14 |
| 0.5 | 83.84 | 0.1129 | 56.86 |
| 1 | 83.84 | 0.1109 | 56.39 |

| Fixed power transmission | | | |
|---|---|---|---|
| **Output power** | **PSR %** | **Avg. Cost per successful transmission mJ** | **Protocol Efficiency %** |
| -18 dBm | 83.83 | 0.0596 | 56.00 |
| -12 dBm | 83.84 | 0.0616 | 58.72 |
| -6 dBm | 83.84 | 0.0730 | 59.51 |
| 0 dBm | 83.85 | 0.0912 | 59.75 |

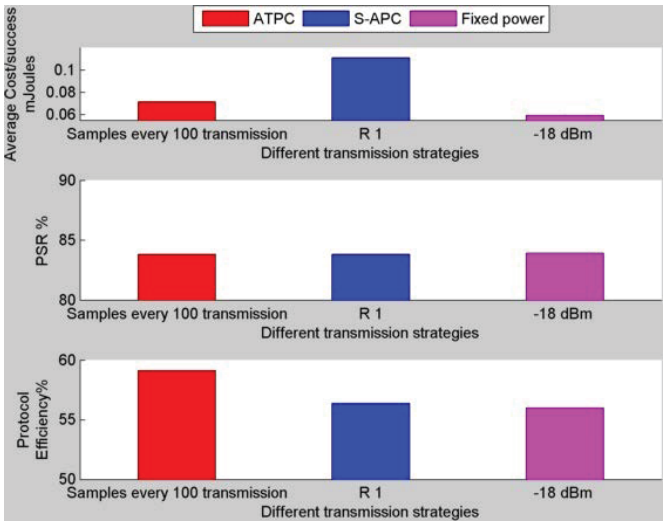


**Figure 132. University dining hall.** *Comparison of the **cost** due to different transmission strategy in University dining hall during busy hours shows that the proposed S-APC protocol is less energy efficient than ATPC and fixed power transmission.*

From Figure 132 it can be observed that S-APC is less energy efficient than ATPC and Fixed power transmission. As expected, the PSR values are all same because packets are only successfully transmitted in good channel state.

### 8.4.3 Town Shopping centre with average $E_b/N_0$ reduced by 40 dB

Table 33 represents the average of the performance comparison values from the three sets of data when the $E_b/N_0$ is further reduced by 20 dB.

**Table 33. Average cost, PSR and protocol efficiency at shopping center when $E_b/N_0$ is reduced by 40 dB**

| ATPC : RSSI based adaptive power control | | | |
|---|---|---|---|
| **Channel scanning frequency** | **PSR %** | **Avg. Cost per successful transmission mJ** | **Protocol Efficiency %** |
| Every time the sensor transmits | 86.7233 | 0.0598 | 62.41 |
| Every 5 transmissions | 86.6433 | 0.0599 | 57.81 |
| Every 10 transmissions | 86.3833 | 0.0597 | 57.47 |
| Every 50 transmissions | 85.9474 | 0.0582 | 61.10 |
| Every 100 transmissions | 93.50 | 0.0581 | 61.17 |

| **S-APC : Non-RSSI based adaptive power control** | | | |
|---|---|---|---|
| **Drop-off factor R** | **PSR %** | **Avg. Cost per successful transmission mJ** | **Protocol Efficiency %** |
| 0.01 | 85.37 | 0.1225 | 59.63 |
| 0.05 | 85.36 | 0.1131 | 57.84 |
| 0.1 | 85.35 | 0.1085 | 56.85 |
| 0.5 | 85.35 | 0.1003 | 55.96 |
| 1 | 85.37 | 0.0982 | 53.99 |
| **Fixed power transmission** | | | |
| **Output power** | **PSR %** | **Avg. Cost per successful transmission mJ** | **Protocol Efficiency %** |
| -18 dBm | 83.81 | 0.0570 | 57.10 |
| -12 dBm | 85.11 | 0.0575 | 60.02 |
| -6 dBm | 85.23 | 0.0677 | 62.07 |
| 0 dBm | 85.36 | 0.0842 | 61.27 |

Similar to the data set distributions of the last two sub-sections, the distribution of the average $E_b/N_0$ is between two extremes of -20 dB and 20 dB. That has resulted in PSR values of all the three sets of strategies (ATPC, fixed power and adaptive) are approximately same and proportional to the time spent in good channel state. Figure 133 shows that the proposed adaptive protocol is not energy efficient.

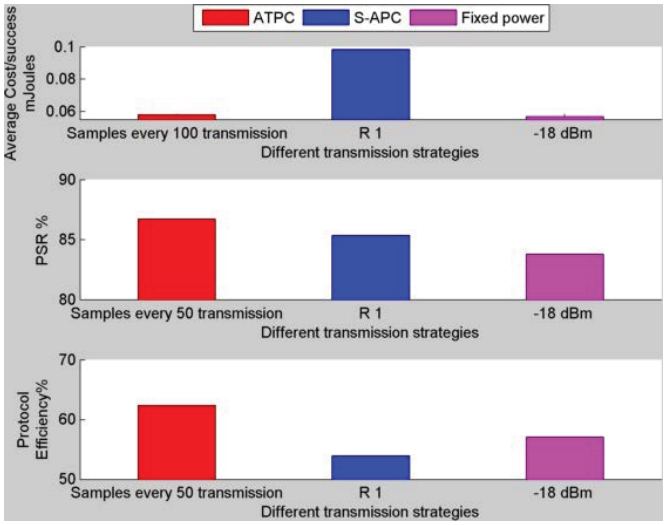


**Figure 133. Shopping centre Weekend.** *Comparison of the **cost** due to different transmission strategy shows that ATPC and fixed power transmissions are significantly more energy efficient than the proposed S-APC protocol.*

Output power manipulation does not work when the channel link quality swing between a bad and a good channel. The ATPC protocol is more efficiently able to track the channel changes. The primary reason is that ATPC uses RSSI information for channel estimation.

The S-APC protocol, on the other hand, tracks the link quality based on the outcome of packet transmission attempt. In the two state channel model, the scope of power adaption can actually nominally reduces energy consumption as compared to fixed power transmission.

## 8.5 Discussions

The observations and analysis of the simulation results are divided into three main sections. In section 8.2 the empirical RSSI values and the derived $E_b/N_0$ are fed in the simulation. Results show that when the average $E_b/N_0$ is good (> 55 dB), the performance of the adaptive protocol is comparable to ATPC and fixed power transmission. In section 8.3, the average $E_b/N_0$ is reduced by 20 dB. Now the $E_b/N_0$ is around 30-35 dB and is considered an average channel. Results of section 8.3 suggest that the adaptive protocol has outperformed the ATPC and fixed power transmission in terms of PSR, energy saving and efficiency by significant margins. But as the overall channel condition or link quality further deteriorates, the adaptive protocol has become less effective. This is demonstrated from the results of section 8.4. The average $E_b/N_0$ is now less than 20 dB. ATPC can track the link quality per transmission basis and has shown to be more energy efficient than the proposed adaptive protocol. It is best to stick to a fixed power than control the output power when link quality is poor.

# Chapter 9 Conclusions

The primary objective of any adaptive communication protocol that operates in the wireless sensor domain is to maximise the operational lifetime of the wireless sensors. The principle contributions of the proposed adaptive power control protocol in this thesis can be divided into two categories. The communication protocol introduces a new paradigm of adaptive power control that does not use the link quality information (in the form of RSSI or LQI) to adjust the output power. The adaptive protocol has four states, each of which signifies one transmission cycle. In each state, there are certain numbers of power levels that can be used to successfully deliver the packet. Any state transition in increasing order means that channel condition has been deteriorating. Similarly, state transition in decreasing order of states means that channel condition has been improving. The system always transmits at a power level in the lower state that is one step below the power level in the higher state. It uses the most recent outcome of the result of packet delivery and the corresponding power level to switch from a lower state to a higher state. The switching from a higher state to a lower state is guided by an exponential drop-off algorithm. The adaptive protocol is found to be most energy efficient when it has room for power manipulation. The energy cost per successful transmission is compared with fixed power scheme and other forms of adaptive power control protocol that uses RSSI or beacon packets for link quality estimation. Exhaustive simulations, followed by extensive experiments, have demonstrated the usefulness and effectiveness of the adaptive protocol to save energy. Especially in mobile sensor scenarios, the adaptive protocol can save up-to 30% energy. The proposed adaptive protocol can work most energy efficiently when the radio channel is in the transition state. When the radio link is either in connected or disconnected region, there is little scope of output power manipulation. In transition state it can ramp up or down the output power level.

The drop-off factor (R) is an important parameter in the adaptive protocol as it determines how fast the system will switch back to a lower state to transmit at a lower power. The experimental data show that the value of R can be set in between 0.5 and 1 to achieve optimal energy consumption. A low value of R means that the system will switch back to a lower power level slowly. Therefore in scenarios when the system has switched to a higher state level in response to momentary drop in signal level, a low R value means that even if the channel condition improves, the system will come down to lower state level slowly. Hence, the energy cost may rise. On the other hand, if R is set at 1, it will drop fast. But if the link quality change is not transient, the system will oscillate between the states. The experiments that were conducted have covered some common indoor radio channel scenarios. For future work, different R values can be set in the different states and the experiments repeated. The R values should be distributed in such a manner that the system can drop-off fastest when in the highest state level and gradually becomes

slower with lower state levels in order to create a balance between switching up and switching down between states. The application of the proposed adaptive power control protocol is not only limited to wireless sensor network but can be employed in any link layer power and retransmission control algorithms that aim to conserve energy.

The adaptive protocol can also be tested on other RF modules which have more than four programmable power levels.

The adaptive protocol has also indicated that since the non-RSSI based protocol can perform better than RSSI-based protocols, the use of this protocol would reduce the deployment cost of wireless sensors. This is because the cost of a transceiver module that supports RSSI is at least 10 times more expensive than the nRF24L01p RF module that was used in the thesis.

# Chapter 10 Future work

It can be observed from the results and the analysis of the previous chapters that there can be an optimal value of the drop-off factor R which yields maximum energy savings which is radio environment dependent. The future research objective is to make R adaptive and change as the radio environment changes. The system will constantly track the PSR and increase or decrease the R value.

In other word, one of the future research plans are to do away with the limitations of the existing protocol that has been proposed in the thesis by adding intelligence when the sensor is in the fringes of its communicable distance.

Its applicability will also be tested in a multi-hop sensor network. A sensor network can be built in different scenarios including farm lands, offices, commercial building and in smart home setups. The adaptive protocol can run in the background and can be compared to existing adaptive protocols in terms of energy efficiency. I also propose to implement the adaptive protocol in the field of robotics where they are used in, for example, mining and fire-fighting sectors.

Extensive research in the field of Internet of Things (IoT) has enabled close interaction between the physical world and computing devices through the exchange of data. It has resulted in the improvement of overall efficiency and accuracy of different systems ranging from managing airports' passenger flow to heating buildings and caring for the elderly. All these have eventually translated into economic benefits. Sensors are an integral part of the wide network of hardware devices and software that constitute IoT. These sensors are the primary components to build connectivity between the sensory world and the data processing devices. In general, these sensors are connected to their base stations through wireless links. Some of them are mobile. Moreover, majority of these sensors are battery powered and therefore have limited computational capacity and operational lifetime. The success of these ubiquitous sensor networks will depend on the reliability of the data transfer for a reasonably long period of time without battery replacement. This is because the economic viability of IoT can be undermined by the huge operational costs of battery replacement and associated maintenance. The sensors consume maximum energy while transmitting and receiving data. Therefore, the core research focus is to develop energy efficient communication protocols for the sensor networks in order to enable the sensors to exchange data for an extended period of time. These protocols can be stacked in the data link layer and the medium access control (MAC) layer. They should be simple and computationally inexpensive.

# Reference

[1] V. Weber, "Smart Sensor Networks: Technologies and Applications for Green Growth," OECD Secretariat (www.oecd.org/dataoecd/39/62/44379113.pdf), December 2009. Last accessed : January 2012

[2] A. Mainwaring, J. Polastre, R. Szewczyk, D. Culler and J. Anderson, "Wireless Sensor Networks for Habitat Monitoring," in *WSNA*, ISBN:1-58113-589-0, pp. 88-97, 2002.

[3] T. Harms, S. Sedigh and F. Bastianini, "Structural Health Monitoring of Bridges Using Wireless Sensor Networks," in *IEEE Instrumentation & Measurement Magazine*, ISSN: 1094-6969, pp. 14-18, December 2010.

[4] M. Fraser, A. Elgamal, X. He and J. P. Conte, "Sensor Network for Structural Health Monitoring of a Highway Bridge," in *Journal of Computing in Civil Engineering*, ISSN:0887-3801, Vol. 24, Issue 1, pp. 11-24, 2010.

[5] S. Ullah, H. Higgin, M. A. Siddiqui and K. S. Kwak, "A Study of Implanted and Wearable Body Sensor Networks," in *KES International conference on Agent and multi-agent systems: technologies and applications (KES-AMSTA)*, pp. 464-473, March 2008.

[6] G. Virone, A. Wood, L. Selavo, Q. Cao, L. Fang, T. Doan, Z. He, R. Stoleru, S. Lin and J. Stankovic, "An Advanced Wireless Sensor Network for Health Monitoring," in *Transdisciplinary Conference on Distributed Diagnosis and Home Healthcare (D2H2)*, April, 2006.

[7] W. S. Conner, J. Heidemann, L. Krishnamurthy, X. Wang and M. Yarvis, "Workplace Applications of Sensor Networks," USC/ISI Technical Report ISI-TR-2004-591, 2004.

[8] M. Weiser, "Ubiquitous Computing," March 1996. http://www.ubiq.com/weiser/UbiHome.html. Last accessed: August 2012

[9] "What is Ambient Intelligence?," Philips, http://www.research.philips.com/technologies/projects/ami/. Last accessed: August 2012

[10] "Ubiquitous Sensor Networks (USN), ITU-T Technology Watch Briefing Report Series," 2008.

[11] "The ISA100 Standards Overview & Status," 2008. https://www.isa.org/pdfs/microsites1134/isa100-overview-oct-2008. Last accessed: February 2013

[12] K. S. Low, W. N. N. Win and M. J. Er, "Wireless Sensor Networks for Industrial Environments," in *International Conference on Computational Intelligence for Modelling, Control and Automation;International Conference on Intelligent Agents, Web Technologies and Internet Commerce*, ISBN: 0-7695-2504-0, pp. 271-276, 2005.

[13] G. Zhao, "Wireless Sensor Networks for Industrial Process Monitoring and Control: A Survey," *Digital Technology Laboratory Network Protocols and Algorithms,* ISSN 1943-3581, vol. 3, no. 1, pp. 46-63, 2011.

[14] H. v. d. Bent, "Wireless Technology in Industrial Automation", White Paper Yokogawa, https://www.yokogawa.com/de/dcs/funkloesungen/de_dokumente/ISA100-whitepaper.pdf . Last accessed: February 2013

[15] T. Katsumi and K. Kenji, "Ubiquitous Sensor Network System," *NEC technical journal,* vol. 1, no. 1, pp. 79-82, 2005.

[16] "HealthCare Solutions," http://www.swisslog.com/-/media/Swisslog/Documents/HCS/RoboCourier_Autonomous_Mobile_Robots/Brochures/AMR_100_AMR_Overview.pdf. Last accessed: December 2013

[17] "Mobile Robot For Delivering Goods In Healthcare Facilities", http://www.challenge.toradex.com/projects/10169-mobile-robot-for-delivering-goods-in-healthcare-facilities. Last accessed: December 2013

[18] T. Rault, A. Bouabdallah and Y. Challal, "Energy Efficiency in Wireless Sensor Networks: a top-down survey," in *Computer Networks, doi:10.1016/j.comnet.2014.03.027* , vol. 67, pp. 104-122, 2014.

[19] R. Fensli, E. Gunnarson and T. Gundersen, "A Wearable ECG-recording System for Continuous Arrhythmia Monitoring in a Wireless Tele-Home-Care Situation," in *IEEE Symposium on Computer-Based Medical Systems*, ISBN: 0-7695-2355-2 , pp. 407-412, June 2005.

[20] G. T. Borujeny, M. Yazdi, A. Keshavarz-Haddad and A. R. Borujeny, "Detection of Epileptic Seizure Using Wireless Sensor Networks," in *Journal of Medical Signals and Sensors,* vol. 3, no. 2, pp. 63-68, 2013.

[21] A. Hadjidj, M. Souil, A. Bouabdallah, Y. Challal and H. Owen, "Wireless Sensor Networks for Rehabilitation Applications: Challenges and Opportunities," in *Journal of Network and Computer Applications, doi:10.1016/j.jnca.2012.10.002* , Vol. 36, Issue 1, pp. 1-15, Jan 2013.

[22] E. R. Berlekamp, Robert E. Peile, Stephen P. Pope, "The application of error control to communications," in *IEEE Communications Magazine,* ISSN: 0163-6804 , Vol. 25, Issue 4, pp. 44-57, 1987.

[23] W. A. Shay, "Understanding Data Communications and Networks," Chapter 5, PWS publishing company, 1995. ISBN-10: 053495054X

[24] "powercastco.com/applications/wireless-sensor-networks/," http://www.powercastco.com/applications/wireless-sensor-networks/. Last accessed: December 2013

[25] K. Furset and P. Hoffman, "High pulse drain impact on CR2032 coin cell battery capacity," 2011. (https://www.dmcinfo.com/Portals/0/Blog%20Files/High%20pulse%20drain%20impact%20on%20CR2032%20coin%20cell%20battery%20capacity.pdf). Last accessed: December 2013

[26] "perpetuapower.com/battery_limitations.htm," PERPETUA, http://www.perpetuapower.com/battery_limitations.htm. Last accessed: April 2014

[27] "Perpetual Power Solutions to Save $1 billion in Labor Costs," ONWORLD, March 2010. http://onworld.com/html/newsperpower.htm. Last accessed: April 2014

[28] S. Keeping, "Internet of Things: Designing Sensor-Based Devices with Coin Cell Batteries", AVNET, http://www.em.avnet.com/en-us/design/technical-articles/Pages/Articles/Internet-of-Things-Designing-Sensor-Based-Devices-with-Coin-Cell-Batteries.aspx. Last accessed: April 2014

[29] "ENERGIZER CR2320", "http://data.energizer.com/PDFs/cr2320.pdf. Last accessed: December 2013

[30] "CR2032 COIN CELL BATTERIES", Monnit, http://www.monnit.com/Products/Accessories/Cables,-Antennas-and-Batteries/Accessories/CR2032-Coin-Cell-Batteries. Last accessed: April 2014

[31] "Wireless Sensor Tags", WirelessTag, http://wirelesstag.net/specs.html#tag.

[32] “SG-Link®-LXRS® Wireless Strain Node” LORD Microstrain sensing system, http://www.microstrain.com/wireless/sg-link. Last accessed: April 2014

[33] SAMSUNG, http://www.samsung.com/us/mobile/cell-phones-accessories/EB-B600BUBESTA. Last accessed: June 2014

[34] “gsmarena", http://www.gsmarena.com/apple_iphone_5-4910.php. Last accessed: June 2014

[35] A. Vandervell, "trustedreviews.com/nokia-lumia-1520-review-battery-life-and-verdict-page-5," 31 March 2014. http://www.trustedreviews.com/nokia-lumia-1520-review-battery-life-and-verdict-page-5. Last accessed: June 2014

[36] C. F. Chiasserini and R. R. Rao, "Pulsed battery discharge in communication devices," in *5th annual ACM/IEEE international conference on Mobile computing and networking*, ISBN:1-58113-142-9 , pp. 88-95, 1999.

[37] H. Karl and A. Willig, "Protocols and Architectures for Wireless Sensor Networks," Wiley publishers, Chapter 6, 2007.

[38] "2.4 GHz IEEE 802.15.4 / ZigBee-ready RF Transceiver," Texas Instruments, http://www.ti.com/lit/ds/symlink/cc2420.pdf. Last accessed: December 2011

[39] "nRF24L01+ Single Chip 2.4GHz Transceiver Product Specification v1.0," Nordic Semiconductors Inc., http://www.nordicsemi.com/eng/Products/2.4GHz-RF/nRF24L01P. Last accessed: June 2012

[40] "CC2500 Single Chip Low Cost Low Power RF Transceiver," Texas Instruments, http://www.ti.com/lit/ds/symlink/cc2500.pdf. Last accessed: June 2012

[41] J.P. Sheu, K.-Y. Hsieh and Y.-K. Cheng, "Distributed Transmission Power Control Algorithm for Wireless Sensor Networks," *Journal Of Information Science And Engineering*, vol. 25, no. 5, pp. 1447-1463, 2009.

[42] I. Rhee, A. Warrier, M. Aia and J. Min, "Z-MAC: a Hybrid MAC for Wireless Sensor Networks," *IEEE/ACM Transactions On Networking*, ISSN: 1063-6692, Vol. 16, no. 3, pp. 511-524, 2008.

[43] Yucel Altunbasak, Georgia Institute of Technology, "Wireless MAC," http://users.ece.gatech.edu/yucel/wmac.pdf. Last accessed: April 2012

[44] W. Ye, J. Heidemann and D. Estrin, "An Energy-Effcient MAC Protocol for Wireless Sensor Networks," in *IEEE INFOCOM*, ISBN: 0-7803-7476-2, Vol. 3,

pp. 1567-1576 , 2002.

[45] J. Polastre, J. Hill and D. Culler, "Versatile Low Power Media Access for Wireless Sensor Networks," in *SenSys,* ISBN:1-58113-879-2, pp. 95-107, 2004.

[46] A. Goldsmith, Wireless Communication, Cambridge University Press, Chapter 4 and 9, 2005.

[47] K. Srinivasan and P. Levis, "RSSI is Under Appreciated," in *Workshop on Embedded Networked Sensors (EmNets),* 2006.

[48] N. Baccour, A. Koubaa, L. Mottola, M. A. Zuniga, H. Youssef, C. A. Boana and M. Alves, "Radio Link Quality Estimation in Wireless Sensor Networks: A Survey," in *ACM Transactions on Sensor Networks, doi. 10.1145/2240116.2240123* , Vol. 8, no. 4, pp. 1-35, 2012.

[49] S. Lin, J. Zhang, G. Zhou, T. H. Lin Gu and J. A. Stankovic, "ATPC: Adaptive Transmission Power Control for Wireless Sensor Networks," in *SenSys*, ISBN:1-59593-343-3, pp. 223-236, 2006.

[50] S. Soltani, M. U. Ilyas and H. Radha, "An Energy Efficient Link Layer Protocol forPower-Constrained Wireless Networks," in *International Conference on Computer Communications and Networks (ICCCN),* ISSN: 1095-2055, pp. 1-6, 2011

[51] L. Zheng, W. Wang, A. Mathewson, B. O'Flynn and M. Hayes, "An Adaptive Transmission Power Control Method for Wireless Sensor Networks," in *ISSC, doi. 10.1049/cp.2010.052* , pp. 261-265, 2010.

[52] J. Ko and A. Terzis, "Power Control for Mobile Sensor Networks: An Experimental Approach," in *SECON,* ISBN: 978-1-4244-7150-8, pp. 261-265, 2010.

[53] J. Jeong, D. Culler and J.-H. Oh, "Empirical Analysis of Transmission Power Control Algorithms for Wireless Sensor Networks," in International Conference on Networked Sensing Systems, ISBN: 1-4244-1231-5, pp. 27-34, 2007.

[54] A. Sheth and R. Han, "An Implementation of Transmit Power Control in 802.11b Wireless Networks," University of Colorado at Boulder, 2002.

[55] Y. Fu, M. Sha, G. Hackmann and C. Lu, "Practical Control of Transmission Power for Wireless Sensor Networks," in *IEEE International Conference on Network Protocols*, ISBN: 978-1-4673-2445-8, pp. 1-10, Oct 2012.

[56] G. Hackmann, O. Chipara and C. Lu, "Robust Topology Control for Indoor Wireless Sensor Networks," in *ACM conference on Embedded network sensor systems*, ISBN: 978-1-59593-990-6 , pp. 57-70, 2006.

[57] D. Lal, A. Manjeshwar, F. Herrmann, E. Uysal-Biyikoglu and A. Keshavarzian, "Measurement and characterization of link quality metrics in energy constrained wireless sensor networks," in *GLOBECOM*, ISBN: 0-7803-7974-8, Vol. 1, pp. 446-452, 2003.

[58] Dania Marabissi, Daniele Tarchi, Romano Fantacci, and Francesco Balleri, "Efficient Adaptive Modulation and Coding Techniques for WiMAX Systems," in *ICC*, ISBN: 978-1-4244-2075-9, pp. 3383-3387, 2008.

[59] J. Eberspächer, H.J. Vögel, C. Bettstetter and C. Hartmann, GSM - Architecture, Protocols and Services, Wiley, 2009, Chapter 4.

[60] Y. Zhao and M. S. Hsiao, "Reducing power consumption by utilizing retransmission in short range wireless network," in *LCN*, ISBN: 0-7695-1591-6, pp. 523-533, Nov 2002.

[61] J. Jeong and C. T. Ee, "Forward Error Correction in Sensor Networks," 2003, http://www.cs.berkeley.edu/~jaein/papers/cs294_9_paper_fec.pdf. Last accessed: December 2012

[62] "TinyOS," January 2013, http://www.tinyos.net/. Last accessed: December 2011

[63] "CC1000 Single Chip Very Low Power RF Transceiver," Texas Instruments, January 2006, http://www.ti.com/lit/ds/symlink/cc1000.pdf. Last accessed: December 2011

[64] D. Schmidt, M. Berning and N. Wehn, "Error correction in single-hop wireless sensor networks - A case study," in *Conference & Exhibition of Design, Automation & Test in Europe*, ISSN: 1530-1591, pp. 1296-1301, Apr 2009.

[65] S. Chouhan and R. Bose, "Integrated Energy Analysis of Error Correcting Codes and Modulation for Energy Efficient Wireless Sensor Nodes," in *IEEE Transactions on Wireless Communications*, ISSN: 1536-1276, Vol. 8, no. 10, pp. 5348-5355, 2009.

[66] S. H. Hwang, B. Kim and Y.-S. Kim, "A hybrid ARQ scheme with power ramping," in *Vehicular Technology Conference*, ISSN: 1090-3038, pp. 1579 – 1583, 2001.

[67] "DL-SCH HARQ Modeling," Matlab, http://au.mathworks.com/help/lte/examples/dl-sch-harq-modeling.html. Last accessed: December 2012

[68] J. P. Linnartz, "Maximum Ratio Combining Diversity," http://www.wirelesscommunication.nl/reference/chaptr05/diversit/mrc.htm. Last accessed: December 2012

[69] I. Stanojev, O. Simeone, Y. Bar-Ness and D. Kim, "On the Energy Efficiency of Hybrid-ARQ Protocols in Fading Channels," in *ICC*, ISBN: 1-4244-0353-7, pp. 3173-3177, 2007.

[70] M. Sajadieh, F. R. Kschischang and A. Leon-Garcia, "A Block Memory Model for Correlated Rayleigh Fading Channels," in *ICC*, ISBN: 0-7803-3250-4, pp. 282-286, 1996.

[71] D. Tse and P. Viswanath, Fundamentals of Wireless Communication, Cambridge University Press, 2005, Chapter 3.

[72] T. Rappaport, Wireless Communications- principles and practice, Prentice Hall PTR, 2002. Chapter 5

[73] S. J. Howard and K. Pahlavan, "Doppler Spread Measurements Of Indoor Radio Channel,"in *Electronics Letters* , ISSN: 0013-5194, Vol. 26, no. 2, pp. 107-108, 1990.

[74] R. Jain, "Channel Models," Feb 2007, http://www.cse.wustl.edu/~jain/cse574-08/ftp/channel_model_tutorial.pdf. Last accessed: December 2012

[75] C. W. Kim, T. S. P. See, T. M. Chiam, Y. Ge, Z. N. Chen and S. Sun, "Channel Characterization of Walking Passerby's Effects on 2.48-GHz Wireless Body Area Network," in *IEEE Transactions On Antennas And Propagation*, ISSN: 0018-926X, Vol. 61, no. 3, pp. 1495-1498, 2013.

[76] "Universal Mobile Telecommunications System (UMTS); Selection procedures for the choice of radio transmission technologies of the UMTS (UMTS 30.03 version 3.1.0)," UMTS, 2011.

[77] ITU-R, "Propagation data and prediction methods for the planning of indoor radiocommunication systems and radio local area networks in the frequency range 300 MHz to 100 GHz," 2015

[78] X. Huang and A. Ozdaglar, "Power Control and Network Design in Mobile Sensor Networks," in *International Symposium on Modeling and Optimization in Mobile,*

*Ad Hoc and Wireless Networks*, pp. 1-10, 2006.

[79] A. Farrokh, V. Krishnamurthy and R. Schober, "Optimal Power and Retransmission Control Policies over Fading Channels with Packet Drop Penalty Costs," in *ICC*, ISBN: 978-1-4244-2075-9, pp. 4021-4027, 2008.

[80] K. Zheng and H. Li, "Reinforcement learning for energy efficient wireless transmission: Green communications for a green hand transmitter," in *ICNC*, ISBN: 978-1-4673-0008-7, pp. 272-276, 2012.

[81] H. S. Wang and N. Moayeri, "Finite-State Markov Channel-A Useful Model for Radio Communication Channels," in *IEEE Transactions On Vehicular Technology*, ISSN: 0018-9545, Vol. 44, no. 1, pp. 163-171, 1995.

[82] P. Sadeghi, R. A. Kennedy, P. B. Rapajic and R. Shams, "Finite-State Markov Modeling of Fading Channels," in *IEEE Signal Processing Magazine*, ISSN: 1053-5888, pp. 57-80, 2008.

[83] Q. Zhang and S. A. Kassam, "Finite-State Markov Model for Rayleigh Fading Channels," in *IEEE Transactions On Communications*, ISSN: 0090-6778, Vol. 47, no. 11, pp. 1688-1692, 1999.

[84] "Texas Instruments Power Calculator Revision V 1.0," Texas Instruments, http://www.ti.com/tool/rf-powercalc. Last accessed: December 2011

[85] "Silab Battery Life Calculator v1.6," Silicon Labs, http://www.silabs.com/support/pages/batterylifeestimator.aspx. Last accessed: December 2011

[86] W. Stallings, "Data and Computer Communications," MaxwellMacMillan Internation Edition, Chapter 5, 1989.

[87] B. Schweber, "Understanding the Basics of Low-Noise and Power Amplifiers in Wireless Designs," Digi-key Electronics, October, 2013. http://www.digikey.com/en/articles/techzone/2013/oct/understanding-the-basics-of-low-noise-and-power-amplifiers-in-wireless-designs. Last accessed: December 2013

[88] "2.4G Wireless nRF24L01p with PA and LNA," http://www.elecfreaks.com/wiki/index.php?title=2.4G_Wireless_nRF24L01p_with_PA_and_LNA. Last accessed: December 2013

[89] "Arduino Mega 2560," http://arduino.cc/en/Main/arduinoBoardMega2560. Last

accessed: December 2013

[90] T. Liu and A. E. Cerpa, "Data-driven Link Quality Prediction Using Link Features," *ACM Transactions on Sensor Networks, doi. 10.1145/2530535,* Vol. 10, no. 2, pp. 37-61, 2014.

[91] A. Keshavarzian, E. Uysal-Biyikoglu, D. Lal and K. Chintalapudi, "From experience with indoor wireless networks:A link quality metric that captures channel memory," *IEEE Communication letters,* ISSN: 1089-7798, Vol. 11, no. 9, pp. 729-731, 2007.

[92] "Sigmoid Function," Wolfram Mathworld, http://mathworld.wolfram.com/SigmoidFunction.html. Last accessed: December 2013

[93] J. P. Linnartz, "Appropriate Choice of Packet Length," JPL's Wireless Communicaiton Reference website, 1995. http://www.wirelesscommunication.nl/reference/chaptr03/fading/effthr.htm.

[94] S. H. Gerez, "Implementation of Digital Signal Processing:Some Background on GFSK Modulation," Feb 2013. http://wwwhome.ewi.utwente.nl/~gerezsh/sendfile/sendfile.php/gfsk-intro.pdf?sendfile=gfsk-intro.pdf . Last accessed: December 2012

[95] R. H. Clarke and W. L. Khoo, "3-D Mobile Radio Channel Statistics," in *IEEE Transactions On Vehicular Technology,* ISSN: 0018-9545, Vol. 46, no. 3, pp. 798-799, 1997.

[96] "arduino.cc", http://www.arduino.cc/en/Main/Software. Last accessed: December 2013

[97] "3rd Generation Partnership Project; Technical Specification Group Radio Access Network" 3GPP, 2012. http://www.qtc.jp/3GPP/Specs/25951-900.pdf.

[98] Z. Tian, D. Yuan and Q. Liang, "Energy Efficiency Analysis of Error Control Schemes in Wireless Sensor Networks," in *International Wireless Communications and Mobile Computing Conference,* ISBN: 978-1-4244-2201-2, pp. 401-405, 2008.

[99] "Si4464/Si4463/Si4461/Si4460 High-Performance, Low-Current Transceiver," Silicon Labs, http://www.silabs.com/Support%20Documents/TechnicalDocs/Si4464-63-61-60.pdf. Last accessed: December 2012

[100] D. Basu, G. S. Gupta, G. Moretti and X. Gui, "Protocol for improved energy efficiency in wireless sensor networks to support mobile robots," in International Conference on Automation, Robotics and Applications (ICARA), *doi. 10.1109/ICARA.2015.7081152*, pp. 230-237, Queenstown, Feb 2015.

[101] D. Basu, G. S. Gupta, G. Moretti and X. Gui, "Performance comparison of a novel adaptive protocol with the fixed power transmission in wireless sensor networks," Journal of Sensor and Actuator Networks, *doi:10.3390/jsan4040274*, pp. 274-292, September 2015.

[102] A. S. Tanenbaum, Computer Networks, Chapter 4, 4th ed., Prentice Hall PTR, 2002.

[103] "IEEE Standard for Information technology— Telecommunications and information exchange between systems—Local and metropolitan area networks—Specific requirements Part 3: Carrier sense multiple access with Collision Detection (CSMA/CD) Access Method and Ph," IEEE Computer Society, 2002.

[104] U. Essays, " Microcontrollers Used In Wireless Sensor Networks Computer Science Essay," 2013. http://www.ukessays.com/essays/computer-science/microcontrollers-used-in-wireless-sensor-networks-computer-science-essay.php. Last accessed: December 2014

[105] T. S. Rappaport, Wireless Communciations Principles and practice, Chapter 4, 2nd ed., Prentice Hall PTR, 2002.

[106] G. Grimmett and D. Stirzaker, "Using Random Numbers Modeling and Simulation of Biological Systems 21-366B," http://www.math.cmu.edu/~shlomo/courses/BioSystems/Lectures/RandomWalk.pdf. Last accessed: December 2014

[107] "Random Numbers Random Walk - Computational Physics," http://www.astro.umass.edu/~schloerb/ph281/Lectures/RandomNumbers/RandomNumbers.pdf. Last accessed: December 2014

[108] J. Zhao and R. Govindan, "Understanding Packet Delivery Performance In Dense Wireless Sensor Networks," in *Sensys*, pp. 1-13, 2003.

[109] "802.11 Beacons Revealed," http://www.wi-fiplanet.com/tutorials/print.php/1492071. Last accessed: December 2014

[110] CISCO, "802.11 Fundamentals," September 2014,

http://www.cisco.com/c/en/us/td/docs/solutions/Enterprise/Borderless_Networks/Unified_Access/CMX/CMX_802Fund.pdf. Last accessed: December 2014

[111] "NetSurveyor — 802.11 Network Discovery / WiFi Scanner," http://nutsaboutnets.com/netsurveyor-wifi-scanner/ . Last accessed: December 2014

# Research publications

**Refereed conference papers**

1) Debraj Basu, Gourab Sen Gupta, Giovanni Moretti, Xiang Gui, **"Energy Efficient Adaptive Power Control in Indoor Wireless Sensor Networks",** 3rd International Conference on "Foundations & Frontiers in Computer, Communication and Electrical Engineering, India, 15-16th Jan 2016 (accepted)

2) Debraj Basu, Gourab Sen Gupta, Giovanni Moretti, Xiang Gui, **"Protocol for Improved Energy Efficiency in Wireless Sensor Networks to Support Mobile Robots**", IEEE Automation, Robotics and Applications (ICARA), Queenstown, New Zealand, pp. 230-237

3) Debraj Basu, Gourab Sen Gupta, Giovanni Moretti, Xiang Gui, **"Investigation into the Impact of Protocol Design on Energy Consumption of Low Power Wireless Sensors",** IEEE Sensors Applications Symposium (SAS), Queenstown, New Zealand, pp.69-74

4) Debraj Basu, Giovanni Moretti, Gourab Sen Gupta, Stephen Marsland, **"Wireless sensor network based smart home: Sensor selection, deployment and monitoring"**, IEEE Sensors Applications Symposium (SAS), 2013, Galveston, USA, Feb 19-21, pp. 49-54

5) Debraj Basu, Gourab Sen Gupta, Giovanni Moretti, **"Issues of data reliability in indoor channel: Impact on the energy efficiency of battery powered wireless sensor nodes",** International Conference on Networks, ICON 2012, Singapore, pp. 465-470

6) Debraj Basu, "**Energy Management in Wireless Sensor Networks: An Optimization problem**", "National Conference on Electrical, Electronics And Computer Engineering", CALCON-2011, Kolkata, India, pp. 191-195

**Journal papers (Published/Accepted)**

1) Debraj Basu, Gourab Sen Gupta, Giovanni Moretti, Xiang Gui, **"Effectiveness of a novel power control algorithm in heart rate monitoring of a mobile adult: energy efficiency comparison with fixed power transmission",** International Journal of Sensor Networks and Data Communications (accepted January 2016)

2) Debraj Basu, Gourab Sen Gupta, Giovanni Moretti, Xiang Gui, **"Performance comparison of a new non-RSSI based transmission power control protocol with RSSI based methods: Experimentation with real world data"**,

International Journal of Engineering and Technology Innovation (IJETI) (accepted November 2015)

3) Debraj Basu, Gourab Sen Gupta, Giovanni Moretti, Xiang Gui, **"Performance comparison of a novel adaptive protocol with the fixed power transmission in wireless sensor networks",** Journal of Sensor and Actuator Networks, Multidisciplinary Digital Publishing Institute (MDPI AG), October 2015, pp. 274-292

4) Debraj Basu, Giovanni Moretti, Gourab Sen Gupta, Stephen Marsland, "**Towards a monitoring smart home for the elderly: One experience in retrofitting a sensor network into an existing home",** Journal of Ambient Intelligence and Smart Environments, IOS press 2013, pp. 639-656

**Journal papers (under review)**

1) Debraj Basu, Gourab Sen Gupta, Giovanni Moretti, Xiang Gui, "**A non-RSSI based energy efficient power control algorithm for mobile wireless sensors"**, International journal of communication systems (WILEY)

# Appendix

## A.1 The nRF24L01p radio frequency transmitter and receiver


**Fig A.1.1 nRF24L01p transmitter with the temperature sensor**

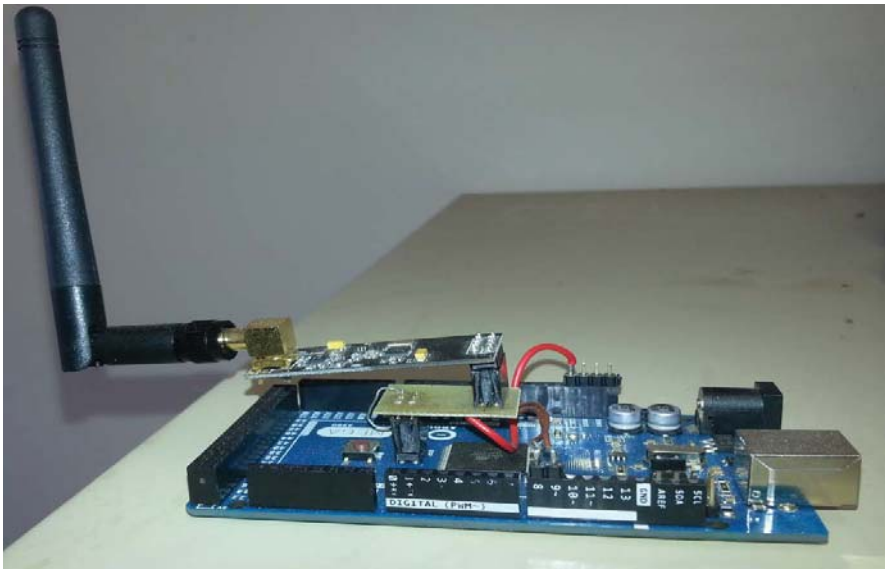


**Fig A.1.2 nRF24L01p receiver (with added PA and LNA)**

The transmitter and the receiver are both set with Arduino MEGA.

## B. Some experimental scenarios and radio propagation environments

### B.1 Within University building

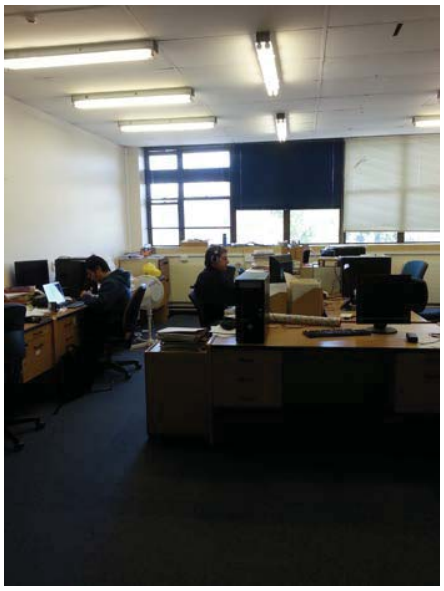

**Fig B.1.1 Sample radio environment**

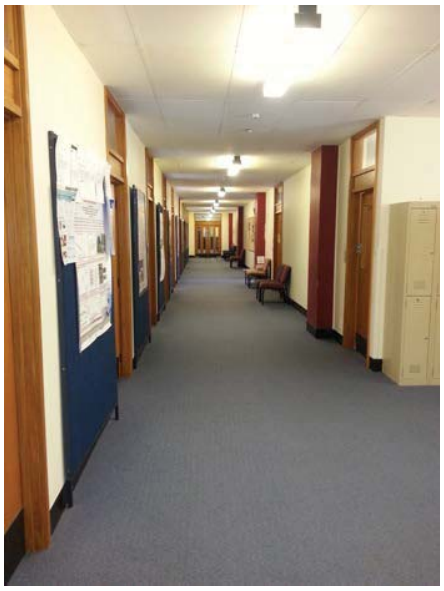

**Fig B.1.2 Sample radio environment**

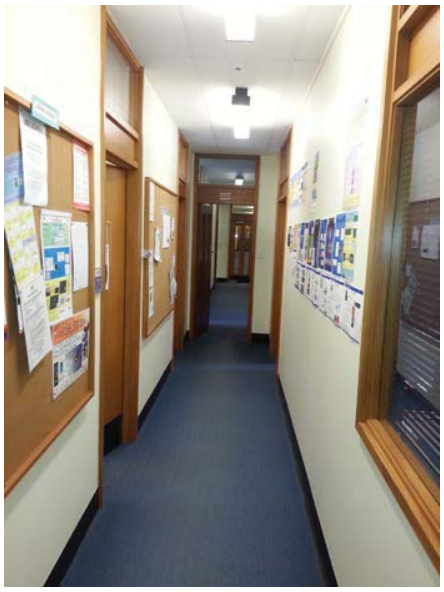

**Fig B.1.3 Sample radio environment**

## B.2 Super Market

**Fig B.2.1 Sample radio environment of super market**

## B.3 Shopping Mall food court during busy hours


**Fig B.3.1 Sample radio environment of Shopping Mall food court**

## B.4 University dining hall during busy hours

**Fig B.4.1 Sample radio enviornment of University dining hall during busy hours**